New Developments in State-Specific Multireference Coupled-Cluster Theory

Dissertation zur Erlangung des Grades
„Doktor der Naturwissenschaften"
im Promotionsfach Chemie

am Fachbereich Chemie, Pharmazie und Geowissenschaften
der Johannes Gutenberg-Universität in Mainz

von

Eric Prochnow
geboren in Radebeul

Mainz, 2010

Contents

1 Introduction

Quantum chemistry has nowadays gained a prominent role in chemical research thanks to advances in methodological developments and increasing computing power. As a consequence the areas of application of quantum chemistry have grown considerably, leading to strong interactions between theoreticians and experimentalists.

The starting point in quantum chemistry is the Schrödinger equation which provides the basis for describing atoms and molecules. However, analytic solutions of the Schrödinger equation can be found only for few model systems such as the hydrogen atom or the hydrogen molecule ion H_2^+. Due to this fact the purpose of quantum chemistry is to find proper approximate numerical solutions. These solutions can be classified by the accuracy obtained as well as the computational effort required. The application of methods yielding highly accurate results with a quantitative determination of properties is limited to rather small molecules due to the demanding computational effort. For larger molecular systems such as biomolecules or molecular clusters, more pragmatic approaches need to be applied in order to make the computations affordable.

One of the most successful and accurate methods in quantum chemistry is coupled-cluster (CC) theory.[1–4] Within CC theory, a hierarchy of methods which systematically converges towards the exact solution of the Schrödinger equation can be formulated. The most commonly used approximations are the coupled-cluster method with single and double excitations (CCSD),[5] CCSD with a perturbative treatment of triple excitations [CCSD(T)][6] and coupled-cluster singles, doubles, and triples (CCSDT).[7–9] The CCSD(T) method is in particular worth to be mentioned here as it has become the *gold standard* due to its high accuracy in reproducing experimental values.[10] For example, CCSD(T) allows the computation of relative energies within chemical accuracy (about 4 kJ mol^{-1}).[10] The extension of the applicability of CC theory - in particular of the CCSD(T) method - to larger systems is desirable and represents one of the current challenges in quantum chemistry. However, this task is limited by the computational resources available. Thus, in order to circumvent computational limitations, various implementations of CC methods as CCSD and CCSD(T) have been presented which take advantage of parallel computing.[11–20]

The CC methods mentioned above are based on the assumption that the wave func-

tion is well represented by a single electronic configuration. As one configuration or determinant is used here as reference, these approaches are called single-reference methods. Despite the success of these single-reference CC (SRCC) methods, there are a large number of problems for which the underlying assumption that the wave function is dominated by one reference determinant breaks down. Biradical systems,[21] bond breaking processes,[22] transition states,[23] excited states,[24] and transition metal compounds[25] are classic examples of problematic cases for SRCC calculations. An example where several references are of importance is the bond stretching of hydrogen fluoride (HF). In Fig. 1.1 the corresponding potential energy surface (PES) is plotted together with the electronic configuration of the valence orbitals. In the region of the equilibrium geometry (the minimum of the PES) the highest occupied and lowest unoccupied molecular orbitals (HOMO and LUMO, respectively) are the 3σ and 4σ orbitals. The 3σ orbital is doubly occupied yielding a closed-shell singlet electronic configuration. When the bond is stretched the 3σ and 4σ orbitals split into the $1s$ atomic orbital (AO) of the hydrogen atom and the $2p_z$ AO of fluorine. At larger distances these two AOs are singly occupied yielding two doublets coupled to an open-shell singlet electronic configuration that needs to be described by a linear combination of the two possible distributions of the electrons as indicated at the right hand side of Fig. 1.1. Between the equilibrium structure and the dissociation limit the aforementioned electronic configurations mix. Thus, a consistent description of the whole PES requires the inclusion of all determinants that can be generated by distributing two electrons in the corresponding two MOs.

Beside the necessity of using multireference methods for the description of the whole PES of molecules, such approaches are also important when investigating the equilibrium structure of a degenerate or quasi-degenerate system. An interesting class of compounds where this is the case are biradical systems as they often represent intermediate species in chemical reactions.[26] However, in many cases, such intermediate species cannot be observed in experiment due to their high instability and reactivity. To access these compounds theoretically as well as to study the corresponding chemical reactions and reaction paths, quantum chemical methods capable to deal with multireference cases need to be used. The need of multireference methods becomes obvious when, for example, biradical systems derived from pyridine by removing two hydrogen atoms are considered. The existence of these compounds has been proven in experimental investigations.[27,28] However, for the 2,6-isomer computational studies of these compounds yield either a monocyclic or a bicyclic structure as depicted in Fig. 1.2. The monocyclic form contains two radical centers (as in Fig. 1.2 the pictures of the two quasi-degenerate molecular

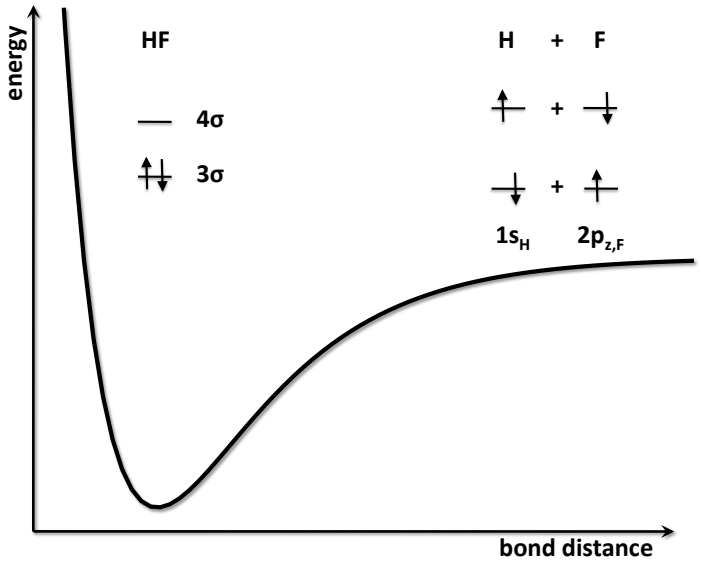

Figure 1.1: Schematic representation of the potential energy surface of hydrogen fluoride (HF). The electronic configurations at the equilibrium structure (closed-shell singlet) and for large bond distances (two doublets coupled to an open-shell singlet) are shown for the valence orbitals. The electronic configuration at larger distances consists of a linear combination of the two electronic occupations depicted.

orbitals demonstrate) which are missing in the bicyclic structure as the electrons form a single bond. The equilibrium geometry obtained from a computation depends on the method used as single-reference approaches are often not able to properly describe the monocyclic form and thus favor the bicyclic geometry.[29–31] Therefore, a consistent study of all minima on the PES of such didehydrocompounds requires the use of multireference approaches to identify the correct equilibrium structure.

In order to extend the applicability of SRCC methods to multireference problems two different strategies have been applied. The first strategy consists in adapting the underlying theory of SRCC to treat special multireference problems. This can be achieved, for example, by choosing one formal reference. One determinant in the MRCC calculation is then identical to that determinant while the other ones are included by higher, i.e., triple, quadruple, ..., excitations that lead to singly and doubly excited determinants of the corresponding reference determinant[32,33] (For other approaches see for example Refs. 34,35). The second strategy that has been started in the late 70s, focuses on the development of genuine MRCC methods. The first formulations presented within genuine

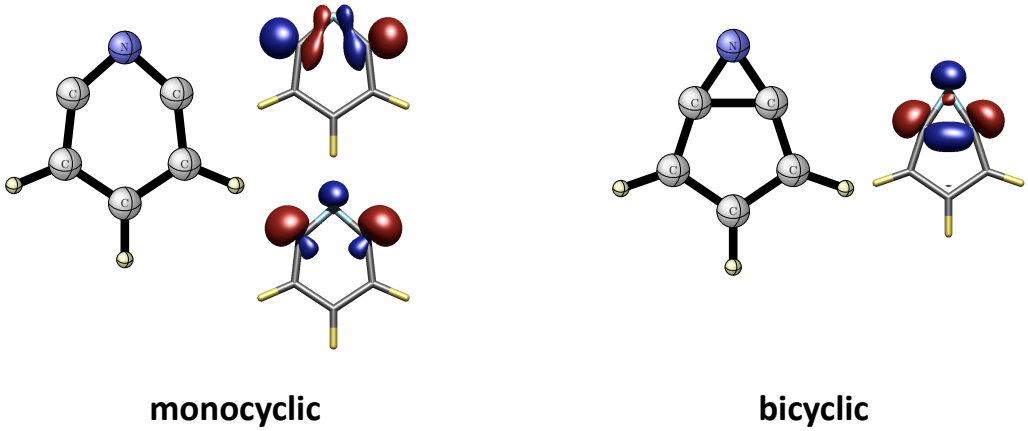

Figure 1.2: Monocyclic and bicyclic structure of the 2,6-didehydropyridine molecule. Depicted are the quasi-degenerate MOs of the monocyclic form as well as the MO corresponding to the additional single-bond in the bicyclic structure. (The corresponding orbitals have been obtained in a RHF/cc-pCVTZ calculation using the Mk-MRCCSD/cc-pCVTZ geometry.)

MRCC theory belong to the class of valence-universal or Fock-space (FS) MRCC.[36,37] In FS-MRCC theory an operator acts on a closed-shell reference generating determinants with a variable number of electrons, i.e., beside determinants with the same number of electrons also determinants containing more or less electrons. In this way ionization energies, electron affinities, and excitation energies can be directly computed. Furthermore, multireference states become accessible. This is obvious when considering a state that needs to be described by all determinants generated by distributing two electrons in two MOs (similar to the situation when stretching the bond of the HF molecule). Within the FS approach, this state, for example, can be reached by starting from the closed-shell determinant of the double anion and removing two electrons in all possible ways to obtain the various determinants. Later, Jeziorski and Monkhorst presented the Hilbert-space or state-universal (SU) MRCC approach.[38] SU-MRCC uses a generalized version of the single-reference CC ansatz containing a set of important determinants, the so-called model space, to describe the multireference problem. In this way solutions of the Schrödinger equation for a given set of states is generated simultaneously. However, both the FS and SU approaches suffer from divergence problems in the iterative

solution of the coupled-cluster equations. This phenomenon is generally attributed to the so-called intruder state problem that arises when excited determinants drop in the energy region of the determinants contained in the reference space and, thus, the energy difference of the reference and excited determinants becomes very small.[3] To avoid the intruder state problem, state-specific (SS) MRCC approaches have been proposed[39–43] for which the SU-MRCC has been slightly modified to focus on one electronic state at a time. Furthermore, state-specific methods only need to satisfy the Schrödinger equation for the state of interest and, therefore, are more flexible approaches that are probably more accurate than state-universal methods.[44] However, there is no unique way to define a state-specific MRCC theory and, accordingly, different formulations are possible.[45]

Much effort has been devoted to the development of the so-called Brillouin-Wigner (BW) MRCC ansatz.[39,40] However, the BW-MRCC ansatz is not a size-extensive theory, i.e., the energy does not scale properly with the increasing size of the system, necessitating, as in configuration-interaction approaches,[46] the consideration of size-extensivity corrections.[47] In contrast to the BW-MRCC approach, the state-specific MRCC method suggested by Mukherjee and coworkers (Mk-MRCC)[41,42] is a size-extensive theory. Based on benchmark studies it could be shown that Mk-MRCC shows faster convergence towards the full-configuration interaction (FCI) limit than BW-MRCC and yields more accurate energies than SU-MRCC theory.[44] Hanrath presented the exponential multireference wave function ansatz (MRexpT).[43] In this approach the standard ansatz where excited determinants are labeled with respect to the corresponding reference determinant is replaced by a labeling where the amplitudes are indexed by the determinants they are exciting to. As Hanrath pointed out,[48] the MRexpT approach is more complex and computationally demanding than the Mk-MRCC ansatz as the computational scaling is worse.[43] In light of these factors, this work focuses on the further development of a state-specific MRCC theory based on the Mk-MRCC approach.

In comparison to SRCC, the Mk-MRCC ansatz not only introduces an additional layer of complexity in the theoretical formulation, but also increases the computational requirements. Therefore, applications of the Mk-MRCC method are usually limited to model systems that are smaller than the molecules accessible to SRCC calculations. This work deals with three points that considerably extend the routine application of the Mk-MRCC method:

- Building an efficient MRCC algorithm for the computation of Mk-MRCC energies and properties.

- Developing analytic first derivatives for the routine location of equilibrium geometries or transition states on the potential energy surfaces of systems with many degrees of freedom.
- Developing a proper parallelization scheme as the high computational effort of the Mk-MRCC approach necessitates calculations distributed on many computers.

This dissertation focuses on the three above topics and it is structured as follows:

In Chapter 2 the theoretical background for the treatment of multireference problems is presented and quantum chemical methods which are relevant for this work are discussed. Furthermore, the general theory of analytic derivative techniques for the calculation of electronic structures and molecular properties is introduced.

For the implementation of the theoretical approaches presented in this work, the highly-efficient computer code CFOUR[49] has been chosen as underlying program system. However, CFOUR lacks a multireference algorithm to perform multireference coupled-cluster computations in a routine way. The strategies used to obtain a multireference coupled-cluster algorithm by adapting a single-reference code combined with an efficient implementation capable to perform Mk-MRCC energy calculations are discussed in Chapter 3.

For the computation of molecular properties, analytical derivatives have become a standard tool in quantum chemistry increasing the range of applicability towards larger systems. Chapter 4 deals with the derivation of analytic expressions for the energy gradient of Mk-MRCC theory using a strategy analogous to the one used in single-reference coupled-cluster theory. Explicit expressions and details for implementation of the first derivative by adapting the single-reference infrastructure of CFOUR are presented for the Mk-MRCCSD (Section 4.5) and Mk-MRCCSDT (Section 4.7) approximations.

Computations at the CCSDT or Mk-MRCCSDT level of theory, i.e., a full inclusion of triple excitations, are always limited to relatively small systems due to the time-limiting steps in the treatment of triple excitations. In Chapter 5 the strategy, implementation, and benchmark investigation of a parallelization scheme of CCSDT and Mk-MRCCSDT computations is presented. These developments allow to increase the size of the systems for which the full treatment of triple excitations can currently be applied.

Finally, Chapter 6 summarizes the results presented in this work and provides an outlook in the future development of MRCC theory.

2 Theoretical Background

2.1 The Electronic Schrödinger Equation

The starting point for the description of atomic and molecular systems is the nonrelativistic time-independent Schrödinger equation:

$$\hat{H}\ \Psi_i = E_i\ \Psi_i\ . \tag{2.1}$$

This eigenvalue equation yields the energy E_i and the wave function Ψ_i for a state i and a given Hamiltonian $\hat{H}$. The Hamiltonian contains all possible interactions of the nuclei and electrons of a molecular system and is defined using atomic units as

$$\begin{aligned}\hat{H} = &\underbrace{-\sum_K \frac{1}{2m_K}\nabla_K^2}_{\hat{T}_n} \underbrace{-\sum_i \frac{1}{2}\nabla_i^2}_{\hat{T}_e} \\ &\underbrace{-\sum_{i,K}\frac{Z_K}{|\mathbf{r}_i - \mathbf{R}_K|}}_{\hat{V}_{en}} + \underbrace{\sum_{KL}\frac{Z_K Z_L}{|\mathbf{R}_K - \mathbf{R}_L|}}_{\hat{V}_{nn}} + \underbrace{\sum_{i,j}\frac{1}{|\mathbf{r}_i - \mathbf{r}_j|}}_{\hat{V}_{ee}}\ .\end{aligned} \tag{2.2}$$

The first two terms in Eq. (2.2) are the kinetic energy contributions of the nuclei ($\hat{T}_n$) and the electrons ($\hat{T}_e$), respectively. ∇_K^2 and ∇_i^2 represent the Laplacians with respect to the coordinates of the nucleus $\mathbf{R}_K$ and the electron $\mathbf{r}_i$, while m_K is the mass of nucleus K. The last three terms describe the Coulomb interactions of electrons and nuclei with charge Z_K. The individual contributions are the electron-nucleus ($\hat{V}_{en}$) attraction as well as the nucleus-nucleus ($\hat{V}_{nn}$) and electron-electron ($\hat{V}_{ee}$) repulsion.

In order to separate the nuclear and electronic problems, the Born-Oppenheimer (BO) approximation[50] is introduced. The BO approximation consists in writing the total wave function as a product of nuclear and electronic wave function $\Psi_n(\mathbf{R})$ and $\Psi_e(\mathbf{r}, \mathbf{R})$:

$$\Psi = \Psi_n(\mathbf{R})\Psi_e(\mathbf{r}, \mathbf{R})\ . \tag{2.3}$$

The nuclear wave function depends on the coordinates of the nuclei whereas the electronic wave function $[\Psi_e(\mathbf{r},\mathbf{R})]$ depends on the position of the electrons and parametrically on the coordinates of the nuclei. $\Psi_e(\mathbf{r},\mathbf{R})$ is determined as the solution of the electronic Schrödinger equation

$$\hat{H}_e\Psi_e(\mathbf{r},\mathbf{R}) = \left(\hat{T}_e + \hat{V}_{en} + \hat{V}_{ee}\right)\Psi_e(\mathbf{r},\mathbf{R}) = E_e(\mathbf{R})\Psi_e(\mathbf{r},\mathbf{R}) \ . \tag{2.4}$$

Once $E_e(\mathbf{R})$ has been determined, $\Psi_n(\mathbf{R})$ can be obtained from the nuclear Schrödinger equation given as

$$\hat{H}_n\Psi_n(\mathbf{R}) = \left(\hat{T}_n + \hat{V}_{nn} + E_e(\mathbf{R})\right)\Psi_n(\mathbf{R}) = E_n\Psi_n(\mathbf{R}) \ . \tag{2.5}$$

Due to the fact that usually an exact solution of the electronic Schrödinger equation is not possible, a number of approximate approaches have been developed. Methods which are relevant for this work are briefly discussed in the following sections.

2.2 Hartree-Fock Theory

In Hartree-Fock theory[46] the electronic wave function of an N electron system is approximated by a single Slater determinant:

$$\Psi_e(\mathbf{r}) = (N!)^{-1/2} \ \cdot \ \begin{vmatrix} \varphi_i(1) & \varphi_j(1) & \cdots & \varphi_k(1) \\ \varphi_i(2) & \varphi_j(2) & \cdots & \varphi_k(2) \\ \vdots & \vdots & \ddots & \vdots \\ \varphi_i(N) & \varphi_j(N) & \cdots & \varphi_k(N) \end{vmatrix} , \tag{2.6}$$

which is the antisymmetric product of N spin orbitals (φ_i). The spin orbital $\varphi_i(j)$ depends on the spatial coordinates $\mathbf{r}_j$ and the spin σ_j of the electron j, i.e.,

$$\varphi_i(\mathbf{r}_j,\sigma_j) = \varphi_i(j) = \varphi_i = |i\rangle \ , \tag{2.7}$$

and is often written in terms of a spatial orbital $\phi_i(\mathbf{r}_j)$ and a spin part $\omega(\sigma_j)$ as

$$\varphi_i(\mathbf{r}_j,\sigma_j) = \phi_i(\mathbf{r}_j)\omega(\sigma_j) \ . \tag{2.8}$$

Using Eq. (2.6) and the variational principle the Hartree-Fock equations are obtained. In canonical representation these equations are

$$\hat{F}\,|i\rangle = \epsilon_i\,|i\rangle\,, \quad i = 1, \ldots, N\ , \tag{2.9}$$

where ϵ_i denotes the energy of orbital i. The Fock operator,

$$\hat{F} = \hat{h} + \sum_i \left(\hat{J}_i - \hat{K}_i\right)\ , \tag{2.10}$$

consists of the one-electron operator $\hat{h}$ as well as the Coulomb ($\hat{J}_j$) and the exchange operator ($\hat{K}_j$) which are defined via

$$\hat{h}(1) = -\frac{1}{2}\nabla_1^2 - \sum_K \frac{Z_K}{|\mathbf{r}_1 - \mathbf{R}_K|}\ , \tag{2.11}$$

$$\hat{J}_j\varphi_i(1) = \left[\int \mathrm{d}\tau_2\ \varphi_j^*(2)\frac{1}{r_{12}}\varphi_j(2)\right]\varphi_i(1)\ , \tag{2.12}$$

$$\hat{K}_j\varphi_i(1) = \left[\int \mathrm{d}\tau_2\ \varphi_j^*(2)\frac{1}{r_{12}}\varphi_i(2)\right]\varphi_j(1)\ , \tag{2.13}$$

with the integration carried out over spin and spatial coordinates ($\tau_i \hat{=} \mathbf{r}_i\sigma_i$). The Fock operator represents an effective one-particle operator. The contribution of $\hat{J}_j$ describes the Coulomb interactions of an electron with the mean field of the other electrons. The Hartree-Fock exchange operator, $\hat{K}_j$, arises due to the antisymmetry of the wave function.

The spatial orbitals ϕ_i are usually expanded as a linear combination of atomic orbitals (LCAO), i.e.,

$$\phi_i = \sum_\mu^M c_{\mu i}\chi_\mu\ . \tag{2.14}$$

The basis functions χ_μ are normally chosen to be Gaussian functions and are weighted by the coefficients $c_{\mu i}$. Although the exact expansion requires in principle a summation over an infinite number of atomic orbitals, for practical reasons the expansion (2.14) is truncated to include only a certain number of terms. Inserting Eq. (2.14) in the Hartree-Fock equations (2.9) yields the Roothaan-Hall equations,[51,52] a generalized matrix eigenvalue problem,

$$\mathbf{FC} = \mathbf{SC}\epsilon\ , \tag{2.15}$$

with the coefficient matrix $\mathbf{C}$ defined as $(\mathbf{C})_{\mu i} = c_{\mu i}$. The elements of the overlap matrix $\mathbf{S}$ are $S_{\mu\nu} = \langle\mu|\nu\rangle$ while the elements of the diagonal matrix ϵ can be identified with the orbital energies. For the closed-shell case, the elements of the Fock matrix $\mathbf{F}$ are given by

$$F_{\mu\nu} = h_{\mu\nu} + \sum_{\lambda,\sigma} D_{\lambda\sigma} \left[\langle\mu\sigma|\nu\lambda\rangle - \frac{1}{2} \langle\mu\sigma|\lambda\nu\rangle \right] , \tag{2.16}$$

with the one-particle density matrix $D_{\lambda\sigma}$ defined as

$$D_{\lambda\sigma} = 2 \sum_{i} c^*_{\lambda i} c_{\sigma i} , \tag{2.17}$$

and the matrix element $h_{\mu\nu}$ as

$$h_{\mu\nu} = \int dr_1 \phi^*_\mu(1) \hat{h}(1) \phi_\nu(1) . \tag{2.18}$$

Here, the short hand notation for the two-electron integrals,

$$\langle\mu\sigma|\nu\lambda\rangle = \int \mathrm{d}r_1 \int \mathrm{d}r_2 \phi^*_\mu(1) \phi^*_\sigma(2) \frac{1}{r_{12}} \phi_\nu(1) \phi_\lambda(2) \tag{2.19}$$

$$\langle\mu\sigma|\lambda\nu\rangle = \int \mathrm{d}r_1 \int \mathrm{d}r_2 \phi^*_\mu(1) \phi^*_\sigma(2) \frac{1}{r_{12}} \phi_\lambda(1) \phi_\nu(2) , \tag{2.20}$$

has been used. Eq. (2.15) can be solved using an iterative self-consistent procedure.[46] At convergence the Hartree-Fock energy (E_{HF}) is given as

$$E_{\mathrm{HF}} = \frac{1}{2} \sum_{\mu,\nu} D_{\nu\mu} \left(h_{\mu\nu} + F_{\mu\nu} \right) . \tag{2.21}$$

In Hartree-Fock theory the Coulomb interaction is described only in a mean-field manner, i.e., the motion of one electron depends on the mean field of the other electrons and not on their individual position. While this is an approximation, the exchange correlation due to the antisymmetric form of the wave function is treated exactly. The difference of the exact energy (E_{exact}) and the Hartree-Fock energy is called the correlation energy E_{corr}:

$$E_{\mathrm{corr}} = E_{\mathrm{exact}} - E_{\mathrm{HF}} . \tag{2.22}$$

2.3 Two-Configurational Self-Consistent Field Theory

When the assumption, that the wave function is dominated by one determinant, does not hold, Hartree-Fock theory as presented in the previous section is not a suitable starting point. For the treatment of multireference problems, single-reference Hartree-Fock theory has been generalized to a wave function ansatz represented by a linear combination of reference determinants Φ_i weighted by the coefficients c_i:

$$\Psi = \sum_i c_i \Phi_i \ , \tag{2.23}$$

yielding the multiconfigurational self-consistent field (MCSCF) theory.[53,54]

A special case of MCSCF theory is the two-configurational self-consistent field (TCSCF) approach[55] where the wave function is composed of a linear combination of two closed-shell reference determinants Φ_t and Φ_s,

$$\Psi = c_t \Phi_t + c_s \Phi_s \ , \tag{2.24}$$

with the weighting coefficients c_t and c_s, also known as CI coefficients. The index s (t) here denotes the determinant for which the active orbital s (t) is occupied, i.e.,

$$\begin{aligned} |\Phi_t\rangle &= \left|(\text{core})^2 \phi_t \bar{\phi}_t\right\rangle \\ |\Phi_s\rangle &= \left|(\text{core})^2 \phi_s \bar{\phi}_s\right\rangle \ , \end{aligned} \tag{2.25}$$

with ϕ_t ($\bar{\phi}_t$) occupied by an electron with α (β) spin. $(\text{core})^2$ stands for the orbitals outside the active space that are doubly occupied for both reference determinants. In contrast to Hartree-Fock theory both the orbitals ϕ_i and the weighting coefficients need to be determined via the variational principle. To obtain a set of equations for calculating the CI coefficients, the energy functional $\tilde{E}$,

$$\begin{aligned} \tilde{E} &= E_{\text{TCSCF}} - \lambda(c_t^2 + c_s^2 - 1) \\ &= c_t^2 \underbrace{\left\langle \Phi_t \middle| \hat{H} \middle| \Phi_t \right\rangle}_{H_{tt}} + c_s^2 \underbrace{\left\langle \Phi_s \middle| \hat{H} \middle| \Phi_s \right\rangle}_{H_{ss}} + 2 c_t c_s \underbrace{\left\langle \Phi_t \middle| \hat{H} \middle| \Phi_s \right\rangle}_{H_{ts}} - \lambda(c_t^2 + c_s^2 - 1) \end{aligned} \tag{2.26}$$

is minimized with respect to the CI coefficients where λ denotes the Lagrange multiplier for the normalization condition of the coefficients. This yields a set of equations given

by

$$\begin{pmatrix} H_{tt} & H_{st} \\ H_{st} & H_{ss} \end{pmatrix} \begin{pmatrix} c_t \\ c_s \end{pmatrix} = E_{\mathrm{TCSCF}} \begin{pmatrix} c_t \\ c_s \end{pmatrix} \ . \tag{2.27}$$

The determination of the orbitals ϕ_p can be carried out in an analogous way as in Hartree-Fock theory by minimizing the energy with respect to the orbitals. For this purpose the energy functional $\tilde{E}$ can be extended by the orthonormality condition of the orbitals yielding

$$\tilde{\tilde{E}} = \tilde{E} + \sum_{i,j} \left(\epsilon_{ij} + \epsilon_{ji}\right) \left(\langle i|j\rangle - \delta_{ij}\right) \ , \tag{2.28}$$

where ϵ_{ij} and ϵ_{ji} denote Lagrange multipliers. As the set of orbitals ϕ_q represents a complete orthonormal basis, a new set of orbitals ϕ'_p can be obtained via the transformation

$$\phi'_p = \sum_q U_{qp} \phi_q \tag{2.29}$$

with the expansion coefficients U_{qp}. Inserting Eq. (2.29) into Eq. (2.28) for all orbitals and differentiating the Lagrangian with respect to the coefficients U_{pq} finally yields the variational conditions given by

$$c_t^2 F_{ai}^t + c_s^2 F_{ai}^s = 0 \tag{2.30}$$

$$c_t^2 F_{at}^t + c_t c_s K_{at}^s = 0 \tag{2.31}$$

$$c_s^2 F_{ti}^s - c_t c_s K_{ti}^s = 0 \tag{2.32}$$

$$c_t^2 F_{st}^t - c_s^2 F_{st}^s + c_t c_s K_{st}^s - c_t c_s K_{st}^t = 0 \ , \tag{2.33}$$

where the Fock matrices $\mathbf{F}^t$ and $\mathbf{F}^s$ are defined as

$$F_{pq}^t = h_{pq} + \sum_j \left(2\langle pj|qj\rangle - \langle pj|jq\rangle\right) \tag{2.34}$$

$$F_{pq}^s = h_{pq} + \sum_j \left(2\langle pj|qj\rangle - \langle pj|jq\rangle\right) \ . \tag{2.35}$$

The sums include the index of the corresponding doubly occupied active orbital t and s, respectively. The exchange matrices $\mathbf{K}^t$ and $\mathbf{K}^s$ contain the two-electron integrals,

$$K_{pq}^t = \langle pt|tq\rangle \tag{2.36}$$

$$K_{pq}^s = \langle ps|sq\rangle \ . \tag{2.37}$$

To determine the orbitals via solving

$$\mathbf{F}^{\text{eff}}\mathbf{U} = \mathbf{F}^{\text{eff}}_{\text{diag}}\mathbf{U} \ , \tag{2.38}$$

an iterative procedure may be used for which the effective Fock matrix $\mathbf{F}^{\text{eff}}$,

$$\mathbf{F}^{\text{eff}} = \begin{pmatrix} F^{\text{eff}}_{ij} & F^{\text{eff}}_{ti} & F^{\text{eff}}_{si} & F^{\text{eff}}_{ai} \\ F^{\text{eff}}_{ti} & F^{\text{eff}}_{tt} & F^{\text{eff}}_{st} & F^{\text{eff}}_{at} \\ F^{\text{eff}}_{si} & F^{\text{eff}}_{st} & F^{\text{eff}}_{ss} & F^{\text{eff}}_{as} \\ F^{\text{eff}}_{ai} & F^{\text{eff}}_{at} & F^{\text{eff}}_{as} & F^{\text{eff}}_{ab} \end{pmatrix} \ , \tag{2.39}$$

is set up containing individual blocks for different kind of indices, i.e., occupied-occupied, occupied-active, occupied-virtual ... The variational conditions [Eqs. (2.30) - (2.33)] are used to build the off-diagonal blocks, i.e., virtual-occupied, virtual-active, active-occupied and active-active, of the effective Fock matrix,

$$F^{\text{eff}}_{ai} = c_t^2 F^t_{ai} + c_s^2 F^s_{ai} \tag{2.40}$$

$$F^{\text{eff}}_{at} = c_t^2 F^t_{at} + c_t c_s K^s_{at} \tag{2.41}$$

$$F^{\text{eff}}_{ti} = c_s^2 F^s_{ti} - c_t c_s K^s_{ti} \tag{2.42}$$

$$F^{\text{eff}}_{st} = c_t^2 F^t_{st} - c_s^2 F^s_{st} + c_t c_s K^s_{st} - c_t c_s K^t_{st} \ . \tag{2.43}$$

When $\mathbf{F}^{\text{eff}}$ is then diagonalized to obtain a new set of orbital coefficients U_{pq} the variational conditions are fulfilled as the off-diagonal elements become zero. The remaining diagonal blocks can in principle be freely chosen which only affects the convergence behavior of the iterative procedure. According to Eq. (2.29) U_{pq} yields a new set of orbitals that are used in conjunction with the CI coefficients to solve Eq. (2.27) and to construct a new effective Fock matrix.

2.4 Coupled-Cluster Theory

To obtain the exact wave function the Hartree-Fock wave function $|\Psi_0\rangle$ can be taken as a starting point. $|\Psi_0\rangle$ is constructed from the N energetically lowest spin orbitals, where N denotes the number of electrons, that are obtained by solving the Roothaan-Hall equations within a finite AO-basis consisting of M basis functions. Replacing the N occupied spin orbitals $(\varphi_i, \varphi_j, \varphi_k, \ldots)$ of $|\Psi_0\rangle$ by the $n_{\text{vrt}} = M - N$ virtual, i.e.,

unoccupied, spin orbitals $(\varphi_a, \varphi_b, \varphi_c, \ldots)$ in all possible combinations, leads to a set of further N-electron Slater determinants $(\Psi_i^a, \Psi_{ij}^{ab}, \ldots)$, which spans a complete many-electron basis for a given AO basis. Therefore, the exact non-relativistic electronic wave function can be written in terms of these excited determinants.

This idea is used in coupled-cluster (CC) theory[1–4,56–58] where the ansatz for the wave function is chosen to be

$$|\Psi_{\mathrm{CC}}\rangle = e^{\hat{T}} |\Psi_0\rangle \ . \tag{2.44}$$

The cluster operator $\hat{T}$ consists of single $(\hat{T}_1)$, double $(\hat{T}_2)$ up to N-tuple $(\hat{T}_N)$ excitations of electrons from occupied to virtual spin orbitals, i.e.,

$$\hat{T} = \hat{T}_1 + \hat{T}_2 + \ldots + \hat{T}_N \ . \tag{2.45}$$

The excitation operators are defined as

$$\hat{T}_N = \frac{1}{(N!)^2} \sum_{i,j,k,\ldots}^{N} \sum_{a,b,c,\ldots}^{n_{\mathrm{vrt}}} t_{ijk\ldots}^{abc\ldots} \, \hat{a}_a^\dagger \hat{a}_i \hat{a}_b^\dagger \hat{a}_j \hat{a}_c^\dagger \hat{a}_k \ldots \ , \tag{2.46}$$

where the contribution to the wave function of the excitations are weighted by the amplitudes $t_{ijk\ldots}^{abc\ldots}$ while $\hat{a}_a^\dagger$ and $\hat{a}_i$ denote second quantization creation and annihilation operators, respectively. The exponential of the cluster operator is expanded in a Taylor series giving

$$e^{\hat{T}} = 1 + \hat{T} + \frac{1}{2}\hat{T}^2 + \frac{1}{6}\hat{T}^3 + \ldots \ , \tag{2.47}$$

showing that in contrast to configuration interaction (CI),[59] the wave function is not linear in the amplitudes due to the appearance of products of cluster operators. A consequence of the exponential parametrization [(2.44)] is that coupled-cluster theory is a size-consistent approach as the exponential $e^{\hat{T}_{\mathrm{AB}}}$ of a compound system of non-interacting subsystems A and B can be recast as

$$e^{\hat{T}_{\mathrm{AB}}} = e^{\hat{T}_{\mathrm{A}} + \hat{T}_{\mathrm{B}}} = e^{\hat{T}_{\mathrm{A}}} e^{\hat{T}_{\mathrm{B}}} \ , \tag{2.48}$$

where the exponentials $e^{\hat{T}_{\mathrm{A}}}$ and $e^{\hat{T}_{\mathrm{B}}}$ only act on the individual subsystems. Inserting the coupled-cluster ansatz for the wave function (2.44) into the Schrödinger equation leads to

$$\hat{H} e^{\hat{T}} |\Psi_0\rangle = E e^{\hat{T}} |\Psi_0\rangle \ . \tag{2.49}$$

Due to the complexity and nonlinearity of the latter equation a variational solution is not viable. Instead, Eq. (2.49) is solved by using projection techniques. Therefore, Eq. (2.49) is first multiplied by $e^{-\hat{T}}$ from the left and then projected on the reference determinant $\langle\Psi_0|$ as well as all possible excited determinants $\left\langle\Psi_{ijk\ldots}^{abc\ldots}\right|$ to obtain an expression for the energy E and a set of equations to determine the amplitudes $t_{ijk\ldots}^{abc\ldots}$, i. e.,

$$\left\langle\Psi_0\middle|\bar{H}\middle|\Psi_0\right\rangle = E \tag{2.50}$$

$$\left\langle\Psi_{ijk\ldots}^{abc\ldots}\middle|\bar{H}\middle|\Psi_0\right\rangle = 0\ , \tag{2.51}$$

where $\bar{H}$ denotes the similarity-transformed Hamiltonian given by

$$\bar{H} = e^{-\hat{T}}\hat{H}e^{\hat{T}}\ . \tag{2.52}$$

These equations may be further simplified using the Baker-Campbell-Hausdorff (BCH) expansion[60] of $\bar{H}$,

$$\bar{H} = \hat{H} + \left[\hat{H},\hat{T}\right] + \frac{1}{2!}\left[\left[\hat{H},\hat{T}\right],\hat{T}\right] + \ldots\ , \tag{2.53}$$

which, due to the structure of the Hamiltonian having only one- and two-electron operators, truncates at the fifth term. A further analysis of the CC equations can be carried out using Wick's theorem or diagrammatic techniques.[2,3] Using the complete cluster operator in Eq. (2.46), i.e., a full coupled-cluster (FCC) ansatz, yields the exact solution of the Schrödinger equation which is equivalent to the full configuration-interaction (FCI) wave function. However, due to the high computational cost, the FCC approach is only applicable to very small systems. Thus, for practical reasons, the cluster operator is truncated at a certain level of excitation. The resulting approximations, presented in Table 2.1, are named according to the excitations included in the cluster operator. For example, CCSD denotes "coupled-cluster singles and doubles" whereas CCSDT is the acronym for "coupled-cluster singles, doubles and triples". Derivations for various truncation levels of the cluster operator as well as detailed expressions for implementation are given in the literature.[7,8,61–64]

The computational scaling behavior of CCSDT prevents its application to relatively small systems. In order to circumvent this drawback approximate approaches for the treatment of triple excitations with a reduced scaling behavior have been developed. In the most successful method, namely CCSD(T),[6] the energy corrections are obtained via perturbation theory arguments and by replacing the corresponding amplitudes by the converged CCSD amplitudes. This correction is added to the CCSD energy. This means

Table 2.1: Truncation scheme of the cluster operator $\hat{T}$, its corresponding naming and the formal computational scaling with the size of the system.

$\hat{T} = \hat{T}_1 + \hat{T}_2$	CCSD	$\mathcal{O}(N^6)$
$\hat{T} = \hat{T}_1 + \hat{T}_2 + \hat{T}_3$	CCSDT	$\mathcal{O}(N^8)$
$\hat{T} = \hat{T}_1 + \hat{T}_2 + \hat{T}_3 + \hat{T}_4$	CCSDTQ	$\mathcal{O}(N^{10})$
	$\vdots$	

that the computation of triples effects is performed in a noniterative manner. The CCSD energy correction is defined by the fourth-order and one of the fifth-order terms yielding the final CCSD(T) energy as

$$E_{\mathrm{CCSD(T)}} = E_{\mathrm{CCSD}} + E^{[4]} + E^{[5]} \ . \tag{2.54}$$

For HF references, the individual contributions using spin-orbitals are defined via

$$E^{[4]} = \frac{1}{36} \sum_{ijk}^{N} \sum_{abc}^{n_{\mathrm{vrt}}} t_{ijk}^{abc} D_{ijk}^{abc} t_{ijk}^{abc} \tag{2.55}$$

$$E^{[5]} = \frac{1}{4} \sum_{ijk}^{N} \sum_{abc}^{n_{\mathrm{vrt}}} \langle jk||bc\rangle \, t_i^a t_{ijk}^{abc} \ , \tag{2.56}$$

where D_{ijk}^{abc} consists of diagonal Fock matrix elements and is defined as

$$D_{ijk}^{abc} = f_{ii} + f_{jj} + f_{kk} - f_{aa} - f_{bb} - f_{cc} \ . \tag{2.57}$$

The triples amplitudes t_{ijk}^{abc} are determined via

$$D_{ijk}^{abc} t_{ijk}^{abc} = \sum_{e} P(i/jk) P(a/bc) t_{jk}^{ae} \langle bc||ei\rangle + \sum_{m} P(i/jk) P(a/bc) t_{mi}^{bc} \langle jk||ma\rangle \ , \tag{2.58}$$

where the doubles amplitudes (t_{ij}^{ab}) are the converged amplitudes from CCSD. The permutation operator $P(i/jk)$ is defined as

$$P(i/jk) f(ijk) = f(ijk) - f(jik) - f(kji) \ , \tag{2.59}$$

and $\langle pq||rs\rangle$ denotes the usual antisymmetrized two-electron integrals, i.e.,

$$\langle pq||rs\rangle = \langle pq|rs\rangle - \langle pq|sr\rangle \ , \tag{2.60}$$

in the molecular-orbital (MO) representation. In comparison to CCSDT, the formal scaling is reduced by one power to $\mathcal{O}(N^7)$. Additionally, the calculation of the (T) correction represents a noniterative step for which the triples amplitudes do not need to be stored.

2.5 State-Specific Multireference Coupled-Cluster Theory

To obtain the exact wave function within CC theory an exponential operator is applied to a reference function as presented in Eq. (2.44). This equation may be recast in a more general way. The exact wave function $|\Psi\rangle$ may also be obtained by applying a wave operator $\hat{\Omega}$ to a reference function $\left|\Psi^P\right\rangle$ as

$$|\Psi\rangle = \hat{\Omega}\left|\Psi^P\right\rangle \ . \tag{2.61}$$

In the case of single-reference CC, $\left|\Psi^P\right\rangle$ is usually chosen as a Hartree-Fock determinant $|\Psi_0\rangle$ while $\hat{\Omega}$ is defined by

$$\hat{\Omega} = e^{\hat{T}}\,|\Psi_0\rangle\,\langle\Psi_0| \ . \tag{2.62}$$

For the development of a multireference method the wave operator from Eq. (2.62) needs to be generalized. Jeziorski and Monkhorst (JM) proposed a general state-universal approach[38] where the wave operator is separated into individual contributions from different reference determinants (Φ_μ),

$$\hat{\Omega} = \sum_{\mu=1}^{d} e^{\hat{T}_\mu}\,|\Phi_\mu\rangle\,\langle\Phi_\mu| \ , \tag{2.63}$$

with $\hat{T}_\mu$ as a reference specific cluster operator and d as the number of reference determinants. The reference function $\left|\Psi_\alpha^P\right\rangle$ of state α is then chosen as a linear combination of reference determinants Φ_μ with weighting coefficients c_μ^α defined as

$$\left|\Psi_\alpha^P\right\rangle = \sum_\mu c_\mu^\alpha\,|\Phi_\mu\rangle \ . \tag{2.64}$$

The wave operator from Eq. (2.63) acts on the approximate wave function $\left|\Psi_\alpha^P\right\rangle$ to obtain the exact wave function for state α:

$$\left|\Psi_\alpha\right\rangle = \hat{\Omega}\left|\Psi_\alpha^P\right\rangle = \sum_{\mu=1}^{d} e^{\hat{T}_\mu}\left|\Phi_\mu\right\rangle c_\mu^\alpha \ . \tag{2.65}$$

The wave operator satisfies the Schrödinger equation for all d eigenstates, i.e.,

$$\hat{H}\hat{\Omega}\left|\Psi_\alpha^P\right\rangle = E^\alpha\hat{\Omega}\left|\Psi_\alpha^P\right\rangle \quad \text{for } \alpha = 1,\ldots,d \ . \tag{2.66}$$

This approach yields the energy of all d states simultaneously and is referred to as state-universal MRCC (SU-MRCC).

State-specific multireference coupled-cluster (SS-MRCC) approaches also rely on the JM wave operator formalism. However, in contrast to SU-MRCC, the state-specific wave operator, denoted by $\hat{\Omega}_\alpha$, acts on only one state α at a time and, thus, Eq. (2.66) is only satisfied for that specific state.

The state-universal wave operator [Eq. (2.63)] as well as the state-specific variant ($\hat{\Omega}_\alpha$) are written as a sum of exponential functions derived from reference determinants Φ_μ that form a model space M of dimension d. When the model space contains all determinants generated by distributing m electrons in n_{act} orbitals, M is called a complete model space (CMS). The cluster operator $\hat{T}_\mu$, in analogy to SRCC [see Eq. (2.45)], excites electrons from the occupied to the virtual spin orbitals of Φ_μ and is typically truncated at a certain excitation level n

$$\hat{T}_\mu = \hat{T}_1^\mu + \hat{T}_2^\mu + \ldots + \hat{T}_n^\mu, \tag{2.67}$$

where the k-fold excitation operator $\hat{T}_k^\mu$ is written as

$$\hat{T}_k^\mu = \sum_{i<j\ldots}^{\text{occ}(\mu)} \sum_{a<b\ldots}^{\text{vir}(\mu)} t_{ij\ldots}^{ab\ldots}(\mu)\hat{a}_a^+\hat{a}_i\hat{a}_b^+\hat{a}_j\ldots \ . \tag{2.68}$$

To avoid redundancies, $\hat{T}_\mu$ is restricted to excitations that lead to determinants outside the model space M and internal excitations that map Φ_μ onto M are set to zero. The cluster operator $\hat{T}_\mu$ may be expressed in a more compact form as

$$\hat{T}_\mu = \sum_{q\in Q(\mu)} t_q(\mu)\hat{\tau}_q(\mu), \tag{2.69}$$

by denoting the excitation indices with the compound index q. Here $Q(\mu)$ is the excitation manifold for determinant Φ_μ and consists of all single, double, up to n-tuple excitations starting from this determinant, excluding internal excitations, $\hat{\tau}_q(\mu)$ is the operator for excitation q ($\cdots \hat{a}_b^\dagger \hat{a}_j \hat{a}_a^\dagger \hat{a}_i$), and $t_q(\mu)$ is the corresponding amplitude $[t_{ij\ldots}^{ab\cdots}(\mu)]$. The excited determinant $\Phi_q(\mu)$ can then be written as

$$|\Phi_q(\mu)\rangle = \hat{\tau}_q(\mu)\,|\Phi_\mu\rangle \ , \tag{2.70}$$

and the projection operator $\hat{P}$ onto the model space as well as its orthogonal complement $\hat{Q}$ can be defined as

$$\hat{P} = \sum_\mu |\Phi_\mu\rangle \langle\Phi_\mu| \ , \tag{2.71}$$

and

$$\hat{Q} = 1 - \hat{P} \ . \tag{2.72}$$

The Schrödinger equation [Eq. (2.66)] with the state-specific variant of the wave operator ($\hat{\Omega}_\alpha$) is multiplied from the left by $\hat{P}$ yielding

$$\hat{P}\hat{H}\hat{\Omega}_\alpha \left|\Psi_\alpha^P\right\rangle = E_\alpha \hat{P}\hat{\Omega}_\alpha \left|\Psi_\alpha^P\right\rangle \ . \tag{2.73}$$

Using the relations[65]

$$\hat{P}\hat{\Omega}_\alpha = \hat{P} \tag{2.74}$$

$$\left|\Psi_\alpha^P\right\rangle = \hat{P}\,|\Psi_\alpha\rangle \tag{2.75}$$

$$\hat{P}\hat{P} = \hat{P} \ , \tag{2.76}$$

Eq. (2.73) is recast as

$$H^{\text{eff}} \left|\Psi_\alpha^P\right\rangle = E_\alpha \left|\Psi_\alpha^P\right\rangle \tag{2.77}$$

where H^{eff} is defined by

$$H^{\text{eff}} = \hat{P}\hat{H}\hat{\Omega}_\alpha \ . \tag{2.78}$$

The SS-MRCC energy E^α and the expansion coefficients c_μ^α are obtained from the eigenvalue equation

$$\sum_\nu H_{\mu\nu}^{\text{eff}} c_\nu^\alpha = E^\alpha c_\mu^\alpha \ , \tag{2.79}$$

where the matrix elements of the effective Hamiltonian $H^{\text{eff}}_{\mu\nu}$ are defined as

$$H^{\text{eff}}_{\mu\nu} = \left\langle \Phi_\mu \middle| \hat{H} e^{\hat{T}_\nu} \middle| \Phi_\nu \right\rangle \overset{\text{CMS}}{=} \left\langle \Phi_\mu \middle| e^{-\hat{T}_\nu} \hat{H} e^{\hat{T}_\nu} \middle| \Phi_\nu \right\rangle \ . \tag{2.80}$$

The second equality in Eq. (2.80) holds only for a complete model space where

$$\hat{T}^\dagger_\nu \left| \Phi_\mu \right\rangle = 0 \ . \tag{2.81}$$

Eq. (2.81) holds due to two conditions. The first one is that intermediate normalization is employed, i.e.,

$$\begin{aligned}
1 &= \left\langle \Psi^P_\alpha \middle| \Psi_\alpha \right\rangle = \left\langle \Psi^P_\alpha \middle| \hat{\Omega}^\dagger \middle| \Psi^P_\alpha \right\rangle = \left\langle \Psi_\alpha \middle| \hat{P} \hat{\Omega}^\dagger \hat{P} \middle| \Psi_\alpha \right\rangle \\
&= \sum_{\mu,\nu,\sigma} \left\langle \Psi_\alpha \middle| \Phi_\mu \right\rangle \left\langle \Phi_\mu \middle| e^{\hat{T}^\dagger_\nu} \middle| \Phi_\nu \right\rangle \left\langle \Phi_\nu \middle| \Phi_\sigma \right\rangle \left\langle \Phi_\sigma \middle| \Psi_\alpha \right\rangle \\
&= \sum_{\mu,\nu} \left\langle \Psi_\alpha \middle| \Phi_\mu \right\rangle \left\langle \Phi_\mu \middle| e^{\hat{T}^\dagger_\nu} \middle| \Phi_\nu \right\rangle \left\langle \Phi_\nu \middle| \Psi_\alpha \right\rangle \\
&= \left\langle \Psi_\alpha \middle| \hat{P} \middle| \Psi_\alpha \right\rangle + \sum_{\substack{\mu \\ \nu \neq \mu}} \left\langle \Psi_\alpha \middle| \Phi_\mu \right\rangle \left\langle \Phi_\mu \middle| e^{\hat{T}^\dagger_\nu} \middle| \Phi_\nu \right\rangle \left\langle \Phi_\nu \middle| \Psi_\alpha \right\rangle \\
&= \left\langle \Psi_\alpha \middle| \hat{P} \hat{P} \middle| \Psi_\alpha \right\rangle + \sum_{\substack{\mu \\ \nu \neq \mu}} \left\langle \Psi_\alpha \middle| \Phi_\mu \right\rangle \left\langle \Phi_\mu \middle| e^{\hat{T}^\dagger_\nu} \middle| \Phi_\nu \right\rangle \left\langle \Phi_\nu \middle| \Psi_\alpha \right\rangle \\
&= \underbrace{\left\langle \Psi^P_\alpha \middle| \Psi^P_\alpha \right\rangle}_{1} + \underbrace{\sum_{\substack{\mu \\ \nu \neq \mu}} \left\langle \Psi_\alpha \middle| \Phi_\mu \right\rangle \left\langle \Phi_\mu \middle| e^{\hat{T}^\dagger_\nu} \middle| \Phi_\nu \right\rangle \left\langle \Phi_\nu \middle| \Psi_\alpha \right\rangle}_{0} \ ,
\end{aligned} \tag{2.82}$$

where Eqs. (2.63), (2.65), (2.71), (2.75) and (2.76) have been used. The contribution of the second term in the last line of Eq. (2.82) has to be zero in the case of intermediate normalization and, therefore, the corresponding internal excitations need to be zero. The second condition is that a complete model space is used. When using an incomplete model space determinants outside the model space could be reached by applying $\hat{T}^\dagger_\nu$ to $|\Phi_\mu\rangle$ which would then be nonzero. Recasting the right-hand side of Eq. (2.80) and using Eq. (2.81) yields

$$\begin{aligned}
\left\langle \Phi_\mu \middle| e^{-\hat{T}_\nu} \hat{H} e^{\hat{T}_\nu} \middle| \Phi_\nu \right\rangle &= \left\langle e^{-\hat{T}^\dagger_\nu} \Phi_\mu \middle| \hat{H} e^{\hat{T}_\nu} \middle| \Phi_\nu \right\rangle = \left\langle \left(1 + \hat{T}^\dagger_\nu + \ldots \right) \Phi_\mu \middle| \hat{H} e^{\hat{T}_\nu} \middle| \Phi_\nu \right\rangle \\
&= \left\langle \Phi_\mu \middle| \hat{H} e^{\hat{T}_\nu} \middle| \Phi_\nu \right\rangle \ .
\end{aligned} \tag{2.83}$$

In the following it will always be assumed that the model space is complete.[i]

For the derivation of the amplitude equations, Eq. (2.65) using the state-specific wave operator $[\hat{\Omega}_\alpha]$ is inserted into the Schrödinger equation yielding

$$\sum_\mu \left[\hat{H} e^{\hat{T}_\mu} \left|\Phi_\mu\right\rangle c_\mu^\alpha - E^\alpha e^{\hat{T}_\mu} \left|\Phi_\mu\right\rangle c_\mu^\alpha \right] = 0 \ . \tag{2.84}$$

It is obvious here that the use of a state-specific form of the wave operator introduces a redundancy problem: the number of equations that can be derived from Eq. (2.84) is smaller than the number of t-amplitudes contained in the $\hat{T}_\mu$ operators. Thus, supplementary conditions, the so-called sufficiency conditions, need to be introduced. However, in SS-MRCC this choice of sufficiency conditions is not unique, and various approaches are possible, for example the ansatz suggested by Mukherjee[41,42] or Brillouin-Wigner MRCC,[40,67] which adopt different sufficiency conditions. For the case of Mk-MRCC theory, Eq. (2.84) can be recast using the resolution of identity, $\hat{1} = e^{\hat{T}_\mu}(\hat{P} + \hat{Q})e^{-\hat{T}_\mu}$, and interchanging indices μ and ν as

$$\sum_\mu \left[\sum_\nu e^{\hat{T}_\nu} \left|\Phi_\mu\right\rangle H_{\mu\nu}^{\mathrm{eff}} c_\nu^\alpha + e^{\hat{T}_\mu} \hat{Q} \bar{H}_\mu \left|\Phi_\mu\right\rangle c_\mu^\alpha - E^\alpha e^{\hat{T}_\mu} \left|\Phi_\mu\right\rangle c_\mu^\alpha \right] = 0 \ , \tag{2.85}$$

with $\bar{H}_\mu = e^{-\hat{T}_\mu} \hat{H} e^{\hat{T}_\mu}$, in analogy to $\bar{H}$ in SRCC theory, as a reference-specific similarity-transformed Hamiltonian. The Mk-MRCC sufficiency conditions are chosen in such a manner that Eq. (2.85) is satisfied by setting the individual terms in the summation over μ to zero. In this way, a matching number of amplitudes and equations is ensured.[41] After multiplication with $e^{-\hat{T}_\mu}$ and projection onto the excited determinants $\Phi_q(\mu)$, the amplitude equations are resulting,

$$\left\langle \Phi_q(\mu) \middle| \bar{H}_\mu \middle| \Phi_\mu \right\rangle c_\mu^\alpha + \sum_{\nu(\neq\mu)} \left\langle \Phi_q(\mu) \middle| \hat{Y}^{\mu,\nu} \middle| \Phi_\mu \right\rangle H_{\mu\nu}^{\mathrm{eff}} c_\nu^\alpha = 0, \tag{2.86}$$

with $\hat{Y}^{\mu,\nu} = e^{-\hat{T}_\mu} e^{\hat{T}_\nu}$. The first term of Eq. (2.86) is similar to the amplitude equations of SRCC with the exception that this part is specific for a reference μ. Explicit expressions for SRCC amplitude equations can be found in the literature.[22,68] The second term is the coupling term between amplitudes of determinant ν and μ. For the derivation of

[i] Formulations for incomplete model spaces, for example for Mk-MRCC, have been given by Pahari *et al.* in Ref. 66.

explicit expressions, the resolution of the identity with respect to reference μ,

$$\begin{aligned}\hat{I} = |\Phi_\mu\rangle \langle\Phi_\mu| + \sum_{m}^{\mathrm{occ}(\mu)} \sum_{e}^{\mathrm{vrt}(\mu)} |\Phi_m^e(\mu)\rangle \langle\Phi_m^e(\mu)| \\ + \frac{1}{4} \sum_{mn}^{\mathrm{occ}(\mu)} \sum_{ef}^{\mathrm{vrt}(\mu)} \left|\Phi_{mn}^{ef}(\mu)\right\rangle \left\langle\Phi_{mn}^{ef}(\mu)\right| + \dots\end{aligned} \tag{2.87}$$

is inserted in the coupling term. In the case of Mk-MRCCSD the coupling terms are given by[22]

$$\left\langle \Phi_i^a(\mu) \middle| \hat{Y}^{\mu,\nu} \middle| \Phi_\mu \right\rangle = t_i^a(\nu/\mu) - t_i^a(\mu) \ , \tag{2.88}$$

for single excitations and

$$\begin{aligned}\left\langle \Phi_{ij}^{ab}(\mu) \middle| \hat{Y}^{\mu,\nu} \middle| \Phi_\mu \right\rangle = -t_{ij}^{ab}(\mu) + P(ij) t_i^a(\mu) t_j^b(\mu) - P(ij)P(ab) t_i^a(\mu) t_j^b(\nu/\mu) \\ + t_{ij}^{ab}(\nu/\mu) + P(ij) t_i^a(\nu/\mu) t_j^b(\nu/\mu) \ ,\end{aligned} \tag{2.89}$$

for double excitations. For Mk-MRCCSDT, triples coupling terms need to be taken into account. The expression for them is given by[68]

$$\begin{aligned}\left\langle \Phi_{ijk}^{abc}(\mu) \middle| \hat{Y}^{\mu,\nu} \middle| \Phi_\mu \right\rangle = \Delta t_{ijk}^{abc}(\nu/\mu,\mu) + P(i/jk)P(a/bc) \Delta t_i^a(\nu/\mu,\mu) \Delta t_{jk}^{bc}(\nu/\mu,\mu) \\ + P(abc) \Delta t_i^a(\nu/\mu,\mu) \Delta t_j^b(\nu/\mu,\mu) \Delta t_k^c(\nu/\mu,\mu) \ .\end{aligned} \tag{2.90}$$

The permutation operators $P(ij)$ and $P(i/jk)$ are defined via

$$P(ij) f(i,j) = f(i,j) - f(j,i) \tag{2.91}$$

$$P(i/jk) f(i,j,k) = f(i,j,k) - f(j,i,k) - f(k,j,i) \tag{2.92}$$

$$\begin{aligned}P(abc) f(a,b,c) = f(a,b,c) - f(b,a,c) - f(c,b,a) - f(a,c,b) \\ + f(c,a,b) + f(b,c,a) \ .\end{aligned} \tag{2.93}$$

In Eq. (2.90) the difference $\Delta t_{ij\dots}^{ab\dots}(\nu/\mu,\mu)$ has been introduced defined via

$$\Delta t_{ij\dots}^{ab\dots}(\nu/\mu,\mu) = t_{ij\dots}^{ab\dots}(\nu/\mu) - t_{ij\dots}^{ab\dots}(\mu) \ . \tag{2.94}$$

The so-called *common* amplitudes of operator $\hat{T}_\nu$ and $\hat{T}_\mu$ are given by

$$t_{ij\ldots}^{ab\cdots}(\nu/\mu) = \begin{cases} t_{ij\ldots}^{ab\cdots}(\nu) & \text{if } i,j\ldots \in \text{occ}(\mu) \text{ and occ}(\nu) \\ & \text{and } a,b\ldots \in \text{vir}(\mu) \text{ and vir}(\nu) \\ 0 & \text{else .} \end{cases} \tag{2.95}$$

The computational cost for solving the amplitude equations (2.86) is dominated by the first term. The formal scaling is $d \cdot N^6$ for Mk-MRCCSD and $d \cdot N^8$ for Mk-MRCCSDT, with d the number of reference determinants. The computational costs for calculating the coupling terms in Eqs. (2.88) - (2.90) are $d \cdot N^2$, $d \cdot N^4$ and $d \cdot N^6$, respectively. This scaling is two orders of magnitudes smaller than the required time for the computation of the single-reference term in Eq. (2.86). The ansatz for the Mk-MRCC approach yields a size-extensive theory.[ii] This has been shown by Mahapatra *et.al.*[42] by proving the connected[iii] nature of the effective Hamiltonian [Eq. (2.80)] and the individual terms of the amplitude equations [Eq. (2.86)].

Although the Mk-MRCC ansatz is one of the most promising candidates in the field for routine application, the approach still has its deficiencies. The most significant drawback is the lack of a full invariance of the energy with respect to rotations of the orbitals.[69,70] While rotations among doubly occupied and unoccupied orbitals leaves the energy unchanged, the energy depends on rotations among active orbitals.[22] However, the origin of the lack of orbital invariance in Mk-MRCC theory is not clear. Li and Paldus suggested that the invariance may arise from an inconsistent truncation of the cluster operator $\hat{T}_\mu$.[71] When considering the singles and doubles truncation the cluster operator generates different sets of excited determinants that only partly overlap, i.e.,

$$\text{span}(\hat{T}_\mu^{\text{SD}} |\Phi_\mu\rangle) \neq \text{span}(\hat{T}_\nu^{\text{SD}} |\Phi_\nu\rangle) \text{ for } \mu \neq \nu, \tag{2.96}$$

where $\text{span}(\hat{T}_\mu^{\text{SD}} |\Phi_\mu\rangle)$ denotes the set spanned by the excited determinants derived from Φ_μ by applying the corresponding $\hat{T}_\mu^{\text{SD}}$. As a consequence of that, the Mk-MRCC wave function (Ψ_α) does not satisfy the residual relation

$$\left\langle \Phi_l \middle| \left(\hat{H} - E^\alpha\right) \middle| \Psi_\alpha \right\rangle = 0 \tag{2.97}$$

[ii] A theory is called size-extensive if the correct scaling of the energy with the number of particles or units in a system is guaranteed.

[iii] A term is called connected if the individual factors share at least one index with another factor, e.g., in the CC energy equation the Hamiltonian shares at least one index with every cluster operator in the expression.

for all excited determinants Φ_l belonging to the set

$$\Phi_l = \cup_\mu \text{ span}(\hat{T}_\mu^{\text{SD}} |\Phi_\mu\rangle) \ , \tag{2.98}$$

as has been pointed out in Ref. 48. Recently, the Mk-MRCCSDtq scheme has been proposed, where, beside the full treatment of single and double excitations, only parts of triple and quadruple excitations, i.e., only triple (quadruple) excitations that have one (two) active and virtual index (indices) belonging to active space orbitals, are considered.[70] The Mk-MRCCSDtq method has a computational scaling of $d^2 \cdot N^6$ which is d times larger than the scaling of Mk-MRCCSD preventing its routine application. Using Mk-MRCCSDtq it has been demonstrated that an equal set of excited determinants for each reference determinant does not guarantee orbital invariance.[70] Another question that has been raised by Das *et. al.* is the fact whether the accuracy of Mk-MRCC is sufficient to describe the whole potential energy surface (PES). In comparison to other methods, as for example multireference configuration interaction (MRCI), for which the computational cost has the same magnitude, the accuracy observed is worse for Mk-MRCC theory.[69] However, it might be argued that due to the structure of the JM ansatz the accuracy of these methods can only directly be compared if the MRCI excitation manifold can be fully spanned for each individual $\hat{T}_\mu |\Phi_\mu\rangle$.[70]

2.6 Molecular Properties as Analytical Derivatives

In chemistry molecules are characterized via their molecular properties, such as the structure, vibrational frequencies, or nuclear magnetic shielding constants. In most cases, molecular properties can be determined as derivatives of the energy with respect to the corresponding perturbations.[72] For example, first derivatives with respect to nuclear displacements define the forces on nuclei which are needed to locate stationary points (minima or transition states) on the potential energy surface. Furthermore, second derivatives with respect to nuclear coordinates allow to characterize stationary points as minima or transition states and to compute harmonic vibrational frequencies.[72]

Energy derivatives can be computed in quantum chemical calculations via numerical or analytical techniques.[72] Following the numerical strategy, the first derivative with respect to a perturbation χ may be expressed as

$$\frac{dE}{d\chi}\Big|_{x=x_0} \approx \frac{E(x_0 + \Delta\chi) - E(x_0 - \Delta\chi)}{2\Delta\chi} \ , \tag{2.99}$$

where $\Delta\chi$ represents a finite change of the perturbation. However, the possible accuracy when calculating the difference quotient is already limited for the computation of first derivatives.[72] This effect is even worse when higher derivatives are to be calculated. Furthermore, the computational cost is relatively high as numerical differentiation requires for example for gradients two additional energy calculations for each degree of freedom. Analytic differentiation circumvents the mentioned problems. Here analytic expressions for the derivatives are used. However, the necessary work for deriving and implementing analytic expressions is higher than for numerical differentiation. Nevertheless, computation of the derivatives via analytic approaches increases the accuracy and reduces the computational cost considerably. Therefore, analytic derivatives are nowadays used as standard techniques in quantum chemistry.[72–76]

2.7 Analytic Gradients in Coupled-Cluster Theory

Since a major part of this work deals with the derivation of analytic first derivatives for SS-MRCC theory using a similar strategy as in SRCC, analytic gradients for SRCC are briefly discussed at this point. For the derivation of SRCC gradients an approach is presented that can easily be extended to SS-MRCC.

To obtain expressions for the first derivatives of the energy it is convenient to exploit the Hellmann-Feynman theorem,

$$\frac{dE}{d\chi} = \left\langle \Psi \middle| \frac{d\hat{H}}{d\chi} \middle| \Psi \right\rangle \ , \tag{2.100}$$

as only derivatives of the Hamiltonian need to be considered. Eq. (2.100) only holds if the electronic energy E is stationary with respect to the variation of the wave function parameters.[77] However, when using the energy expression from SRCC theory this condition is not satisfied as the SRCC approach is non-variational. To circumvent this problem the technique of Lagrange multipliers may be used to set up a Lagrangian $\tilde{E}$ which fulfills the stationarity condition. Within the SRCC approach a Lagrangian may be constructed that has the form

$$\tilde{E} = \left\langle \Psi_0 \middle| \bar{H} \middle| \Psi_0 \right\rangle + \sum_q \lambda_q \left\langle \Psi_q \middle| \bar{H} \middle| \Psi_0 \right\rangle \ . \tag{2.101}$$

The first term of Eq. (2.101) corresponds to the CC energy expression [Eq. (2.50)], the

second one to the CC amplitude equations [Eq. (2.51)] multiplied by the corresponding Lagrange multipliers λ_q. Eq. (2.101) may be rewritten in a shorter form,

$$\tilde{E} = \left\langle \Psi_0 \middle| (1 + \hat{\Lambda}) \bar{H} \middle| \Psi_0 \right\rangle \ , \tag{2.102}$$

where the de-excitation operator $\hat{\Lambda}$ is given, in analogy to the cluster operator, by

$$\langle \Psi_0 | \, \hat{\Lambda} = \sum_q \lambda_q \langle \Psi_q | \ . \tag{2.103}$$

$$\hat{\Lambda} = \hat{\Lambda}_1 + \hat{\Lambda}_2 + \dots \tag{2.104}$$

$$\hat{\Lambda}_k = \frac{1}{(k!)^2} \sum_{i,j\dots}^{\text{occ}} \sum_{a,b\dots}^{\text{vir}} \lambda_{ab\dots}^{ij\dots} \hat{a}_i^+ \hat{a}_a \hat{a}_j^+ \hat{a}_b \dots \ . \tag{2.105}$$

According to Eq. (2.102), $\tilde{E}$ is stationary with respect to the λ-amplitudes when the amplitude equations [Eq. (2.51)] are solved. The stationary condition of the t-amplitudes is fulfilled by solving the so-called lambda equations

$$0 = \left\langle \Psi_0 \middle| \left(1 + \hat{\Lambda}\right) \left(e^{-\hat{T}} \hat{H} e^{\hat{T}} - E_{CC} \right) \middle| \Psi_q \right\rangle \ . \tag{2.106}$$

Using the t- and λ-amplitudes obtained by solving the CC and lambda equations (Eqs. (2.51) and (2.106), respectively), the SRCC gradient may then be formulated as

$$\frac{d\tilde{E}}{d\chi} = \left\langle \Psi_0 \middle| (1 + \hat{\Lambda}) e^{-\hat{T}} \frac{\partial \hat{H}}{\partial \chi} e^{\hat{T}} \middle| \Psi_0 \right\rangle \ . \tag{2.107}$$

It is important to note that no derivatives of $\hat{T}$ and $\hat{\Lambda}$ need to be determined due to the $2n + 1$ and $2n + 2$ rules[10,78,79] provided that $\tilde{E}$ is stationary. Eq. (2.107) may be rewritten as

$$\frac{d\tilde{E}}{d\chi} = \sum_{pq} D_{pq} \frac{\partial f_{pq}}{\partial \chi} + \sum_{pqrs} \Gamma_{pqrs} \frac{\partial \langle pq || rs \rangle}{\partial \chi} \ , \tag{2.108}$$

where the one- and two-particle density matrices D_{pq} and Γ_{pqrs} consist of contributions due to the response of the t-amplitudes and the reference determinant,

$$D_{pq} = D_{pq}^{\text{CC}} + D_{pq}^{\text{ref}} \tag{2.109}$$

$$\Gamma_{pqrs} = \Gamma_{pqrs}^{\text{CC}} + \Gamma_{pqrs}^{\text{ref}} \ . \tag{2.110}$$

The contributions due to the amplitude response, i.e., D_{pq}^{CC} and $\Gamma_{pqrs}^{\mathrm{CC}}$, are

$$D_{pq}^{\mathrm{CC}} = \left\langle \Psi_0 \middle| \left(1 + \hat{\Lambda}\right) e^{-\hat{T}} \left\{ a_p^\dagger a_q \right\} e^{\hat{T}} \middle| \Psi_0 \right\rangle \tag{2.111}$$

$$\Gamma_{pqrs}^{\mathrm{CC}} = \frac{1}{4} \left\langle \Psi_0 \middle| \left(1 + \hat{\Lambda}\right) e^{-\hat{T}} \left\{ a_p^\dagger a_q^\dagger a_s a_r \right\} e^{\hat{T}} \middle| \Psi_0 \right\rangle \ , \tag{2.112}$$

while the contributions D_{pq}^{ref} and $\Gamma_{pqrs}^{\mathrm{ref}}$ are the standard one- and two-particle contribution for a Slater determinant Ψ_0.[10] When one imagines that the perturbation is switched on after the HF calculation, the orbitals are not changed by the perturbation leading to an orbital-unrelaxed approach. The gradient is then defined by Eq. (2.108) containing only derivatives of the corresponding AO integrals. Considering changes of the orbitals due to the external perturbation yields to an orbital-relaxed approach. Here, the fact is taken into account that the MO integral derivatives from Eq. (2.108) contain terms due to the derivative of the MO coefficients in addition to the AO integral derivatives. To separate these contributions, the derivatives of the AO one- and two-electron integrals as well as the overlap matrix rotated into the MO basis are defined (h_{pq}^{χ}, $\langle pq||rs\rangle^{\chi}$ and S_{pq}^{χ}, respectively). The Fock-matrix derivative $f_{pq}^{(\chi)}(\mu)$,

$$f_{pq}^{(\chi)}(\mu) = h_{pq}^{\chi} + \sum_{k}^{\mathrm{occ}(\mu)} \langle pk||qk\rangle^{\chi} \ , \tag{2.113}$$

is introduced, which does not contain contributions due to the derivatives of the MO coefficients $c_{\mu p}$. The derivatives of the MO coefficient $c_{\mu p}$ are parametrized via[80]

$$\frac{\partial c_{\mu p}}{\partial \chi} = \sum_{q} U_{qp}^{\chi} c_{\mu q} \ . \tag{2.114}$$

Using these definitions, Eq. (2.108) is then rewritten as

$$\frac{d\tilde{E}}{d\chi} = \sum_{pq} D_{pq} f_{pq}^{(\chi)} + \sum_{pqrs} \Gamma_{pqrs} \langle pq||rs\rangle^{\chi} - 2 \sum_{pq} I'_{pq} U_{pq}^{\chi} \ . \tag{2.115}$$

The last term in Eq. (2.115) contains terms due to the derivative of the MO coefficients with respect to the perturbation. Explicit expressions for the one-particle intermediate $I'_{pq}(\mu)$ when using a RHF reference function can be found in Ref. 81 or in the Appendix. To avoid explicit determination of the coefficients U_{pq}^{χ} and in this way reduce the computational effort, the last term in Eq. (2.115) is recast using the Z-vector method by Handy

and Schaefer.[82] Finally, an expression for the CC gradient in the AO representation is obtained[83] given by

$$\frac{d\tilde{E}}{d\chi} = \sum_{\mu\nu}^{\mathrm{AO}} D_{\mu\nu} f_{\mu\nu}^{(\chi)} + \sum_{\mu\nu\sigma\rho}^{\mathrm{AO}} \Gamma_{\mu\nu\sigma\rho} \langle \mu\nu || \sigma\rho \rangle^{\chi} + \sum_{\mu\nu}^{\mathrm{AO}} I_{\mu\nu} S_{\mu\nu}^{\chi} \ . \tag{2.116}$$

$D_{\mu\nu}$, $\Gamma_{\mu\nu\sigma\rho}$ and $I_{\mu\nu}$ denote an effective one-particle density matrix, the two-particle density matrix and an one-particle intermediate, respectively, expressed in the AO basis. Explicit expressions of these matrices depend on the applied reference function and can be found in Ref. 84 for restricted Hartree-Fock (RHF) references (see also the Appendix for expressions of $I_{\mu\nu}$) as well as in Refs. 85 and 86 for the use of MCSCF orbitals.

3 Development of an Efficient Multireference Algorithm in CFOUR

In order to reduce the effort required to implement the Mk-MRCC method, it is convenient whenever possible to take advantage of efficient program packages and adapt the CC code therein. Mk-MRCC theory is well suited for such a strategy because the amplitude equations [Eq. (2.86)] can be separated into a single-reference CC-like term for each determinant corresponding to the similarity-transformed Hamiltonian of SRCC theory and a coupling part.[42] The single-reference CC-like term, representing the time-determining step when solving for the amplitudes, is specific for a reference Φ_μ. Therefore, to use a SRCC code, this term may be implemented by looping over all reference determinants. Within this loop the corresponding coupling terms are added to the intermediates.

3.1 Implementation of Mk-MRCCSD

The Mk-MRCC ansatz has been implemented in the quantum-chemical program package CFOUR[49] using the expressions given in Section 2.5. For each reference determinant, occupied and virtual orbitals are defined differently. However, the CFOUR code relies on the separate storage and handling of molecular orbital integrals according to the type of orbitals [e.g. $\langle oo|oo\rangle, \langle oo|ov\rangle, \langle oo|vv\rangle, \ldots$ with o (v) denoting indices for occupied (virtual) orbitals]. Therefore, a straightforward implementation would require the use of multiple MO integral files which in turn would lead to a significant increase in disk space requirements. To avoid this, a different strategy has been chosen in this work which consists in doubling the MOs within the active space so that each active MO belongs to both occupied as well as virtual orbital spaces. For the case of an active space of two orbitals (one occupied and one virtual) the duplication is illustrated in Fig. 3.1. Thus, the whole calculation is based on one set of MO integral files. The active-space orbital doubling is simply accomplished by enlarging the MO coefficient matrix before the transformation of the integrals from the AO to the MO basis. Due to this duplication

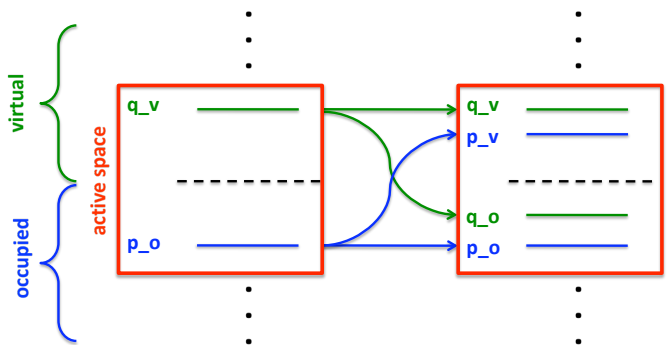

Figure 3.1: Schematic representation of the orbital duplication for an active space containing two orbitals p and q (left-hand side). The indices o and v indicate occupied and virtual orbitals with respect to a specific reference determinant. After the duplication (right-hand side) p and q belong to both the occupied and virtual spaces of the reference determinant.

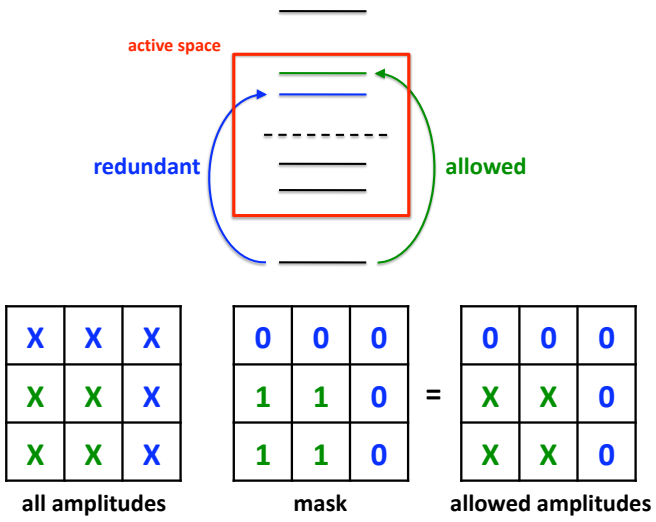

Figure 3.2: Schematic representation of an allowed (green) and a redundant (blue) single excitation within one reference determinant occurring due to the duplication of MOs (top). The orbital depicted in green represents a virtual orbital for this specific reference determinant while the orbital in blue is a redundant orbital due to the duplication. As a calculation yields all excitations the redundant ones need to be set to zero. The redundant t_1-amplitudes are eliminated in a computation by multiplication of each amplitude with the corresponding element of a mask leaving only allowed excitations (bottom). In the matrix depicted, rows denote virtual, columns occupied orbitals.

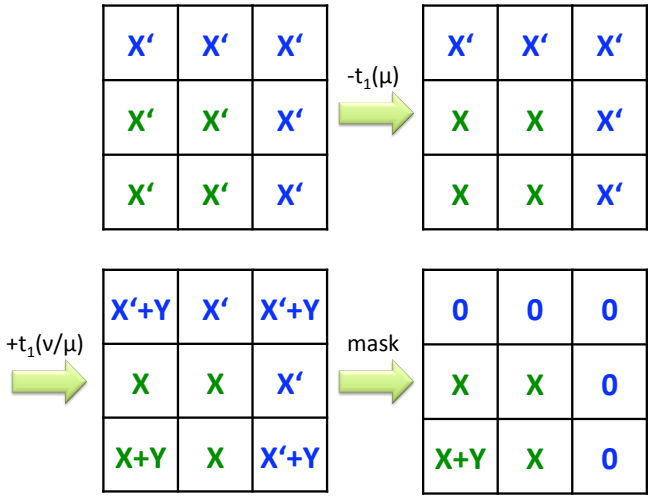

Figure 3.3: Schematic representation of the addition of the coupling terms to the t_1 residuals when computing the amplitude equations for the system described in Fig. 3.2. Symbols in green denote allowed, symbols in blue redundant elements. After computing the SRCC part the top left matrix with the elements X' is obtained. As $t_1(\mu)$ belongs to reference determinant μ only the green part is changed yielding the elements X. When adding $t_1(\nu/\mu)$ allowed and redundant matrix elements are changed (denoted by Y) due to the fact that the these amplitudes belong to a different reference ν. When applying the mask as described in Fig. 3.2 the redundant elements are set to zero.

redundant excitations occur in the amplitude equations which are set to zero to obtain only the proper elements for a certain reference determinant.

Following this approach, for each determinant Φ_μ the enlargement of the orbital space results in redundant excitations as depicted schematically in Fig. 3.2 for a system containing three occupied and three virtual orbitals after duplication. This is due to the fact that all excitations from occupied to virtual orbitals, which include duplicated MOs, are taken into account. The corresponding t-amplitudes need to be set to zero in each iteration. For this purpose a mask containing elements equal to zero or one is created for each reference determinant. The amplitudes are multiplied by the corresponding element of the mask to give either zero or to retain the allowed value.

Before updating the amplitudes, the coupling terms need to be added. Since the amplitudes of all references are stored using the same orbital ordering there is no need to resort them before computing the contribution of the coupling terms. These, as illus-

trated in Fig. 3.3 for the t_1-amplitude equations [Eq. (2.88)] of the system mentioned before, contribute only to allowed elements or to elements which are set to zero at the end as these are redundant excitations within this reference.

In Mk-MRCC theory the energy E^α and the weighting coefficients c_μ^α are obtained by diagonalizing an effective Hamiltonian H^{eff}. According to Eq. (2.80) the diagonal elements of H^{eff} are determined by adding the reference energy and the CC energy for the corresponding reference determinant Φ_μ. The off-diagonal elements are obtained by solving the SRCC amplitude equations [Eq. (2.51)] for projections on excited determinants that are contained in the model space.

The flowchart in Fig. 3.4 summarizes the implementation of Mukherjee's MRCC ansatz using the SRCC code in CFOUR. The current implementation for Mk-MRCCSD has a formal scaling of $d \cdot n_o^2 n_v^4$, where d represents the number of reference determinants, n_o the number of occupied and n_v the number of virtual orbitals, and is available for RHF, unrestricted Hartree-Fock (UHF), TCSCF and restricted open-shell Hartree-Fock (ROHF) open-shell singlet orbitals.

3.2 Implementation of Mk-MRCCSDT

For the implementation of Mk-MRCCSDT energies, the Mk-MRCCSD procedure needs to be extended. After computing the SRCC part for the t_1- and t_2-amplitudes for all reference determinants, the triples part of the code is entered looping over all determinants. Within this loop, the SRCC contribution to the t_3-amplitudes is calculated. The basis scheme in the CFOUR algorithm for the formation of the t_3-amplitudes in an energy calculation including triple excitations is an outer loop over an index triple i, j, k of the t_{ijk}^{abc}-amplitudes.[87] Blocks of a, b, c index triples are computed within this loop one at a time. Afterwards, the coupling terms projected on triple excitations are added and redundant amplitudes are set to zero by using a mask for the triples amplitudes. In this way a new set of t_3-amplitudes is obtained for each a, b, c-block which is directly used to compute the corresponding triples contributions to the t_1- and t_2-amplitudes. The additional steps for the computation of triples beyond Mk-MRCCSD are depicted schematically in Fig. 3.4.

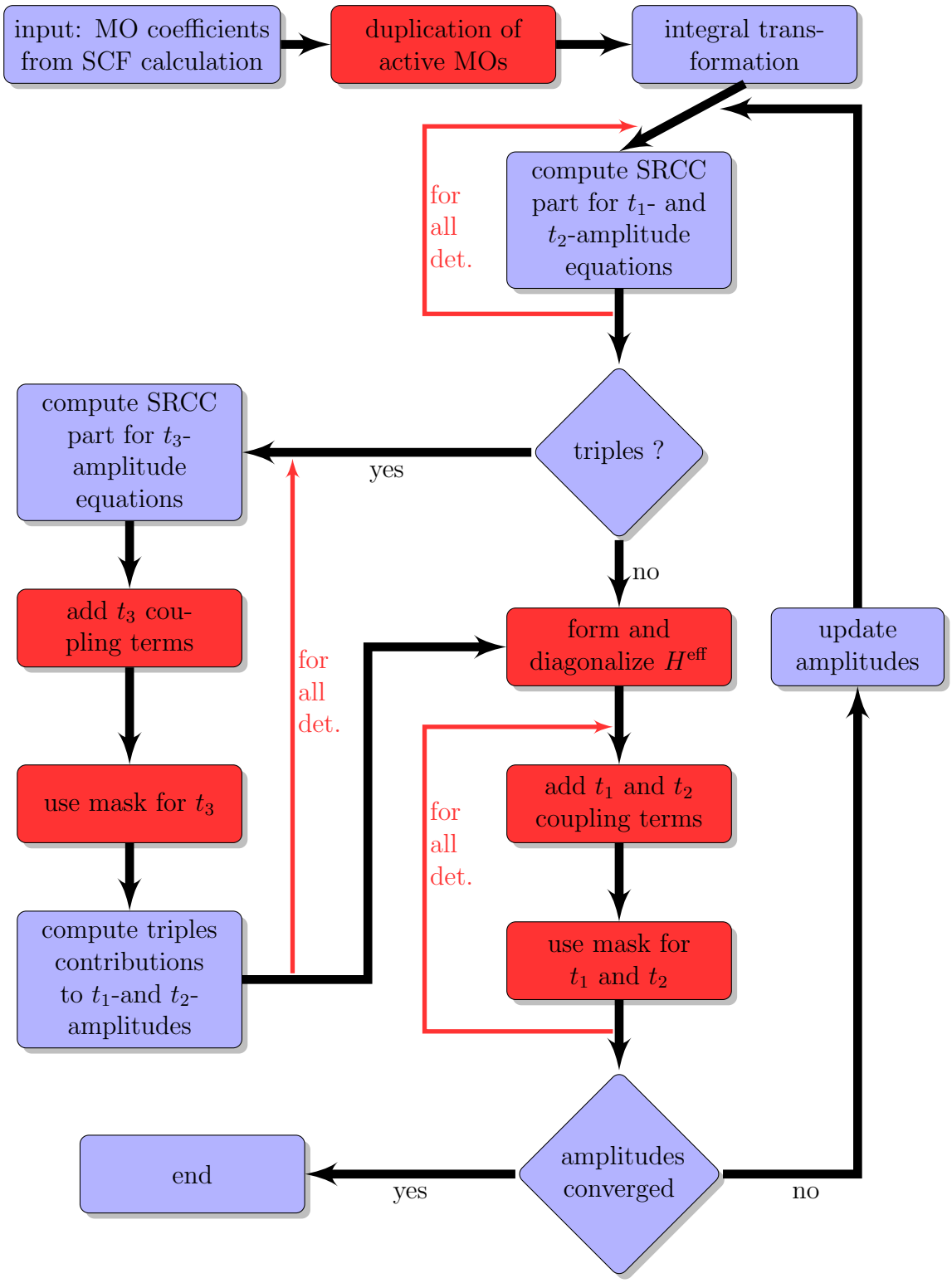

Figure 3.4: Flowchart of a Mk-MRCC energy computation in CFOUR. Only these steps are shown that need to be carried out after the underlying SCF calculation. Information in red denote steps that have been implemented in order to adapt the SRCC code.

4 Analytic First Derivatives for the Mk-MRCC Ansatz

The development of analytic derivative techniques for the coupled-cluster singles and doubles (CCSD) model,[79,81,88–91] CCSD with a perturbative treatment of triple excitations [CCSD(T)][84,92–96] and higher order CC models[87,97–100] offers the possibility of routinely locating minima and transition states on the potential energy surface of molecules and computing vibrational frequencies. However, analytic energy derivatives for multireference methods have been developed only for a few of the approaches proposed in the literature. Szalay and Bartlett implemented analytic gradients for the two-determinant CC method within the state-universal framework that is applicable to open-shell singlet states.[101] Fock space CC analytic gradients in an equation-of-motion (EOM) CC formulation have been developed by Stanton and Gauss.[102] Gradients for the spin-flip EOM-CC ansatz, which is able to describe open-shell singlet states starting from a triplet state reference, have been reported by Krylov and coworkers.[103] Analytic first derivatives have been also presented for active space CC methods using both Hartree-Fock and multi-configurational SCF reference functions.[99] Very recently, Pittner and Šmydke[75] presented a formulation of analytic gradients for the state-universal and the BW-MRCC approach[67,104,105] together with a pilot implementation within a FCI program.

In the following the theory of analytic gradients for the state-specific Mk-MRCC method is presented. Implementations within the Mk-MRCC singles and doubles (Mk-MRCCSD) and Mk-MRCC singles, doubles and triples (Mk-MRCCSDT) approximation based on the algorithm for Mk-MRCC energy computations presented in Chapter 3 are reported. The applicability of the gradient approach is demonstrated for Mk-MRCCSD by geometry optimizations for 2,6-pyridyne (C_5NH_3) and the 2,6-pyridynium cation ($C_5NH_4^+$) while for Mk-MRCCSDT investigations of the equilibrium structure of ozone (O_3), cyclobutadiene (C_4H_4) and a set of arynes, namely 2,6-pyridyne, the 2,6-pyridynium cation and *m*-benzyne (C_6H_4) are reported.

4.1 The Lagrangian of the Mk-MRCC Ansatz

To derive analytic expressions for derivatives of the Mk-MRCC energy with respect to an external perturbation χ, the Lagrangian technique[77,78,106] is used. The first step consists in constructing an appropriate energy functional using the technique of Lagrange multipliers. This functional, often referred to as Lagrangian, is in a second step made stationary with respect to all parameters involved. The expression for the energy gradient then takes a particularly simple form in which the only perturbed quantities involved are the integral derivatives.

For the Mk-MRCC approach, the energy functional $\tilde{E}$ is obtained by augmenting the energy E^α with the constraints for the eigenvalue problem [Eq. (2.79)] and the amplitude equations [Eq. (2.86)]. To these constraints correspond the Lagrange multipliers $\bar{c}^\alpha_\mu$ and $\lambda_q(\mu)$ yielding the following form for $\tilde{E}$:

$$\begin{aligned}\tilde{E} =& E^\alpha + \sum_\mu \bar{c}^\alpha_\mu \left[\sum_\nu H^{\text{eff}}_{\mu\nu} c^\alpha_\nu - E^\alpha c^\alpha_\mu \right] \\ &+ \sum_\mu \sum_{q\in Q(\mu)} \bar{c}^\alpha_\mu \lambda_q(\mu) \left[\left\langle \Phi_q(\mu) \middle| \bar{H}_\mu \middle| \Phi_\mu \right\rangle c^\alpha_\mu + \sum_{\nu(\neq\mu)} \left\langle \Phi_q(\mu) \middle| \hat{Y}^{\mu,\nu} \middle| \Phi_\mu \right\rangle H^{\text{eff}}_{\mu\nu} c^\alpha_\nu \right] .\end{aligned} \tag{4.1}$$

Note that $\bar{c}^\alpha_\mu$ is inserted here as a convenient prefactor in the Lagrange multipliers for the amplitude equations in order to simplify the subsequent expressions.

To eliminate E^α from Eq. (4.1) it is required that c^α_μ and the Lagrange multipliers $\bar{c}^\alpha_\mu$ satisfy the biorthonormality condition

$$\sum_\mu \bar{c}^\alpha_\mu c^\alpha_\mu = 1 , \tag{4.2}$$

where the fact has been exploited that the normalization of the eigenvector c^α_μ is not fixed by the eigenvalue problem in Eq. (2.79). Using Eq. (4.2) as a further constraint, the energy functional is written as

$$\begin{aligned}\tilde{E} =& \sum_{\mu\nu} \bar{c}^\alpha_\mu H^{\text{eff}}_{\mu\nu} c^\alpha_\nu + \sum_\mu \sum_{q\in Q(\mu)} \bar{c}^\alpha_\mu \lambda_q(\mu) \Bigg[\left\langle \Phi_q(\mu) \middle| \bar{H}_\mu \middle| \Phi_\mu \right\rangle c^\alpha_\mu \\ &+ \sum_{\nu(\neq\mu)} \left\langle \Phi_q(\mu) \middle| \hat{Y}^{\mu,\nu} \middle| \Phi_\mu \right\rangle H^{\text{eff}}_{\mu\nu} c^\alpha_\nu \Bigg] - \epsilon \left[\sum_\mu \bar{c}^\alpha_\mu c^\alpha_\mu - 1 \right] ,\end{aligned} \tag{4.3}$$

where ϵ is the Lagrange multiplier for the biorthonormality condition, Eq. (4.2).

It should be noted that Pittner and Šmydke[75] presented a Lagrangian for the BW-MRCC approach. At a first glance their energy functional [Eq. (15) in Ref. 75] seems to be identical to the one given in Eq. (4.3), but there is a subtle difference. In BW-MRCC theory, the Lagrange multipliers $\bar{c}_\mu^\alpha$ are simply the coefficients of the left-hand eigenvector of the effective Hamiltonian $H_{\mu\nu}^{\text{eff}}$, while this is not the case for the Mk-MRCC method. The reason is the dependence of the amplitude equations, Eq. (2.86), on the coefficients c_μ^α which renders an explicit determination of the corresponding Lagrange multipliers necessary.

4.2 Mk-MRCC Energy Gradient Expression

The Mk-MRCC energy functional, Eq. (4.3), can be written in a more compact form by introducing the deexcitation operator $\hat{\Lambda}_\mu$ and partitioning this operator into an external and an internal component via

$$\hat{\Lambda}_\mu = \hat{\Lambda}_\mu^{\text{ext}} + \hat{\Lambda}_\mu^{\text{int}} \ , \tag{4.4}$$

with

$$\hat{\Lambda}_\mu^{\text{ext}} = \sum_{q \in Q(\mu)} \hat{\tau}_q^+(\mu) \lambda_q(\mu) \ , \tag{4.5}$$

and[i]

$$\hat{\Lambda}_\mu^{\text{int}} = \sum_{\nu(\neq\mu)} \frac{\bar{c}_\nu^\alpha}{\bar{c}_\mu^\alpha} \left[1 + \sum_{q \in Q(\nu)} \lambda_q(\nu) \left\langle \Phi_q(\nu) \middle| \hat{Y}^{\nu,\mu} \middle| \Phi_\nu \right\rangle \right] |\Phi_\mu\rangle \langle\Phi_\nu| \ . \tag{4.6}$$

$\left\langle \Phi_q(\nu) \middle| \hat{Y}^{\nu,\mu} \middle| \Phi_\nu \right\rangle$ in Eq. (4.6) denotes the coupling terms from the amplitude equations [Eq. (2.86)]. Since the sum in Eq. (4.5) runs over all deexcitations except the internal ones, $\hat{\Lambda}_\mu^{\text{ext}}$ contains no internal deexcitations, i.e.,

$$\left\langle \Phi_\nu \middle| \hat{\Lambda}_\mu^{\text{ext}} \middle| \Phi_\mu \right\rangle = 0 \ , \tag{4.7}$$

[i] In Eq. (4.6) it is assumed that $\bar{c}_\mu^\alpha \neq 0$. When $\bar{c}_\mu^\alpha$ is close to zero, convergence problems may occur.

internal deexcitations are nevertheless introduced via $\hat{\Lambda}_\mu^{\mathrm{int}}$. With these definitions, the Mk-MRCC Lagrangian is recast as

$$\tilde{E} = \sum_\mu \bar{c}_\mu^\alpha \Big\langle \Phi_\mu \Big| (1 + \hat{\Lambda}_\mu) \bar{H}_\mu \Big| \Phi_\mu \Big\rangle c_\mu^\alpha - \epsilon \left[\sum_\mu \bar{c}_\mu^\alpha c_\mu^\alpha - 1 \right] . \tag{4.8}$$

The first derivative of the Mk-MRCC Lagrangian with respect to an external perturbation χ then takes the following form:

$$\frac{d\tilde{E}}{d\chi} = \sum_\mu \bar{c}_\mu^\alpha \left\langle \Phi_\mu \middle| \left(1 + \hat{\Lambda}_\mu\right) e^{-\hat{T}_\mu} \frac{d\hat{H}}{d\chi} e^{\hat{T}_\mu} \middle| \Phi_\mu \right\rangle c_\mu^\alpha . \tag{4.9}$$

In Eq. (4.9), stationarity of $\tilde{E}$ with respect to all wave function parameters (t-amplitudes and coefficients c_μ^α) and Lagrange multipliers (λ-amplitudes, $\bar{c}_\mu^\alpha$, and ϵ) has been assumed, as in this way the $2n+1$ and $2n+2$ rules[78] can be exploited to avoid the appearance of the corresponding derivatives in the gradient expression.

4.3 Lambda Equations and Lagrange Multipliers $\bar{c}_\mu^\alpha$ in the Mk-MRCC Approach

Invoking the stationary condition for the Mk-MRCC energy functional [Eq. (4.8)] with respect to the amplitudes $t_q(\mu)$ leads to the following set of equations

$$\begin{aligned} 0 &= \frac{\partial \tilde{E}}{\partial t_q(\mu)} \\ &= \bar{c}_\mu^\alpha \Big\langle \Phi_\mu \Big| \left(1 + \hat{\Lambda}_\mu\right) \left[\bar{H}_\mu, \hat{\tau}_q(\mu)\right] \Big| \Phi_\mu \Big\rangle c_\mu^\alpha + \sum_\nu \bar{c}_\nu^\alpha \Big\langle \Phi_\nu \Big| \frac{\partial \hat{\Lambda}_\nu^{\mathrm{int}}}{\partial t_q(\mu)} \bar{H}_\nu \Big| \Phi_\nu \Big\rangle c_\nu^\alpha . \end{aligned} \tag{4.10}$$

The first term in Eq. (4.10) (formally) corresponds to the single-reference lambda equations for determinant Φ_μ, with the only difference that the $\hat{\Lambda}_\mu$ operator is defined according to Eq. (4.4). The second term in Eq. (4.10) involves contributions due to the coupling between different reference determinants and is present only in MRCC theory.

Additional equations also arise from the stationarity of the Mk-MRCC energy functional with respect to the coefficients c_μ^α, a property that is not automatically guaranteed due to the dependence of the amplitude equations, Eq. (2.86), on the coefficients c_μ^α.

Differentiating Eq. (4.3) with respect to c_μ^α yields

$$\begin{aligned} 0 &= \frac{\partial \tilde{E}}{\partial c_\mu^\alpha} \\ &= \bar{c}_\mu^\alpha \left[H_{\mu\mu}^{\text{eff}} - E^\alpha - \sum_{q \in Q(\mu)} \lambda_q(\mu) \sum_{\nu(\neq\mu)} \left\langle \Phi_q(\mu) \middle| \hat{Y}^{\mu,\nu} \middle| \Phi_\mu \right\rangle H_{\mu\nu}^{\text{eff}} \frac{c_\nu^\alpha}{c_\mu^\alpha} \right] \\ &\quad + \sum_{\nu(\neq\mu)} \bar{c}_\nu^\alpha \left[H_{\nu\mu}^{\text{eff}} + \sum_{q \in Q(\nu)} \lambda_q(\nu) \left\langle \Phi_q(\nu) \middle| \hat{Y}^{\nu,\mu} \middle| \Phi_\nu \right\rangle H_{\nu\mu}^{\text{eff}} \right] , \end{aligned} \tag{4.11}$$

where the fact that the Lagrange multiplier ϵ can be identified with E^α,[ii] and Eq. (2.86) have been used to eliminate $\left\langle \Phi_q(\mu) \middle| \bar{H}_\mu \middle| \Phi_\mu \right\rangle$.

At this point it becomes obvious why the Lagrange multiplier $\bar{c}_\mu^\alpha$ has to be introduced in Eq. (4.1). For the BW-MRCC approach, where the amplitude equations do not depend on c_μ^α, the corresponding equation is simply the left-hand eigenvalue analog of Eq. (2.79), with $\bar{c}_\mu^\alpha$ representing elements of the left-hand eigenvector. However, for the general case this is not true, and $\bar{c}_\mu^\alpha$ must be identified as a "true" Lagrange multiplier. In summary, Eq. (4.11) represents a linear system of the form

$$\sum_\nu \bar{c}_\nu^\alpha M_{\nu\mu} = 0 \ , \tag{4.12}$$

where the elements of the matrix $\mathbf{M}$ are defined as

$$M_{\mu\mu} = H_{\mu\mu}^{\text{eff}} - E^\alpha - \sum_q \lambda_q(\mu) \sum_{\nu(\neq\mu)} \left\langle \Phi_q(\mu) \middle| \hat{Y}^{\mu,\nu} \middle| \Phi_\mu \right\rangle H_{\mu\nu}^{\text{eff}} \frac{c_\nu^\alpha}{c_\mu^\alpha} \ , \tag{4.13}$$

$$M_{\mu\nu} = H_{\mu\nu}^{\text{eff}} + \sum_q \lambda_q(\nu) \left\langle \Phi_q(\nu) \middle| \hat{Y}^{\nu,\mu} \middle| \Phi_\nu \right\rangle H_{\nu\mu}^{\text{eff}} \ . \tag{4.14}$$

To prove that the matrix $\mathbf{M}$ has a zero eigenvalue, in a first step Eq. (4.12) can be multiplied from the right by c_μ^α and be summed over μ,

$$\sum_{\nu\mu} \bar{c}_\nu^\alpha M_{\nu\mu} c_\mu^\alpha = 0 \ . \tag{4.15}$$

[ii] This is easily seen by differentiating $\tilde{E}$ with respect to $\bar{c}_\mu^\alpha$ which leads to $\sum_\mu H_{\mu\nu}^{\text{eff}} c_\nu^\alpha = \epsilon c_\mu^\alpha$.

Using the biorthonormality condition [Eq. (4.2)] yields the relation

$$\sum_{\nu\mu} \bar{c}_\mu^\alpha H_{\nu\mu}^{\text{eff}} c_\mu^\alpha = E \sum_\mu \bar{c}_\mu^\alpha c_\mu^\alpha = E \ . \tag{4.16}$$

Together with the fact that the vectors $\bar{c}_\mu^\alpha$ and c_μ^α are biorthonormal and, thus, $\bar{c}_\mu^\alpha c_\nu^\alpha = 0$, it can be shown that Eq. (4.12) has a non-trivial solution which provides the required values for the Lagrange multipliers $\bar{c}_\mu^\alpha$.

4.4 Density-Matrix Based Formulation of Mk-MRCC Gradients

For the evaluation of Eq. (4.9) it is computationally advantageous to use a density-matrix based approach.[83,89] To exploit such an ansatz in the case of Mk-MRCC gradients, the Hamiltonian is specified for each reference determinant Φ_μ in second quantization

$$\hat{H} = H_{\mu\mu} + \sum_{pq} f_{pq}(\mu) \{a_p^\dagger a_q\}_\mu + \frac{1}{4} \sum_{pqrs} \langle pq||rs\rangle \, \{a_p^\dagger a_q^\dagger a_s a_r\}_\mu \ , \tag{4.17}$$

where the strings $\{a_p^\dagger a_q\}_\mu$ and $\{a_p^\dagger a_q^\dagger a_s a_r\}_\mu$ denote normal-ordered sequences [iii] of creation $(a_p^\dagger, a_q^\dagger)$ and annihilation (a_r, a_s) operators defined with respect to Φ_μ as Fermi vacuum. $H_{\mu\mu}$ in Eq. (4.17) is the diagonal contribution to the Hamiltonian due to the reference determinant and the Fock-matrix elements $f_{pq}(\mu)$ are defined as

$$f_{pq}(\mu) = h_{pq} + \sum_k^{\text{occ}(\mu)} \langle pk||qk\rangle \ , \tag{4.18}$$

with the sum running over all spin-orbitals that are occupied in Φ_μ.

Inserting Eq. (4.17) into Eq. (4.9), the energy gradient is rewritten as

$$\frac{d\tilde{E}}{d\chi} = \sum_\mu \bar{c}_\mu^\alpha \left[\sum_{pq} D_{pq}(\mu) \frac{d\, f_{pq}(\mu)}{d\chi} + \sum_{pqrs} \Gamma_{pqrs}(\mu) \frac{d\, \langle pq||rs\rangle}{d\chi} \right] c_\mu^\alpha \ , \tag{4.19}$$

[iii] Normal-ordering of creation and annihilation operators with respect to a single Slater determinant reference function means that all annihilation operators are located to the right of all creation operators within the particle-hole formalism. In this formalism normal ordering is not defined relative to a vacuum state but rather relative to a reference state Φ. The one-electron states occupied in Φ are called "hole" states while those unoccupied in the reference are referred to as "particle" states. For a complete discussion of normal ordering within coupled-cluster theory see Ref. 2.

with the one- and two-particle density matrices $D_{pq}(\mu)$ and $\Gamma_{pqrs}(\mu)$ containing contributions due to the response of the t-amplitudes and the reference determinant,

$$D_{pq}(\mu) = D_{pq}^{\mathrm{CC}}(\mu) + D_{pq}^{\mathrm{ref}}(\mu) \tag{4.20}$$

$$\Gamma_{pqrs}(\mu) = \Gamma_{pqrs}^{\mathrm{CC}}(\mu) + \Gamma_{pqrs}^{\mathrm{ref}}(\mu) \ . \tag{4.21}$$

The contributions due to the amplitude response, i.e., $D_{pq}^{\mathrm{CC}}(\mu)$ and $\Gamma_{pqrs}^{\mathrm{CC}}(\mu)$, are

$$D_{pq}^{\mathrm{CC}}(\mu) = \left\langle \Phi_\mu \middle| \left(1 + \hat{\Lambda}_\mu\right) e^{-\hat{T}_\mu} \left\{a_p^\dagger a_q\right\}_\mu e^{\hat{T}_\mu} \middle| \Phi_\mu \right\rangle \tag{4.22}$$

$$\Gamma_{pqrs}^{\mathrm{CC}}(\mu) = \frac{1}{4} \left\langle \Phi_\mu \middle| \left(1 + \hat{\Lambda}_\mu\right) e^{-\hat{T}_\mu} \left\{a_p^\dagger a_q^\dagger a_s a_r\right\}_\mu e^{\hat{T}_\mu} \middle| \Phi_\mu \right\rangle \ , \tag{4.23}$$

while the contributions $D_{pq}^{\mathrm{ref}}(\mu)$ and $\Gamma_{pqrs}^{\mathrm{ref}}(\mu)$ are the standard one- and two-particle contribution for a single Slater determinant Φ_μ.[10] It should be noted that with the modified $\hat{\Lambda}_\mu$ operator defined in Eq. (4.4) the expressions for the density matrices given above are the same as in single-reference CC theory.

In a further step the integral derivatives appearing in Eq. (4.19) may be decomposed into a pure atomic-orbital (AO) integral and an orbital-relaxation contribution. For this purpose, the derivatives of the AO one- and two-electron integrals rotated into the MO basis are denoted with h_{pq}^χ and $\langle pq||rs\rangle^\chi$. Then the derivatives of the MO coefficient $c_{\mu p}$ are parametrized via[80]

$$\frac{\partial c_{\mu p}}{\partial \chi} = \sum_q U_{qp}^\chi c_{\mu q} \ . \tag{4.24}$$

In addition, the Fock-matrix derivative $f_{pq}^{(\chi)}(\mu)$,

$$f_{pq}^{(\chi)}(\mu) = h_{pq}^\chi + \sum_k^{\mathrm{occ}(\mu)} \langle pk||qk\rangle^\chi \ , \tag{4.25}$$

is introduced which does not contain contributions due to the derivatives of the MO coefficients $c_{\mu p}$. Eq. (4.19) is then rewritten as

$$\frac{d\tilde{E}}{d\chi} = \sum_\mu \bar{c}_\mu^\alpha \left[\sum_{pq} D_{pq}(\mu) f_{pq}^{(\chi)}(\mu) + \sum_{pqrs} \Gamma_{pqrs}(\mu) \langle pq||rs\rangle^\chi - 2 \sum_{pq} I'_{pq}(\mu) U_{pq}^\chi \right] c_\mu^\alpha \ . \tag{4.26}$$

The last term in Eq. (4.26) arises from the orbital response with the one-particle intermediate $I'_{pq}(\mu)$ defined by[84]

$$\begin{aligned} I'_{pq}(\mu) = -\frac{1}{2}\Bigg\{ & \sum_{r} f_{pr}(\mu)\Big[D_{rq}(\mu) + D_{qr}(\mu)\Big] \\ & + \sum_{rst} \Big[\langle pr||st\rangle\, \Gamma_{qrst}(\mu) + \langle rp||st\rangle\, \Gamma_{rqst}(\mu) + \langle rs||pt\rangle\, \Gamma_{rsqt}(\mu) \\ & + \langle rs||tp\rangle\, \Gamma_{rstq}(\mu)\Big]\Bigg\} - \sum_{rs} \langle pr||qs\rangle\, D_{rs}(\mu)\delta_{qi}(\mu)\ , \end{aligned} \tag{4.27}$$

where

$$\delta_{qi}(\mu) = \begin{cases} 1 & \text{if } q \in \mathrm{occ}(\mu) \\ 0 & \text{otherwise} \end{cases}\ . \tag{4.28}$$

To avoid explicit determination of the coefficients U^{χ}_{pq}, the last term in Eq. (4.26) is usually reformulated using the Z-vector method by Handy and Schaefer.[82] The final expression for the Mk-MRCC gradient is then given in the AO representation as

$$\frac{d\tilde{E}}{d\chi} = \sum_{\mu} \bar{c}^{\alpha}_{\mu} \left[\sum_{\rho\sigma}^{\mathrm{AO}} D_{\rho\sigma}(\mu) f^{(\chi)}_{\rho\sigma}(\mu) + \sum_{\rho\sigma\tau\upsilon}^{\mathrm{AO}} \Gamma_{\rho\sigma\tau\upsilon}(\mu)\, \langle \rho\sigma||\tau\upsilon\rangle^{\chi} + \sum_{\rho\sigma}^{\mathrm{AO}} I_{\rho\sigma}(\mu) S^{\chi}_{\rho\sigma} \right] c^{\alpha}_{\mu}\ , \tag{4.29}$$

with S^{χ}_{pq} as the derivative of the AO overlap matrix transformed into the MO basis. Note that $D_{\rho\sigma}(\mu)$ represents here the relaxed one-particle density matrix and contains contributions due to orbital relaxation, i.e., all terms arising from the derivatives of the MO coefficients except the ones that belong to AO derivatives of the overlap matrix $S^{\chi}_{\rho\sigma}$, while $I_{\rho\sigma}(\mu)$, which is related but not identical to $I'_{pq}(\mu)$, represents elements of a generalized energy-weighted density matrix. The exact definitions of these quantities depend on the actual choice of the reference function. An appropriate discussion for the case of reference determinants constructed from Hartree-Fock (HF) orbitals can be found in Ref. 84, while the use of multi-configurational self-consistent-field orbitals has been considered in detail in Refs. 85 and 86. As the main focus of this work lies on the use of HF references, explicit expressions for $I_{\rho\sigma}(\mu)$ are provided in the Appendix for this case.

4.5 The Mk-MRCCSD approximation

In the singles and doubles approximation, the cluster operator of Eq. (2.69) is given by

$$\hat{T}_\mu = \hat{T}_1^\mu + \hat{T}_2^\mu \ , \tag{4.30}$$

and the amplitude equations can be written as

$$\left\langle \Phi_i^a(\mu) \middle| \bar{H}_\mu \middle| \Phi_\mu \right\rangle c_\mu^\alpha + \sum_{\nu(\neq\mu)} \left\langle \Phi_i^a(\mu) \middle| \hat{Y}^{\mu,\nu} \middle| \Phi_\mu \right\rangle H_{\mu\nu}^{\text{eff}} c_\nu^\alpha = 0 \ , \tag{4.31}$$

for single and

$$\left\langle \Phi_{ij}^{ab}(\mu) \middle| \bar{H}_\mu \middle| \Phi_\mu \right\rangle c_\mu^\alpha + \sum_{\nu(\neq\mu)} \left\langle \Phi_{ij}^{ab}(\mu) \middle| \hat{Y}^{\mu,\nu} \middle| \Phi_\mu \right\rangle H_{\mu\nu}^{\text{eff}} c_\nu^\alpha = 0 \ , \tag{4.32}$$

for double excitations, respectively. The coupling terms are the ones from Eqs. (2.88) and (2.89). The corresponding lambda equations have the form

$$\bar{c}_\mu^\alpha \left\langle \Phi_\mu \right| \left[1 + \hat{\Lambda}_\mu\right] \left[\bar{H}_\mu, \hat{\tau}_i^a(\mu)\right] \left| \Phi_\mu \right\rangle c_\mu^\alpha + \sum_\nu \bar{c}_\nu^\alpha \left\langle \Phi_\nu \right| \frac{\partial \hat{\Lambda}_\nu^{\text{int}}}{\partial t_i^a(\mu)} \bar{H}_\nu \left| \Phi_\nu \right\rangle c_\nu^\alpha = 0, \tag{4.33}$$

$$\bar{c}_\mu^\alpha \left\langle \Phi_\mu \right| \left[1 + \hat{\Lambda}_\mu\right] \left[\bar{H}_\mu, \hat{\tau}_{ij}^{ab}(\mu)\right] \left| \Phi_\mu \right\rangle c_\mu^\alpha + \sum_\nu \bar{c}_\nu^\alpha \left\langle \Phi_\nu \right| \frac{\partial \hat{\Lambda}_\nu^{\text{int}}}{\partial t_{ij}^{ab}(\mu)} \bar{H}_\nu \left| \Phi_\nu \right\rangle c_\nu^\alpha = 0 \ . \tag{4.34}$$

To derive expressions for the last term in Eqs. (4.33) and (4.34), $\hat{\Lambda}_\nu^{\text{int}}$ needs to be differentiated with respect to $t_i^a(\mu)$ and $t_{ij}^{ab}(\mu)$, which can be done using Eqs. (4.6), (2.88), and (2.89). This yields

$$\begin{aligned}
&\sum_\nu \bar{c}_\nu^\alpha \left\langle \Phi_\nu \right| \frac{\partial \hat{\Lambda}_\nu^{\text{int}}}{\partial t_i^a(\mu)} \bar{H}_\nu \left| \Phi_\nu \right\rangle c_\nu^\alpha \\
&= \bar{c}_\mu^\alpha \sum_{\nu(\neq\mu)} \Bigg[- \lambda_a^i(\mu) + \sum_{n,f} \lambda_{af}^{in}(\mu) t_n^f(\mu) - \sum_{n,f} \lambda_{af}^{in}(\mu) t_n^f(\nu/\mu) \Bigg] H_{\mu\nu}^{\text{eff}} \frac{c_\nu^\alpha}{c_\mu^\alpha} c_\mu^\alpha \\
&\quad + \bar{c}_\mu^\alpha \sum_{\nu(\neq\mu)} \frac{\bar{c}_\nu^\alpha}{\bar{c}_\mu^\alpha} \Bigg[\lambda_a^i(\nu/\mu) - \sum_{n,f} \lambda_{af}^{in}(\nu) t_n^f(\nu) + \sum_{n,f} \lambda_{af}^{in}(\nu/\mu) t_n^f(\mu/\nu) \Bigg] H_{\nu\mu}^{\text{eff}} c_\mu^\alpha \\
&= \bar{c}_\mu^\alpha \sum_{\nu(\neq\mu)} \Bigg[- \lambda_a^i(\mu) H_{\mu\nu}^{\text{eff}} \frac{c_\nu^\alpha}{c_\mu^\alpha} + C_a^i(\mu,\nu) \Bigg] c_\mu^\alpha,
\end{aligned} \tag{4.35}$$

and

$$\begin{aligned}
&\sum_{\nu} \bar{c}_{\nu}^{\alpha} \left\langle \Phi_{\nu} \middle| \frac{\partial \hat{\Lambda}_{\nu}^{\mathrm{int}}}{\partial t_{ij}^{ab}(\mu)} \bar{H}_{\nu} \middle| \Phi_{\nu} \right\rangle c_{\nu}^{\alpha} \\
&= \bar{c}_{\mu}^{\alpha} \sum_{\nu(\neq\mu)} \left[-\lambda_{ab}^{ij}(\mu) H_{\mu\nu}^{\mathrm{eff}} \frac{c_{\nu}^{\alpha}}{c_{\mu}^{\alpha}} + \frac{\bar{c}_{\nu}^{\alpha}}{\bar{c}_{\mu}^{\alpha}} \lambda_{ab}^{ij}(\nu/\mu) H_{\nu\mu}^{\mathrm{eff}} \right] c_{\mu}^{\alpha} \ ,
\end{aligned} \tag{4.36}$$

with

$$\begin{aligned}
C_{a}^{i}(\mu,\nu) = &\left[\sum_{n,f} \lambda_{af}^{in}(\mu) t_{n}^{f}(\mu) - \sum_{n,f} \lambda_{af}^{in}(\mu) t_{n}^{f}(\nu/\mu) \right] H_{\mu\nu}^{\mathrm{eff}} \frac{c_{\nu}^{\alpha}}{c_{\mu}^{\alpha}} \\
&+ \frac{\bar{c}_{\nu}^{\alpha}}{\bar{c}_{\mu}^{\alpha}} \left[\lambda_{a}^{i}(\nu/\mu) - \sum_{n,f} \lambda_{af}^{in}(\nu) t_{n}^{f}(\nu) + \sum_{n,f} \lambda_{af}^{in}(\nu/\mu) t_{n}^{f}(\mu/\nu) \right] H_{\nu\mu}^{\mathrm{eff}} \ .
\end{aligned} \tag{4.37}$$

In these formulas the common lambda amplitudes

$$\lambda_{ab\ldots}^{ij\ldots}(\nu/\mu) = \begin{cases} \lambda_{ab\ldots}^{ij\ldots}(\nu) & \text{if } i,j\ldots \in \mathrm{occ}(\mu) \text{ and } \mathrm{occ}(\nu) \\ & \text{and } a,b\ldots \in \mathrm{vir}(\mu) \text{ and } \mathrm{vir}(\nu) \\ 0 & \text{else,} \end{cases} \tag{4.38}$$

are defined in analogy to the common amplitudes $t_{ij\ldots}^{ab\ldots}(\nu/\mu)$.

Using Eqs. (4.35) and (4.36) the Mk-MRCCSD lambda equations (4.10) may be written in a suitable form for implementation,

$$\lambda_{a}^{i}(\mu) D_{i}^{a}(\mu) = S_{a}^{i}(\mu) + \sum_{\nu(\neq\mu)} C_{a}^{i}(\mu,\nu) \tag{4.39}$$

and

$$\lambda_{ab}^{ij}(\mu) D_{ij}^{ab}(\mu) = S_{ab}^{ij}(\mu) + \sum_{\nu(\neq\mu)} \frac{\bar{c}_{\nu}^{\alpha}}{\bar{c}_{\mu}^{\alpha}} \lambda_{ab}^{ij}(\nu/\mu) H_{\nu\mu}^{\mathrm{eff}} \ , \tag{4.40}$$

with

$$S_{a}^{i}(\mu) = \left\langle \Phi_{\mu} \middle| \left[1 + \hat{\Lambda}_{\mu} \right] \left[\bar{H}_{\mu}, \hat{\tau}_{i}^{a}(\mu) \right] \middle| \Phi_{\mu} \right\rangle + \lambda_{a}^{i}(\mu) \left[f_{ii}(\mu) - f_{aa}(\mu) \right] \tag{4.41}$$

$$\begin{aligned}
S_{ab}^{ij}(\mu) = &\left\langle \Phi_{\mu} \middle| \left[1 + \hat{\Lambda}_{\mu} \right] \left[\bar{H}_{\mu}, \hat{\tau}_{ij}^{ab}(\mu) \right] \middle| \Phi_{\mu} \right\rangle \\
&+ \lambda_{ab}^{ij}(\mu) \left[f_{ii}(\mu) + f_{jj}(\mu) - f_{aa}(\mu) - f_{bb}(\mu) \right] \ .
\end{aligned} \tag{4.42}$$

Here the contributions arising from the diagonal part of the Fock matrix have been separated out. The denominator arrays $D_{ij\ldots}^{ab\cdots}(\mu)$ are given by

$$D_i^a(\mu) = f_{ii}(\mu) - f_{aa}(\mu) + E^\alpha - H_{\mu\mu}^{\text{eff}} \tag{4.43}$$

$$D_{ij}^{ab}(\mu) = f_{ii}(\mu) + f_{jj}(\mu) - f_{aa}(\mu) - f_{bb}(\mu) + E^\alpha - H_{\mu\mu}^{\text{eff}} \,, \tag{4.44}$$

with the Fock-matrix elements $f_{pq}(\mu)$ defined with respect to Φ_μ as the Fermi vacuum [Eq. (4.18)].

4.5.1 Implementation

Based on the expressions given in the previous section, analytic Mk-MRCCSD energy gradients have been implemented in the quantum-chemical program package CFOUR[49] as depicted schematically in Fig. 4.1. As this represents the first step towards a complete multireference CC treatment in the computation of analytic gradients, only the use of two closed-shell reference determinants and restricted Hartree-Fock (RHF) orbitals is discussed in this section. The extension to orbitals obtained for example from a TC-SCF calculation will be discussed in the next section. The utilization of RHF orbitals in selected MRCC applications may be justified by the well-known insensitivity of CC theory to the choice of orbitals[3] and the fact that orbital relaxation effects are treated efficiently in CC theory via single excitations.[3,107] The implementation has a formal scaling of $d \cdot n_o^2 n_v^4$ suitable for large-scale calculations.

In addition to the solution of the amplitude equations [Eq. (2.86)] and the eigenvalue problem in Eq. (2.79), Mk-MRCC gradient calculations require the solution of the lambda equations [Eq. (4.10)] and of the equations for the Lagrange multipliers $\bar{c}_\mu^\alpha$ [Eq. (4.12)]. As the latter two sets of equations depend on each other, they have to be solved simultaneously. The lambda equations have been implemented in a similar way as the amplitude equations with a contribution given in terms of the usual single-reference part and an additional coupling term. The existing CCSD gradient code in CFOUR has been exploited for this purpose using the same strategy as in the case of the amplitude equations. The equations for the Lagrange multipliers $\bar{c}_\mu^\alpha$ are solved by diagonalizing the matrix $\mathbf{M}$ and picking the left-hand eigenvector that corresponds to the zero eigenvalue.

For the density matrices the situation is even simpler, as the corresponding expressions take the same form as those in the single-reference case,[81] so that the code could be used without modification. Again, it is only necessary to loop over the reference

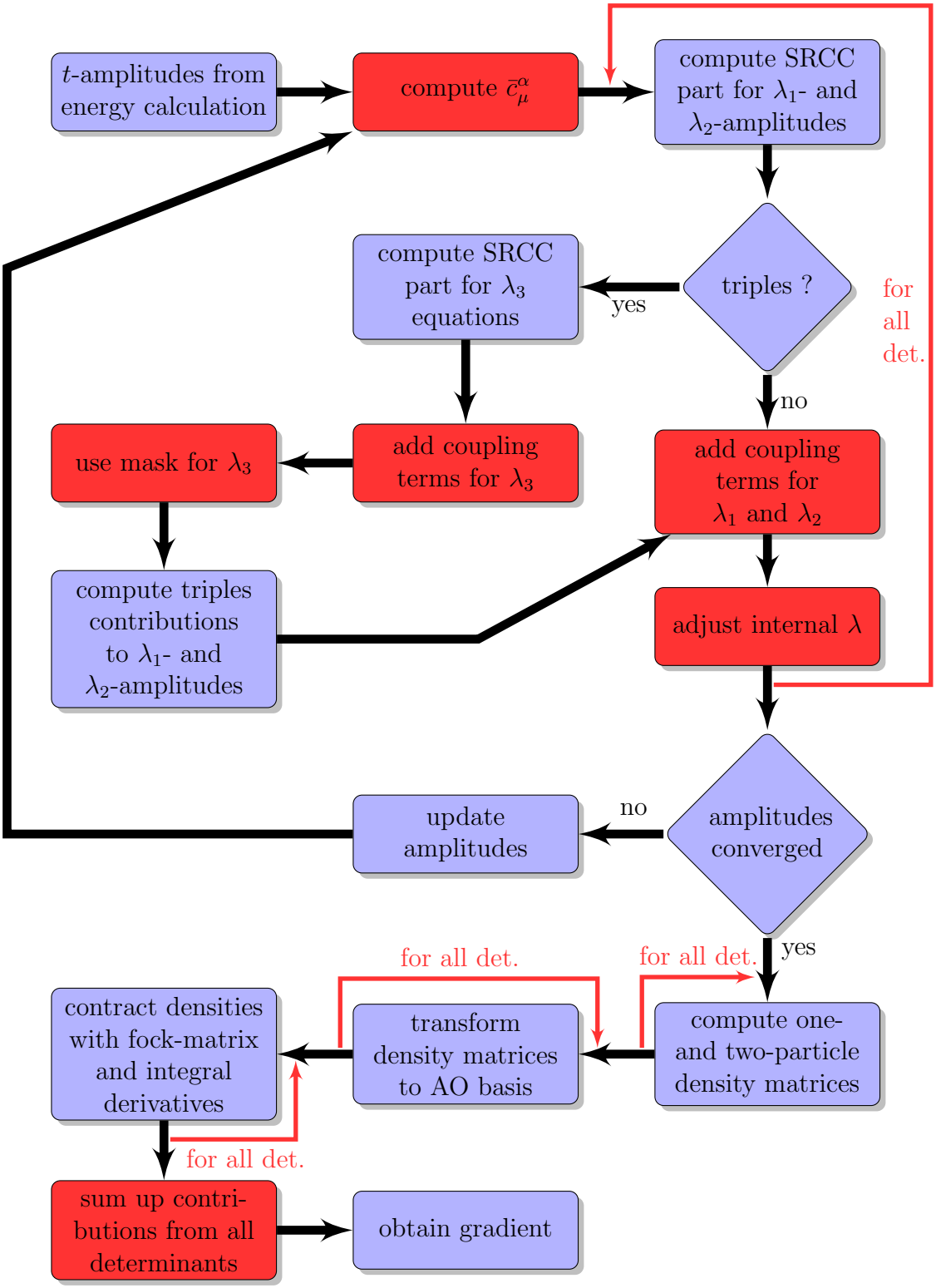

Figure 4.1: Flowchart of a Mk-MRCC gradient computation in CFOUR. Only those steps are shown that need to be carried out after the corresponding Mk-MRCC energy calculation (see Fig. 3.4). Information in red denote steps that have been implemented in order to adapt the SRCC code.

determinants. Back transformation of the density matrices to the AO basis and the contraction with the AO integral derivatives are also carried out as in the single-reference case.

For calculations based on HF orbitals, orbital relaxation can be treated by the Z-vector method as described in Ref. 81. It is only noted that the full orbital invariance of single-reference CC theory, i.e., invariance with respect to rotations within the occupied and virtual orbital space as provided by the HF wave function, cannot be exploited in the case of Mk-MRCC gradients. To circumvent this problem, the gradient calculations are always based on perturbed canonical orbitals,[93,94] i.e., those perturbed orbitals are chosen that diagonalize the first derivative of the Fock matrix. With this choice it is necessary to calculate only the diagonal elements of the occupied-occupied and virtual-virtual block of the density matrix $D_{pq}(\mu)$ in Eq. (4.26) while the off-diagonal elements are calculated as part of the orbital-relaxation contribution.

The implementation of analytic Mk-MRCCSD gradients has been checked by comparing analytically evaluated dipole moments and forces with the corresponding first derivatives obtained using finite-difference techniques. The order of magnitude of the maximum error observed is 10^{-10} a.u. for dipole moments and 10^{-7} a.u. for forces corresponding to the maximum accuracy that could be obtained from numerical differentiation.

4.5.2 Illustrative Examples for Mk-MRCCSD Gradients

The applicability of the analytic Mk-MRCCSD gradient approach is demonstrated by investigating the equilibrium geometry of the 2,6-isomers of the didehydropyridinium (pyridynium) cation and didehydropyridine (pyridyne). This choice of examples has been motivated by the fact that the chemically interesting didehydroarenes (arynes)[21,27,108,109] exhibit a strong biradical character and that their theoretical treatment remains a challenge until today. For the treatment of these degenerate systems, multireference approaches are the natural choice, but the application of these methods is not always straightforward, as the different choice of active orbitals indicate,[110,111] and is often hampered by the size of the systems to be investigated.[110–117] Furthermore, these methods do not necessarily provide conclusive results when for example considering the deviation of the computed energy splitting of *o*- and *p*-benzyne from experiment.[110,111] Attempts have been also undertaken to use high-level single-reference CC methods[118,119] for the investigation of arynes with an emphasis on the use of symmetry-broken unrestricted

reference determinants as a pragmatic solution to the multireference problem in CC theory.[22,120] Another option within CC theory is the treatment by means of the spin-flip equation-of-motion method.[121] Furthermore, several studies can be found in the literature which employ density-functional theory for the computational investigation of arynes.[30,122–126] The benzyne systems have been recently investigated using multireference CC methods in order to demonstrate the usefulness of the developed and implemented Mk-MRCC schemes.[22]

The focus in the following will be on biradicals derived from pyridine, namely pyridyne and protonated pyridyne. In this work the focus lies on the corresponding 2,6-isomers. Due to their large number of degrees of freedom, pyridynes can be considered as good examples to illustrate the use of analytic gradient techniques, as geometry optimization based on single-point energy calculations would be very computationally demanding.

A particularly intriguing aspect of *meta*-arynes, as already mentioned in the introduction, is the possibility that they may exist as monocyclic or bicyclic compounds. While for *meta*-benzyne the bicyclic structure is understood to be an artifact displayed at various levels of theory,[127] the issue has not been settled in the case of the didehydrocompounds of heteroarenes and will be investigated in the following for 2,6-pyridyne and the 2,6-pyridynium cation.

For both examples, two closed-shell determinants are used as reference with the orbitals taken from RHF calculations. The first, Φ_1, corresponds to the HF solution, while the second, Φ_2, is obtained by replacing the highest-occupied MO (HOMO) in the monocyclic form (a_1 symmetry) by the lowest unoccupied MO (LUMO) (b_2 symmetry). The active orbitals are depicted in Fig. 4.2. In all calculations, C_{2v} symmetry has been imposed. The correlation-consistent, core-valence polarized basis sets cc-pCVXZ (X = D,T) of Woon and Dunning were used in all computations.[128] The transition states have been located using the transition state search scheme as implemented in CFOUR.[49]

4.5.2.1 2,6-Pyridynium Cation ($C_5NH_4^+$)

All calculations, except those at the HF-SCF level, yield for the 2,6-pyridynium cation a monocyclic structure, which is depicted in Fig. 4.3.

The multireference character of the 2,6-isomer of the pyridynium cation is clearly seen from the expansion coefficients obtained in the Mk-MRCC calculations. The corresponding values are 0.91 for c_1 and -0.41 for c_2 (Mk-MRCCSD/cc-pCVTZ calculation employing the reference determinants as described before) which means that the relative

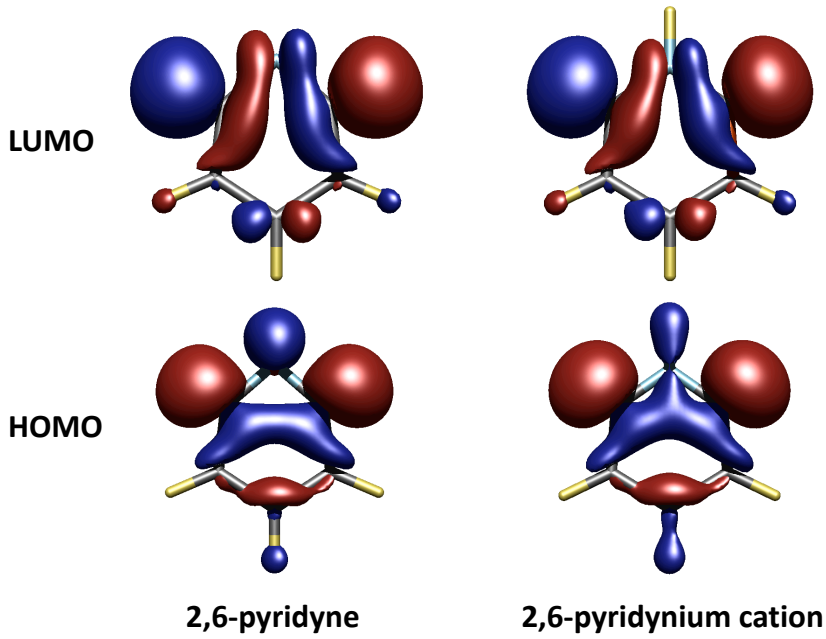

Figure 4.2: The active orbitals of 2,6-pyridyne and the 2,6-pyridynium cation chosen for the Mk-MRCC computations. The orbitals have been obtained in a RHF/cc-pCVTZ calculation using the Mk-MRCCSD/cc-pCVTZ geometry.

contributions (c_1^2 and c_2^2, respectively) of the two reference functions are about 83 and 17%.

The optimized geometries obtained from Mk-MRCCSD calculations using the cc-pCVDZ and cc-pCVTZ basis sets are reported in Tables 4.1 and 4.2 together with results from single-reference approaches. While the HF-SCF approach leads, as already mentioned, to a bicyclic structure (1.4959 Å for the C_2C_6 distance), this artifact is already corrected at the TCSCF level, which yields a monocyclic structure with a long C_2C_6 distance of 2.2299 Å. The same is also observed in all electron-correlated calculations, which for this reason, do not differ dramatically in the obtained geometrical structures. Still, some differences are noted, and in Fig. 4.3 as additional information the C_2C_6 distance as obtained in the various CC calculations is provided. This distance, together with the $C_2N_1C_6$ angle, is a good indicator for the adequacy of the description of the multireference character. From the values in Table 4.1 it is obvious that the single-reference CCSD calculations are far from converged with respect to the electron-correlation treatment. The change in the C_2C_6 distance due to triple excitations is

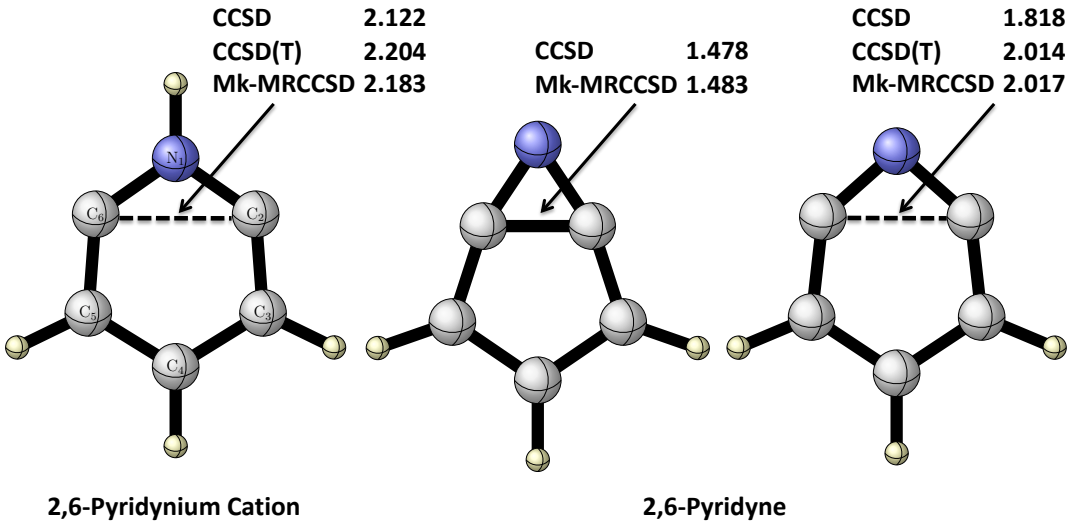

Figure 4.3: Optimized structures for 2,6-pyridyne and the 2,6-pyridynium cation computed at the CCSD, CCSD(T) and Mk-MRCCSD levels of theory using the cc-pCVTZ basis set. For 2,6-pyridyne both the monocyclic and bicyclic forms are shown. The representative C_2C_6 bond distance is given in Å. RHF orbitals were used in all computations.

rather pronounced and thus renders the CCSD results questionable. On the other hand, the magnitude of the triples corrections also sheds some doubts on the quality of the CCSD(T) calculations. Clearly, single-reference CC approaches are not able to provide a reliable description of the equilibrium geometry for the 2,6-pyridynium cation. The Mk-MRCCSD results can be considered more appropriate in this respect. Nevertheless, the geometrical parameters from this computation turn out to be close to those obtained at the CCSD(T) level. In addition to the standard single-reference CC results, Table 4.1 also lists those obtained from CC treatments based on a symmetry-broken unrestricted HF (UHF) determinant. It is noted that these CC calculations predict a monocyclic structure, though the angle at the radical centers is somewhat wider. It is impossible to rigorously judge the reliability of these symmetry-broken CC calculations, as long as no reliable benchmark data are available. However, from a computational point of view, symmetry-broken CC calculations are significantly more expensive than the present Mk-MRCC calculations. Furthermore, they are seriously affected by spin contamination ($\langle S^2 \rangle = 1.028$ at the CCSD/cc-pCVDZ level), thus making them less

Table 4.1: Geometrical parameters for the 2,6-isomer of the pyridynium cation ($C_5NH_4^+$) as computed at various levels of theory using the cc-pCVDZ basis set. CCSD* and CCSD(T)* indicate results obtained using a symmetry-broken UHF reference determinant.

	SCF	TCSCF	CCSD	CCSD*	CCSD(T)	CCSD(T)*	Mk-MRCCSD
bond lengths [Å]							
N_1C_2	1.2993	1.3287	1.3370	1.3454	1.3502	1.3500	1.3418
C_2C_3	1.3592	1.3587	1.3738	1.3776	1.3814	1.3815	1.3734
C_3C_4	1.4290	1.3979	1.4127	1.4124	1.4174	1.4174	1.4127
N_1H	1.0170	1.0060	1.0215	1.0232	1.0236	1.0248	1.0214
C_3H	1.0763	1.0796	1.0929	1.0923	1.0949	1.0944	1.0929
C_4H	1.0844	1.0820	1.0958	1.0953	1.0973	1.0972	1.0949
C_2C_6	1.4960	2.2299	2.1631	2.2755	2.2402	2.2723	2.2150
bond angles [°]							
$C_2N_1C_6$	70.29	114.09	107.99	115.49	112.12	114.62	111.26
$N_1C_2C_3$	164.11	126.75	130.81	125.64	127.65	126.15	128.43
$C_2C_3C_4$	103.90	116.67	117.30	116.96	117.72	117.18	117.43
$C_3C_4C_5$	113.69	119.07	115.79	119.32	117.14	118.72	117.02
C_2C_3H	128.65	120.47	119.78	120.64	119.84	120.44	120.01

reliable. Concerning the equilibrium geometries obtained at the DFT level, one significant disagreement is noted ($\measuredangle C_2N_1C_6 = 104.3°$ for B3LYP/cc-pVDZ[117] in comparison to 111.26 ° for Mk-MRCCSD/cc-pCVDZ).

Table 4.2 documents the optimized geometries obtained using the larger cc-pCVTZ basis set. The comparison between the CCSD, CCSD(T), and Mk-MRCCSD results lead to similar conclusions as for the cc-pCVDZ basis. The observed changes when going from cc-pCVDZ to cc-pCVTZ (e.g., CCSD: 1.45°, CCSD(T): 1.19°, and Mk-MRCCSD: 0.83° for the angle $C_2N_1C_6$) are rather typical for basis-set effects.

4.5.2.2 2,6-Pyridyne (C_5NH_3)

In order to investigate the equilibrium geometry of 2,6-pyridyne, the geometry has been optimized at the HF-SCF, CCSD, CCSD(T), and Mk-MRCCSD level using the cc-pCVDZ and cc-pCVTZ basis set starting from a small (about 1.1 Å) and a large C_2C_6 distance (about 2.2 Å) to locate stationary points corresponding to a monocyclic and a bicyclic structure (see Fig. 4.3 and Tables 4.3 and 4.4). The results are visualized

Table 4.2: Geometrical parameters for the 2,6-isomer of the pyridynium cation ($C_5NH_4^+$) as obtained at the CCSD, CCSD(T) and Mk-MRCCSD levels of theory using the cc-pCVTZ basis set.

	CCSD	CCSD(T)	Mk-MRCCSD
bond lengths [Å]			
N_1C_2	1.3235	1.3375	1.3292
C_2C_3	1.3570	1.3647	1.3568
C_3C_4	1.3994	1.4041	1.3992
N_1H	1.0105	1.0129	1.0102
C_3H	1.0788	1.0811	1.0788
C_4H	1.0818	1.0834	1.0807
C_2C_6	2.1214	2.2036	2.1834
bond angles [°]			
$C_2N_1C_6$	106.54	110.93	110.43
$N_1C_2C_3$	131.94	128.51	129.05
$C_2C_3C_4$	117.02	117.59	117.27
$C_3C_4C_5$	115.54	116.87	116.94
C_2C_3H	119.95	119.90	120.12

in Fig. 4.4 for the computations with the cc-pCVTZ basis.

While at the the HF-SCF level only the bicyclic structure is found, both CCSD and Mk-MRCCSD calculations yield the monocyclic and the bicyclic forms. However, the CCSD computations predict the bicyclic structure to be more stable by about 1.8 kcal mol^{-1}, whereas the Mk-MRCCSD approach favors the monocyclic form by more than 3.6 kcal mol^{-1}. At the CCSD(T) level only the monocyclic isomer is found to be a minimum on the potential energy surface. The geometry optimization for the bicyclic form (i.e., the one starting with a short C_2C_6 distance) also converged to the monocyclic structure. It is interesting to note that DFT, as HF-SCF calculations, leads to a bicyclic structure (for example, the C_2C_6 distance is 1.561 Å for BPW91/cc-pVDZ), while the complete-active-space SCF calculations in Ref. 30 provide a larger C_2C_6 distance than the CCSD(T) and Mk-MRCCSD computations.

In the case of the monocyclic form of 2,6-pyridyne, the contributions of the two reference determinants in the Mk-MRCC calculations amount to about 86 and 14%, respectively with $c_1 = 0.93$ and $c_2 = -0.37$ (Mk-MRCCSD/cc-pCVTZ calculation at the equilibrium geometry). Again, both reference determinants have a large contribution

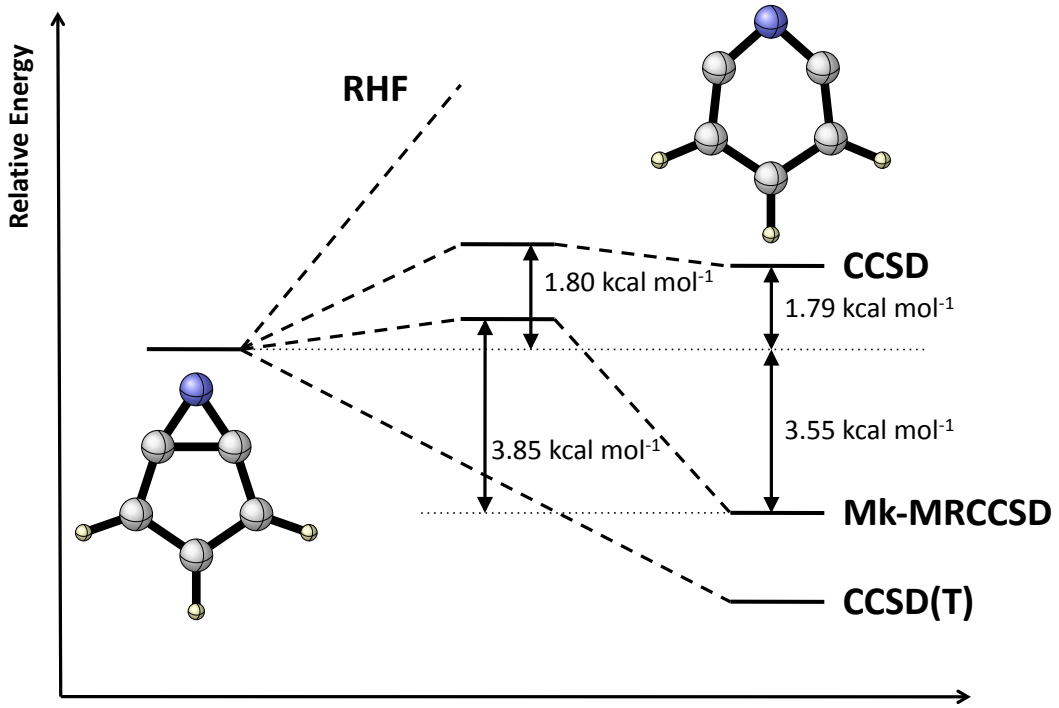

Figure 4.4: Schematic representation of the energetic ordering of the monocyclic and bicyclic forms as well as the corresponding transition state of 2,6-pyridyne as obtained for various levels of theory using the cc-pCVTZ basis set. For all methods the energy is given relative to the bicyclic form.

and 2,6-pyridyne should be considered as a system with rather strong multireference character. To illustrate the influence of the multireference treatment the geometrical parameters determined for the monocyclic form at the Mk-MRCCSD/cc-pCVDZ and Mk-MRCCSD/cc-pCVTZ levels are compared with those obtained at the single-reference CC level. The effect of the multireference treatment is again best monitored by means of the $C_2N_1C_6$ angle or, alternatively, the C_2C_6 distance. The CCSD treatment yields here the smallest angle with 86.15° using the cc-pCVTZ basis set, while CCSD(T) and Mk-MRCCSD calculations favor wider angles of 96.80 and 98.01 degrees, respectively. Consistent with this finding, the CCSD approach yields a shorter C_2C_6 distance (1.8183 Å) than the CCSD(T) and Mk-MRCCSD calculations (2.0144 and 2.0170 Å, respectively). Again, these findings indicate the shortcomings of the single-reference CC treatments and serve as argument in favor of the use of the present Mk-MRCCSD approach.

Table 4.3: Geometrical parameters for the monocyclic structure of 2,6-pyridyne (C_5N_3) computed at the CCSD, CCSD(T) and Mk-MRCCSD levels of theory using the cc-pCVDZ and cc-pCVTZ basis sets.

	cc-pCVDZ			cc-pCVTZ		
	CCSD	CCSD(T)	Mk-MRCCSD	CCSD	CCSD(T)	Mk-MRCCSD
bond lengths [Å]						
N_1C_2	1.3473	1.3596	1.3489	1.3313	1.3470	1.3361
C_2C_3	1.3892	1.3963	1.3896	1.3734	1.3801	1.3735
C_3C_4	1.4056	1.4098	1.4046	1.3936	1.3964	1.3908
C_3H	1.0916	1.0940	1.0920	1.0771	1.0800	1.0777
C_4H	1.0979	1.0995	1.0967	1.0838	1.0855	1.0825
C_2C_6	1.9139	2.0544	2.0469	1.8183	2.0144	2.0170
bond angles [°]						
$C_2N_1C_6$	90.52	98.15	98.70	86.15	96.80	98.01
$N_1C_2C_3$	143.20	137.09	136.91	146.94	138.12	137.45
$C_2C_3C_4$	115.85	117.23	116.97	114.52	117.01	116.80
$C_3C_4C_5$	111.40	113.22	113.55	110.93	112.93	113.49
C_2C_3H	119.91	119.48	119.72	120.74	119.51	119.78

Table 4.4 compares the results for the bicyclic form from CCSD and Mk-MRCCSD computations. As the multireference character for this form is much smaller (i.e., the weights of the two reference determinants in the Mk-MRCC calculations are about 99.9 and 0.1%), the agreement between single- and multireference CCSD results is much better with respect to the monocyclic isomer.

Table 4.3 and 4.4 also illustrate basis-set effects on the computed geometrical parameters. As for the 2,6-pyridynium cation, these changes are in line with the usual expectations when going from the smaller cc-pCVDZ to the larger cc-pCVTZ set, i.e., the bond lengths are shorter when using the larger basis set.

Finally, to calculate the height of the energy barrier at the CCSD and Mk-MRCCSD levels of theory using the cc-pCVTZ basis, the corresponding transition states have been determined by applying an eigenvector-following scheme[129,130] as implemented in CFOUR.[49] The geometries obtained are reported in Table 4.5. The corresponding C_2C_6 distances are 1.7679 Å for CCSD as well as 1.6026 Å for Mk-MRCCSD and lie between the ones of the monocyclic and bicyclic minimum of the PES. At the CCSD level, as depicted in Fig. 4.4, the energy barrier from the bicyclic to the monocyclic structure is

Table 4.4: Geometrical parameters for the bicyclic structure of 2,6-pyridyne (C_5NH_3) computed at the CCSD and Mk-MRCCSD levels of theory using the cc-pCVDZ and cc-pCVTZ basis sets.

	cc-pCVDZ		cc-pCVTZ	
	CCSD	Mk-MRCCSD	CCSD	Mk-MRCCSD
bond lengths [Å]				
N_1C_2	1.3524	1.3500	1.3374	1.3371
C_2C_3	1.3932	1.3919	1.3798	1.3800
C_3C_4	1.4237	1.4206	1.4114	1.4108
C_3H	1.0898	1.0904	1.0753	1.0753
C_4H	1.0984	1.0983	1.0838	1.0837
C_2C_6	1.5071	1.5427	1.4777	1.4830
bond angles [°]				
$C_2N_1C_6$	67.72	69.69	67.07	67.36
$N_1C_2C_3$	163.88	161.92	164.63	164.32
$C_2C_3C_4$	106.41	107.58	105.90	106.12
$C_3C_4C_5$	111.69	111.30	111.85	111.77
C_2C_3H	126.83	125.92	127.21	127.01

predicted to be 1.8 kcal mol^{-1}. The PES from the transition state to the monocyclic form is very flat with an energy difference of only 0.01 kcal mol^{-1}. At the Mk-MRCCSD level the situation is reversed. While the energy barrier from the bicyclic to the monocyclic form is small with a height of 0.3 kcal mol^{-1}, the energy difference of the transition state and the monocyclic structure is 3.55 kcal mol^{-1}.

4.6 Orbital Relaxation for TCSCF Orbitals

In the previous sections the Mk-MRCC approach has been applied using RHF orbitals. Although CC methods are rather insensitive to the choice of orbitals, strong multireference cases in principle necessitate a proper treatment of the orbitals at the MCSCF level of theory. The simplest possible MCSCF orbitals are those obtained from TCSCF computations which also represent the most important case within this work. The theoretical framework for Mk-MRCC gradient calculations using TCSCF orbitals as well as an implementation in CFOUR has been worked out in the diploma thesis of Thomas-Christian Jagau[131] and is also reported in Ref. 132. The framework is briefly

Table 4.5: Geometrical parameters for the transition state between the monocyclic and bicyclic form of 2,6-pyridyne (C_5NH_3) as computed at the CCSD and Mk-MRCCSD levels of theory using the cc-pCVDZ and cc-pCVTZ basis sets.

	cc-pCVDZ		cc-pCVTZ	
	CCSD	Mk-MRCCSD	CCSD	Mk-MRCCSD
bond lengths [Å]				
N_1C_2	1.3426	1.3459	1.3297	1.3308
C_2C_3	1.3889	1.3902	1.3735	1.3756
C_3C_4	1.4119	1.4164	1.3951	1.4022
C_3H	1.0909	1.0907	1.0770	1.0771
C_4H	1.0983	1.0982	1.0839	1.0839
C_2C_6	1.6996	1.6049	1.7679	1.6026
bond angles [°]				
$C_2N_1C_6$	78.54	73.20	83.33	74.05
$N_1C_2C_3$	153.63	158.56	149.40	157.84
$C_2C_3C_4$	111.87	109.44	113.59	109.74
$C_3C_4C_5$	110.46	110.81	110.69	110.79
C_2C_3H	122.59	124.45	121.36	124.28

discussed here as it is of importance in the following sections.

In Section 4.4 it has been demonstrated that the dependence on the used orbitals is restricted to the last term of Eq. (4.26). Thus, when using orbitals different from RHF in energy derivative computations, the gradient expression (4.26) remains the same but the term containing the derivatives of the MO coefficients with respect to the perturbation changes. The evaluation of this contribution to Mk-MRCC gradients requires, in principle, the determination of the coefficients U^{χ}_{pq} by means of the orbitals used. In the case of TCSCF orbitals, U^{χ}_{pq} is obtained by coupled-perturbed TCSCF (CPTCSCF)[133] theory. The corresponding CPTCSCF equations may be written as

$$\begin{pmatrix} \mathbf{A}_{\mathrm{oo}} & \mathbf{A}_{\mathrm{oc}} \\ \mathbf{A}_{\mathrm{co}} & \mathbf{A}_{\mathrm{cc}} \end{pmatrix} \begin{pmatrix} \mathbf{U}^{\chi}_{\mathrm{o}} \\ \mathbf{c}^{\chi} \end{pmatrix} = \begin{pmatrix} \mathbf{B}^{\chi}_{\mathrm{o}} \\ \mathbf{B}^{\chi}_{\mathrm{c}} \end{pmatrix} , \tag{4.45}$$

where $\mathbf{U}^{\chi}_{\mathrm{o}}$ denotes the vector of coefficients U^{χ}_{pq} and $\mathbf{c}^{\chi}$ the derivative of the TCSCF-CI vector. All entries in Eq. (4.45) do not represent single elements but rather blocks with the indices o and c denoting the orbital and CI part, respectively. The elements of the perturbation-independent matrix $\mathbf{A}$ comprise two-electron integrals and Fock-

matrix elements, whereas the elements of the perturbation-dependent vector $\mathbf{B}^\chi$ include derivatives of these quantities.

To reduce the computational effort the solution of the CPTCSCF equations is avoided by using the Z-vector method as is done in Section 4.4 for RHF orbitals. With the orthonormality condition

$$U^\chi_{pq} + U^\chi_{qp} + S^\chi_{pq} = 0 \ , \tag{4.46}$$

and the fact that those elements of $\mathbf{U}^\chi$ which refer to redundant orbital pairs can be chosen as

$$U^\chi_{pq} = -\frac{1}{2} S^\chi_{pq} \ , \tag{4.47}$$

the last term of Eq. (4.26) is reformulated as

$$-2 \sum_{pq} I'_{pq}(\mu) U^\chi_{pq} = -2 \sum_{pq}^{\text{non}} X_{pq}(\mu) U^\chi_{pq} + \sum_{pq}^{\text{red}} I_{pq}(\mu) S^\chi_{pq} \ , \tag{4.48}$$

where $X_{pq}(\mu) = I'_{pq}(\mu) - I'_{qp}(\mu)$ and the sums run over all TCSCF non-redundant (non)[iv] and remaining pairs of orbitals (red), respectively. The first term on the right-hand side of Eq. (4.48) is then recast using Eq. (4.45) as

$$-2 \begin{pmatrix} \mathbf{X}_\text{o} \\ 0 \end{pmatrix}^\mathbf{T} \begin{pmatrix} \mathbf{U}^\chi_\text{o} \\ \mathbf{c}^\chi \end{pmatrix} = -2 \begin{pmatrix} \mathbf{Z}_\text{o} \\ \mathbf{Z}_\text{c} \end{pmatrix}^\mathbf{T} \begin{pmatrix} \mathbf{B}^\chi_\text{o} \\ \mathbf{B}^\chi_\text{c} \end{pmatrix} \ , \tag{4.49}$$

with the vector $\mathbf{Z}$ defined by

$$\begin{pmatrix} \mathbf{Z}_\text{o} \\ \mathbf{Z}_\text{c} \end{pmatrix}^\mathbf{T} \begin{pmatrix} \mathbf{A}_\text{oo} & \mathbf{A}_\text{oc} \\ \mathbf{A}_\text{co} & \mathbf{A}_\text{cc} \end{pmatrix} = \begin{pmatrix} \mathbf{X}_\text{o} \\ \mathbf{0} \end{pmatrix}^\mathbf{T} \ . \tag{4.50}$$

Eq. (4.50) only contains perturbation-independent quantities. Thus, only one set of Z-vector equations need to be solved instead of $(3N - 6)$ CPTCSCF equations, where N is the number of nuclei.[131,132] Detailed expressions of the quantities presented in this section are not relevant for the following discussion and, therefore, are not repeated here. The reader is rather referred to Refs. 85 and 132–134.

[iv] Redundant orbital pairs of molecular orbitals are those for which rotations between the two molecular orbitals does not affect the energy while all other orbital pairs are denoted as non-redundant.[85] In the case of TCSCF, non-redundant orbital pairs are those in the virtual-occupied, virtual-active and active-occupied blocks of $\mathbf{U}^\chi$ as well as the U^χ_{pq} element in the active-active block with $p > q$.[132]

4.6.1 Effect of TCSCF Orbitals on Geometrical Parameters

The changes of geometrical parameters in Mk-MRCCSD geometry optimizations when TCSCF instead of RHF orbitals are used are discussed in the following.[132] The investigation of the 2,6-pyridynes (Section 4.5.2) is extended by computing the equilibrium structure of the monocyclic form using a TCSCF reference function. The active space

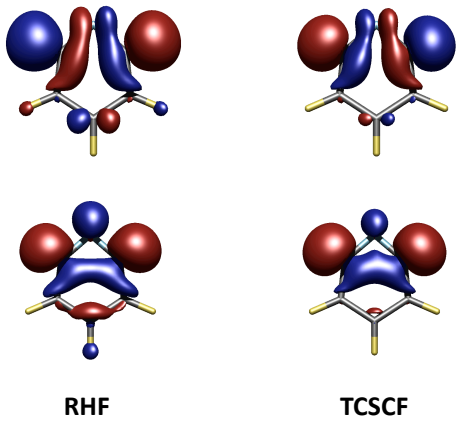

Figure 4.5: Active orbitals of 2,6-pyridyne obtained by optimizing the structures at the Mk-MRCCSD/cc-pCVTZ level of theory using a RHF (left) and TCSCF (right) reference wave function.

for the underlying TCSCF calculation has been chosen as described in Section 4.5.2 for the Mk-MRCCSD computation. The active orbitals are of a_1 and b_2 symmetry and correspond to the HOMO and LUMO in a RHF calculation.

The resulting bond lengths and bond angles are presented in Table 4.6 in comparison to the results obtained using RHF orbitals. The optimized geometries confirm that Mk-MRCC in fact is insensitive to the choice of orbitals. As depicted in Fig. 4.5, the use of TCSCF instead of RHF orbitals does not distinctly change the molecular structure. For this example, the maximum change observed for the bond lengths is about 0.001 Å for the N_1C_2 bond while the bond angles change at most by 1 degree ($\measuredangle C_2N_1C_6$). Regarding the C_2C_6 distance (provided in Table 4.6), the difference between the RHF and TCSCF results is one order of magnitude larger (0.012 Å) than for the bond lengths. The C_2C_6 distance is also an indicator for the relative influence of the reference determinants since the first determinant (with the active orbital of a_1 symmetry) favors short distances while the second one favors longer distances (for a detailed discussion see Ref. 132). The

Table 4.6: Geometrical parameters for the monocyclic structure of 2,6-pyridyne (C_5NH_3) computed at the Mk-MRCCSD/cc-pCVTZ levels of theory using RHF and TCSCF orbitals.

	RHF	TCSCF
bond lengths [Å]		
N_1C_2	1.3361	1.3352
C_2C_3	1.3735	1.3738
C_3C_4	1.3908	1.3908
C_3H	1.0777	1.0776
C_4H	1.0825	1.0828
C_2C_6	2.0170	2.0297
bond angles [°]		
$C_2N_1C_6$	98.01	98.94
$N_1C_2C_3$	137.45	136.81
$C_2C_3C_4$	116.80	116.82
$C_3C_4C_5$	113.49	113.80
C_2C_3H	119.78	119.84

relative contribution of the second determinant is about 14 (16) % when RHF (TCSCF) orbitals are used, which explains the slight lengthening of the C_2C_6 distance.

4.7 The Mk-MRCCSDT Approximation

The implementation of the Mk-MRCCSDT energy gradients requires an extension of the Mk-MRCCSD approach. In the singles, doubles and triples approximation, the cluster operator of Eq. (2.69) is given by

$$\hat{T}_\mu = \hat{T}_1^\mu + \hat{T}_2^\mu + \hat{T}_3^\mu \ . \tag{4.51}$$

The amplitude equations for singles and doubles can be written according to Eqs. (4.31) and (4.32), where, in comparison to Mk-MRCCSD, additional terms due to contributions of t_3-amplitudes occur. The t_3-amplitude equations take the form:

$$\left\langle \Phi_{ijk}^{abc}(\mu) \middle| \bar{H}_\mu \middle| \Phi_\mu \right\rangle c_\mu^\alpha + \sum_{\nu(\neq\mu)} \left\langle \Phi_{ijk}^{abc}(\mu) \middle| \hat{Y}^{\mu,\nu} \middle| \Phi_\mu \right\rangle H_{\mu\nu}^{\mathrm{eff}} c_\nu^\alpha = 0 \ . \tag{4.52}$$

The corresponding singles and doubles lambda equations are Eqs. (4.33) - (4.34), again, in comparison to Mk-MRCCSD, augmented by contributions due to t_3- and λ_3-amplitudes, and

$$\bar{c}_\mu^\alpha \Big\langle \Phi_\mu \Big| \Big[1 + \hat{\Lambda}_\mu\Big] \left[\bar{H}_\mu, \hat{\tau}_{ij}^{ab}(\mu)\right] \Big| \Phi_\mu \Big\rangle c_\mu^\alpha + \sum_\nu \bar{c}_\nu^\alpha \Big\langle \Phi_\nu \Big| \frac{\partial \hat{\Lambda}_\nu^{\text{int}}}{\partial t_{ijk}^{abc}(\mu)} \bar{H}_\nu \Big| \Phi_\nu \Big\rangle c_\nu^\alpha = 0 \tag{4.53}$$

for triples. Expressions for the last terms in Eqs. (4.33), (4.34) and (4.53) are obtained by differentiating $\hat{\Lambda}_\nu^{\text{int}}$ with respect to $t_i^a(\mu)$, $t_{ij}^{ab}(\mu)$ and $t_{ijk}^{abc}(\mu)$, respectively, using the expressions of the coupling terms for singles, doubles and triples [Eqs. (2.88) - (2.90)] as well as Eq. (4.6). This yields

$$\begin{aligned}
&\sum_\nu \bar{c}_\nu^\alpha \Big\langle \Phi_\nu \Big| \frac{\partial \hat{\Lambda}_\nu^{\text{int}}}{\partial t_i^a(\mu)} \bar{H}_\nu \Big| \Phi_\nu \Big\rangle c_\nu^\alpha \\
&= C_{\text{Mk-MRCCSD}} + \bar{c}_\mu^\alpha \sum_{\nu(\neq\mu)} \Bigg[- \sum_{mnef} \lambda_{aef}^{imn}(\mu) \Delta t_{mn}^{ef}(\nu/\mu, \mu) \\
&\qquad - \sum_{mnef} P(bc) \lambda_{aef}^{imn}(\mu) \Delta t_m^e(\nu/\mu, \mu) \Delta t_n^f(\nu/\mu, \mu) \Bigg] H_{\mu\nu}^{\text{eff}} \frac{c_\nu^\alpha}{c_\mu^\alpha} c_\mu^\alpha \\
&\quad + \bar{c}_\mu^\alpha \sum_{\nu(\neq\mu)} \frac{\bar{c}_\nu^\alpha}{\bar{c}_\mu^\alpha} \Bigg[+ \sum_{mnef} \lambda_{aef}^{imn}(\nu) \Delta t_{mn}^{ef}(\mu/\nu, \nu) \\
&\qquad + \sum_{mnef} P(bc) \lambda_{aef}^{imn}(\nu) \Delta t_m^e(\mu/\nu, \nu) \Delta t_n^f(\mu/\nu, \nu) \Bigg] H_{\nu\mu}^{\text{eff}} c_\mu^\alpha \ ,
\end{aligned} \tag{4.54}$$

$$\begin{aligned}
&\sum_\nu \bar{c}_\nu^\alpha \Big\langle \Phi_\nu \Big| \frac{\partial \hat{\Lambda}_\nu^{\text{int}}}{\partial t_{ij}^{ab}(\mu)} \bar{H}_\nu \Big| \Phi_\nu \Big\rangle c_\nu^\alpha \\
&= C_{\text{Mk-MRCCSD}} + \bar{c}_\mu^\alpha \sum_{\nu(\neq\mu)} \Bigg[\sum_{me} -\lambda_{abe}^{ijm}(\mu) \Delta t_m^e(\nu/\mu, \mu) H_{\mu\nu}^{\text{eff}} \frac{c_\nu^\alpha}{c_\mu^\alpha} \\
&\quad + \frac{\bar{c}_\nu^\alpha}{\bar{c}_\mu^\alpha} \sum_{me} \lambda_{abe}^{ijm}(\nu) \Delta t_m^e(\mu/\nu, \nu) H_{\nu\mu}^{\text{eff}} \Bigg] c_\mu^\alpha \ ,
\end{aligned} \tag{4.55}$$

and

$$\begin{aligned}
&\sum_\nu \bar{c}_\nu^\alpha \Big\langle \Phi_\nu \Big| \frac{\partial \hat{\Lambda}_\nu^{\text{int}}}{\partial t_{ijk}^{abc}(\mu)} \bar{H}_\nu \Big| \Phi_\nu \Big\rangle c_\nu^\alpha \\
&= \bar{c}_\mu^\alpha \sum_{\nu(\neq\mu)} \Bigg[- \lambda_{abc}^{ijk}(\mu) H_{\mu\nu}^{\text{eff}} \frac{c_\nu^\alpha}{c_\mu^\alpha} + \frac{\bar{c}_\nu^\alpha}{\bar{c}_\mu^\alpha} \lambda_{abc}^{ijk}(\nu/\mu) H_{\nu\mu}^{\text{eff}} \Bigg] c_\mu^\alpha \ ,
\end{aligned} \tag{4.56}$$

where $C_{\text{Mk-MRCCSD}}$ denotes terms already appearing in the Mk-MRCCSD gradient equations. The *common* lambda amplitudes are defined in Eq. (4.38).

4.7.1 Implementation

Based on the expressions given in the previous section, analytic Mk-MRCCSDT energy gradients have been implemented in the quantum-chemical program package CFOUR[49] as depicted in Fig. 4.1. The implementation extends the algorithm presented for Mk-MRCCSD energy gradients and only additional steps necessary for the inclusion of triple excitations are reported here. The implementation currently allows the use of two closed-shell reference determinants and RHF or TCSCF orbitals. The algorithm is suitable for large-scale calculations and has a formal scaling of $d \cdot n_o^3 n_v^5$, where d represents the number of reference determinants, n_o the number of occupied and n_v the number of virtual orbitals.

The computation of the Mk-MRCCSDT gradients requires the calculation of the t_3- and λ_3-amplitude equations as well as the triples contributions to the corresponding singles and doubles amplitudes. The implementation of these contributions has been described in Sec. 3.2.

The basic scheme in the CFOUR algorithm for the formation of the t_3-amplitudes in a CCSDT energy calculation is an outer loop over an index triple i, j, k of the t_{ijk}^{abc}-amplitudes.[87,97] Blocks of a, b, c index triples are computed one at a time within the loop and are stored on disk for the next iteration. Additionally, these i, j, k blocks are used immediately to calculate the contributions to the t_1- and t_2-amplitude equations. For Mk-MRCCSDT an outer loop over reference determinants is introduced together with the computation of the corresponding coupling terms for the i, j, k blocks (For further details see also Ref. 135).

Beside solving the amplitude equations [Eq. (2.86)], Mk-MRCC gradient calculations require the solution of the lambda equations [Eq. (4.10)] and of the equations for the Lagrange multipliers $\bar{c}_\mu^\alpha$ [Eq. (4.12)]. The lambda equations have been implemented in a similar way as the amplitude equations with a contribution given in terms of the usual single-reference part and an additional coupling term. The existing CCSDT gradient code in CFOUR has been exploited for this purpose using the same strategy as in the case of the amplitude equations. For the determination of the Lagrange multipliers $\bar{c}_\mu^\alpha$ the triples contributions are added to the Mk-MRCCSD matrix $\mathbf{M}$ [Eqs. (4.13) and (4.14)] and, subsequently, Eq. (4.12) is solved.

The expressions for the density matrices have the same form as those in the single-reference case,[81,87,97] so that the code can be used without any modification. Back transformation of the density matrices to the AO basis and contraction with the AO integral derivatives are also carried out as in the single-reference case. The corresponding loops over reference determinants have already been introduced for the implementation of Mk-MRCCSD gradients. In the current implementation based on HF or TCSCF orbitals, orbital relaxation can be treated by the Z-vector method as described in Section 4.6 as well as Refs. 131, 81, and 132.

The implementation of analytic Mk-MRCCSDT gradients has been checked in an analogous way as the corresponding Mk-MRCCSD first derivatives as described in Sec. 4.5.1.

4.7.2 Illustrative Examples for Mk-MRCCSDT Gradient Calculations

To illustrate the applicability of the implemented analytic Mk-MRCCSDT gradients three examples are given in the following. For all examples two closed-shell determinants

$$|\Phi_1\rangle = \left|(\text{core})^2(\text{valence}-2\text{e}^-)^2(\text{HOMO})^2\right\rangle \tag{4.57}$$

and

$$|\Phi_2\rangle = \left|(\text{core})^2(\text{valence}-2\text{e}^-)^2(\text{LUMO})^2\right\rangle \ . \tag{4.58}$$

are taken as references using orbitals from TCSCF calculations. HOMO (LUMO) corresponds to the highest-occupied (lowest-unoccupied) MO in a RHF calculation.

In the first example the equilibrium geometry of the ozone molecule (O_3) is investigated as this is a prototypical example for non-dynamical correlation effects and has been widely studied in the literature (for a detailed overview concerning quantum-chemical studies on ozone, see Ref. 136). Though O_3 can be treated rather well with single-reference CC methods if higher excitations are included, the rather large non-dynamical correlation effects render a multireference treatment desirable.

The second example consists in the automerization process of cyclobutadiene (C_4H_4). While for the rectangular equilibrium structure the wave function is dominated by one reference determinant and may be described by single-reference methods, the square transition state is a multireference problem due to the degeneracy of the frontier orbitals (b_{1g} and b_{2g} symmetry in D_{4h} point group). For this reason the automerization of cyclobutadiene has been extensively studied in the literature employing various multiref-

erence methods.[23,103,104,137–140] These theoretical investigations have focused not only on the geometry parameters but also on the energy barrier of the automerization process. As cyclobutadiene is a rather unstable compound, to the best of my knowledge, its experimental isolation has not been successful so far. Studies based on trapping reactions only yield a rough estimate of the height of the automerization barrier.[141]

In the third example, the equilibrium geometries of didehydroarenes (arynes) are investigated. The strong biradical character of these systems has already been pointed out in Section 4.5.2 thus motivating a proper multireference treatment. In this section a study of 2,6-pyridyne, the 2,6-pyridynium cation and *m*-benzyne (C_6H_4), respectively, is presented. The active orbitals chosen in this investigation are in all three cases of a_1 and b_2 symmetry.

4.7.2.1 Ozone (O_3)

In the case of ozone, the contribution of the two reference determinants to the wave function amount to 91 and 9%, respectively (the corresponding expansion coefficients are $c_1 \approx 0.95$ and $c_2 \approx -0.31$ for the Mk-MRCCSDT/cc-pVTZ calculation at the equilibrium geometry). Thus, the wave function has already substantial multireference character.

In Table 4.7, the Mk-MRCCSDT geometry of O_3 is compared to those obtained with different single-reference CC methods and Mk-MRCCSD when using the cc-pVDZ and cc-pVTZ basis.[143] The CCSDT(Q) method[144] includes quadruple excitations in a perturbative manner and can be considered of sufficient accuracy to serve as a standard for comparison. The results obtained using the cc-pVDZ basis indicate that the bond length increases when higher excitations are included [1.2584, 1.2828, and 1.2943 Å for CCSD, CCSDT, and CCSDT(Q), respectively] and that the angle decreases (117.30, 116.50, and 116.21 °).

The geometrical parameters obtained from the Mk-MRCCSD approach (1.2759 Å and 115.95 °) are closer to the CCSDT(Q) result than the results from the corresponding single-reference CCSD calculation. This can be taken as an indication that the explicit consideration of the multireference character in the calculation leads to improved results. On the other hand, the Mk-MRCCSD bond length is still too short in comparison to CCSDT(Q). This indicates that an adequate treatment of dynamical electron correlation at the Mk-MRCC level requires at least the inclusion of triple excitations.

The full inclusion of triple excitations at the Mk-MRCCSDT level further reduces

Table 4.7: Geometrical parameters (bond length in Å and bond angle in degree) of ozone (O_3) computed at the CCSD, CCSDT, CCSDT(Q), Mk-MRCCSD and Mk-MRCCSDT levels of theory using the cc-pVDZ (dz) and cc-pVTZ (tz) basis sets. For the Mk-MRCC methods TCSCF orbitals have been used.

method	basis	R(OO)	∠(OOO)
CCSD	dz	1.2584	117.30
	tz	1.2458	117.64
CCSDT	dz	1.2828	116.50
	tz	1.2695	116.88
CCSDT(Q)	dz	1.2943	116.21
Mk-MRCCSD	dz	1.2759	115.95
	tz	1.2619	116.38
Mk-MRCCSDT	dz	1.2861	116.30
	tz	1.2732	116.64
experiment[142]		1.2717	116.78

the deviation from the CCSDT(Q) results. The bond length and angle computed with Mk-MRCCSDT (1.2861 Å and 116.30 °) are closer to the CCSDT(Q) value than the results obtained at the CCSDT levels of theory. This result supports the previous finding that a well-balanced description of dynamical and non-dynamical correlation effects is necessary for the computation of geometry parameters for the ozone molecule.[47,145]

Table 4.7 contains also results obtained for the cc-pVTZ basis. The comparison with the single-reference results indicate that the same patterns are seen in the Mk-MRCCSD and Mk-MRCCSDT calculations, i.e., the use of larger basis sets yields a shorter distance and a wider angle. Our best values, i.e., 1.2732 Å for the bond length and 116.64 ° for the angle obtained at the Mk-MRCCSDT/cc-pVTZ level of theory, are in excellent agreement with experiment[142] and deviates by just 0.0015 Å and 0.14 °, respectively.

4.7.2.2 Automerization of Cyclobutadiene (C_4H_4)

The cyclobutadiene molecule represents an antiaromatic system with two carbon-carbon single bonds and two double bonds. Between the two equivalent rectangular structures lies the square transition state. The height of the automerization barrier

determines the interconversion of the two rectangular equilibrium structures. This automerization process of cyclobutadiene is depicted in Fig. 4.6.

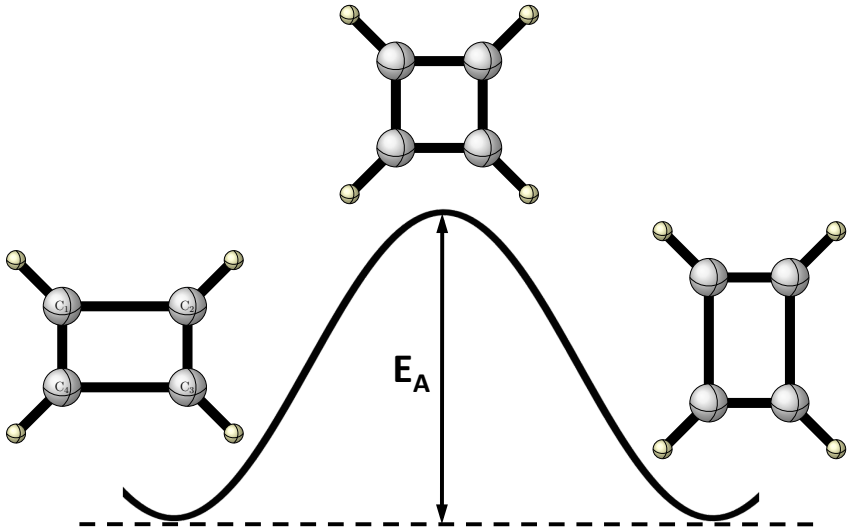

Figure 4.6: Schematic representation of the automerization of cyclobutadiene. Depicted are the rectangular equilibrium structures and the square transition state. E_A represents the energy barrier.

Table 4.8: Geometrical parameters (bond lengths in Å and bond angle in degree) of the cyclobutadiene (C_4H_4) molecule computed for the equilibrium structure. Geometries have been obtained at the CCSD, CCSDT, Mk-MRCCSD and Mk-MRCCSDT levels of theory using the cc-pVDZ basis set. For multireference calculations TCSCF orbitals have been used.

method	$R(C_1C_2)$	$R(C_2C_3)$	R(CH)	$\measuredangle(HC_1C_2)$
CCSD	1.5804	1.3543	1.0924	134.91
CCSDT	1.5784	1.3652	1.0941	134.93
Mk-MRCCSD	1.5708	1.3609	1.0923	134.91
Mk-MRCCSDT	1.5769	1.3660	1.0941	134.93

For the equilibrium geometry, the multireference character of the wave function is rather small with contributions of the two reference determinants of 95% and 5% (the corresponding expansion coefficients are $c_1 \approx 0.98$ and $c_2 \approx -0.22$ for the Mk-MRCCSDT/cc-pVDZ calculation at the equilibrium geometry). Table 4.8 summarizes the geometry

Table 4.9: Bond lengths in Å of the square transition state of the automerization of the cyclobutadiene (C_4H_4) molecule. Geometries have been obtained at the CCSD, CCSDT, Mk-MRCCSD and Mk-MRCCSDT levels of theory using the cc-pVDZ basis set. For multireference calculations TCSCF orbitals have been used.

method	R(CC)	R(CH)
CCSD	1.4565	1.0912
CCSDT	1.4645	1.0930
Mk-MRCCSD	1.4570	1.0913
Mk-MRCCSDT	1.4623	1.0931

parameters of the equilibrium structure obtained at the CCSD, CCSDT, Mk-MRCCSD and Mk-MRCCSDT levels of theory using the cc-pVDZ basis set. Most pronounced are the changes in the C_1-C_2 and C_2-C_3 bond lengths when using different methods. Taking into account triple excitations by the CCSDT method, the CCSD bond lengths (1.5804 and 1.3543 Å) are shortened by 0.002 Å in the case of C_1-C_2 and lengthened by 0.011 Å for C_2-C_3. The bond lengths obtained at the Mk-MRCCSD level are in both cases shorter (by about 0.008 and 0.005 Å) than the CCSDT results. The inclusion of triple excitations at the Mk-MRCCSDT level lengthens both C-C bonds by about 0.006 Å. For Mk-MRCCSDT the C_1-C_2 bond length lies then in between the CCSDT and Mk-MRCCSD results while the C_2-C_3 bond length is slightly longer than the CCSDT result. For C_2-C_3 Mk-MRCCSDT yields a bond length that is probably closer to the convergence limit than CCSDT as the inclusion of triple excitations in both cases lengthens the bond. For the C_1-C_2 bond such a statement is hardly possible as the trends are opposed to each other for single-reference and multireference methods. The changes of the C-H bond length and the H-C_1-C_2 angle show only a small dependence on the method used, with maximum changes of 0.0018 Å and 0.02 °, respectively. The effect of a multireference treatment on these parameters is rather small as it is obvious when comparing the results of the single-reference and the corresponding multireference method.

More pronounced differences in the geometry are expected at the transition state of the automerization process. Here, the two configurations become degenerate, thus providing equal contributions to the wave function. The results obtained for the geometry at the transition state,[v] as given in Table 4.9, indicate that CCSDT predicts the C-C

[v] Starting from the square geometry of the transition state, the structure may be distorted in two ways. One transforms the geometry to a rectangle, one to a rhombus.[146] Optimizing the geometries

Table 4.10: Automerization barrier (E_A) of cyclobutadiene (in kcal mol^{-1}) obtained for geometries optimized at the CCSD, CCSDT, Mk-MRCCSD and Mk-MRCCSDT levels of theory using the cc-pVDZ basis set as well as RHF orbitals for single-reference and TCSCF orbitals for multireference computations.

method	barrier height
CCSD	21.13
CCSDT	7.62
Mk-MRCCSD	7.79
Mk-MRCCSDT	7.87

bond length to be longer than CCSD by 0.008 Å. The Mk-MRCCSD bond length lies in between the CCSD and CCSDT results and is predicted to be only 0.0005 Å longer than the corresponding CCSD bond length. When accounting for triple excitations in Mk-MRCC computations, the C-C bond is longer (by 0.0053 Å) than predicted by Mk-MRCCSD but shorter (by 0.0022 Å) than the CCSDT result. Although these effects are relatively small, it is interesting to note the reversed trend when comparing CCSD and Mk-MRCCSD as well as CCSDT and Mk-MRCCSDT. Again, as for the equilibrium structure, the C-H bond length is less sensitive than the C-C bond length to the method used with a maximum change of 0.0019 Å when comparing the CCSD and Mk-MRCCSDT results.

The automerization barrier obtained at the different levels of theory is presented in Table 4.10. While the energy barrier computed at the CCSD level (21.13 kcal mol^{-1}) is very large and seems, in comparison to the other results and the experimental estimate, to be one order of magnitude too high, CCSDT predicts the barrier to be 7.62 kcal mol^{-1}. However, if multireference effects are treated via the Mk-MRCC approach, the barrier height is significantly improved (7.79 kcal mol^{-1}) already within the singles and doubles approximation, that is 0.17 kcal mol^{-1} larger than the CCSDT energy barrier. For the Mk-MRCCSDT method, the barrier height is predicted to be 7.87 kcal mol^{-1} which is 0.08 and 0.25 kcal mol^{-1} higher than the results obtained at the Mk-MRCCSD and CCSDT level, respectively. A comparison to an experimental number

requires calculations in two different D_{2h} subgroups of D_{4h} symmetry. Therefore, two different sets of MOs are required to follow the proper distortion from the D_{4h} structure. For the computations carried out at the D_{4h} symmetry, the square structure has been slightly distorted by stretching one of the C-C bonds by 10^{-6} Å in order to obtain the proper D_{2h} molecular orbitals. This distortion is very small and has only negligible effect on the computed geometries and energies.

is hardly possible as only a rough estimate of the barrier height (1.6 - 10 kcal mol^{-1}) is reported in the literature.[141] The only possible conclusion from this estimate is that the results observed, except for CCSD, have the correct order of magnitude and lie in the experimentally predicted range for the barrier height. It is interesting to note that the results obtained at the Mk-MRCC level are always over 1 kcal mol^{-1} larger than the corresponding barrier obtained at the BW-MRCC level of theory. The barrier height is predicted to be 6.2-6.5 kcal mol^{-1} for BW-MRCCSD and 5.7-6.1 kcal mol^{-1} for BW-MRCCSD(T),[137] depending on the size-extensivity correction used. Thus, the perturbative triples correction for BW-MRCCSD lowers the energy barrier while a full treatment of triple excitations within the Mk-MRCC model increases the barrier height. For comparison, the multireference configuration-interaction method with singles and doubles (MRCISD) yields an automerization barrier of 7.3 kcal mol^{-1}.[23]

4.7.2.3 Arynes

The optimized structures for the arynes investigated, namely 2,6-pyridyne (C_5NH_3), 2,6-pyridynium cation ($C_5NH_4^+$) and *m*-benzyne (C_6H_4), are depicted in Fig. 4.7. Their multireference character is evident from the expansion coefficients obtained in Mk-MRCC calculations. The corresponding values are 0.92, 0.90 and 0.95 for c_1 while

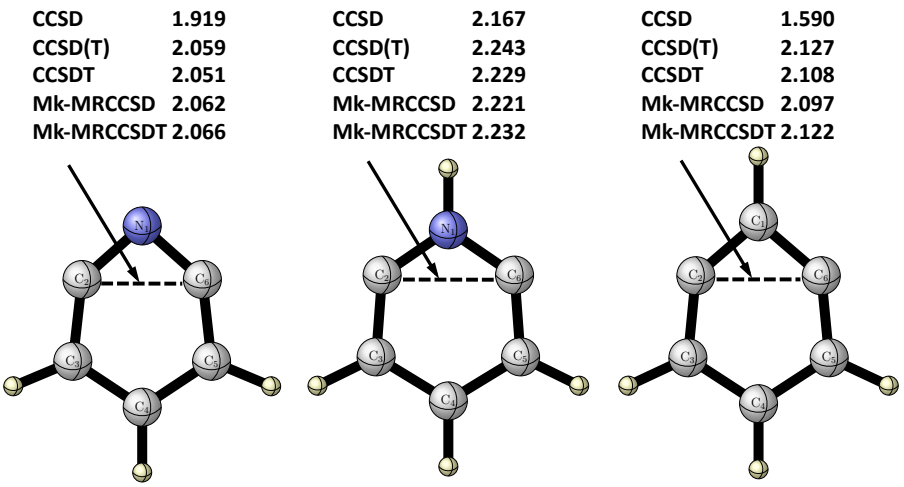

Figure 4.7: Optimized structures for 2,6-pyridyne, the 2,6-pyridynium cation and *m*-benzyne computed at the CCSD, CCSDT, Mk-MRCCSD and Mk-MRCCSDT levels of theory using the cc-pVDZ basis set. The representative C_2C_6 bond distance is in Å. RHF (TCSCF) orbitals were used in single-reference (multireference) computations.

Table 4.11: Geometrical parameters (bond lengths in Å and bond angles in degree) of the 2,6-pyridyne (C_5NH_3) obtained at the CCSD, CCSD(T), CCSDT, Mk-MRCCSD and Mk-MRCCSDT levels of theory using the cc-pVDZ basis set as well as RHF orbitals for single-reference and TCSCF orbitals for multireference computations.

	CCSD	CCSD(T)	CCSDT	Mk-MRCCSD	Mk-MRCCSDT
$R(N_1C_2)$	1.3484	1.3604	1.3581	1.3491	1.3572
$R(C_2C_3)$	1.3908	1.3978	1.3970	1.3914	1.3971
$R(C_3C_4)$	1.4071	1.4112	1.4111	1.4062	1.4112
$R(C_3H)$	1.0923	1.0947	1.0944	1.0926	1.0945
$R(C_4H)$	1.0985	1.1000	1.0998	1.0977	1.0998
$R(C_2C_6)$	1.9192	2.0589	2.0508	2.0617	2.0655
$\measuredangle(C_2N_1C_6)$	90.75	98.35	98.05	99.66	99.09
$\measuredangle(N_1C_2C_3)$	143.02	136.95	137.26	136.26	136.53
$\measuredangle(C_2C_3C_4)$	115.90	117.24	117.10	116.99	117.13
$\measuredangle(C_3C_4C_5)$	111.43	113.27	113.24	113.84	113.58
$\measuredangle(C_2C_3H)$	119.89	119.49	119.57	119.80	119.67

-0.40, -0.44 and -0.32 for c_2 (Mk-MRCCSDT/cc-pVDZ calculation employing the reference determinants as described above) which means that the relative contributions of the two reference functions are about 84, 81 and 90% for the first reference while 16, 19 and 10% for the second one. These ratios of the individual contributions are more or less identical to the ones obtained from the corresponding Mk-MRCCSD calculation where 83, 81 and 90 % are observed for the first as well as 17, 19 and 10 % for the second determinant.

To illustrate the influence of the multireference treatment, the geometrical parameters determined at the Mk-MRCCSD and Mk-MRCCSDT levels are compared with those obtained at the single-reference CC level. The geometrical parameters obtained are summarized in Tables 4.11 - 4.13. The effect of the multireference treatment is best monitored by means of the $C_2N_1C_6$ angle or, alternatively, the C_2C_6 distance. The CCSD treatment yields for all three arynes the smallest $C_2N_1C_6$ angle with 90.75, 108.12 and 71.33 °, while CCSD(T), CCSDT, Mk-MRCCSD and Mk-MRCCSDT calculations favor wider angles. Consistent with this finding, the CCSD approach yields a shorter C_2C_6 distance for 2,6-pyridyne, the 2,6-pyridynium cation, and *m*-benzyne (1.9192, 2.1667 and 1.5902 Å) than the CCSD(T), CCSDT, Mk-MRCCSD and Mk-MRCCSDT calculations. Again, these findings indicate the shortcomings of the single-reference CC treatments, in

Table 4.12: Geometrical parameters (bond lengths in Å and bond angles in degree) for the 2,6-isomer of the pyridynium cation ($C_5NH_4^+$) obtained at the CCSD, CCSD(T) CCSDT, Mk-MRCCSD and Mk-MRCCSDT levels of theory using the cc-pVDZ basis set as well as RHF orbitals for single-reference and TCSCF orbitals for multireference computations.

	CCSD	CCSD(T)	CCSDT	Mk-MRCCSD	Mk-MRCCSDT
$R(N_1C_2)$	1.3381	1.3511	1.3490	1.3429	1.3490
$R(C_2C_3)$	1.3754	1.3829	1.3815	1.3750	1.3810
$R(C_3C_4)$	1.4140	1.4187	1.4187	1.4143	1.4191
$R(N_1H)$	1.0218	1.0239	1.0237	1.0221	1.0237
$R(C_3H)$	1.0935	1.0954	1.0953	1.0936	1.0954
$R(C_4H)$	1.0964	1.0978	1.0978	1.0962	1.0979
$R(C_2C_6)$	2.1667	2.2434	2.2293	2.2205	2.2324
$\measuredangle(C_2N_1C_6)$	108.12	112.24	111.44	111.54	111.67
$\measuredangle(N_1C_2C_3)$	130.72	127.58	128.22	128.27	128.08
$\measuredangle(C_2C_3C_4)$	117.31	117.71	117.58	117.36	117.54
$\measuredangle(C_3C_4C_5)$	115.82	117.18	116.97	117.19	117.08
$\measuredangle(C_2C_3H)$	119.78	119.85	119.90	120.13	120.01

Table 4.13: Geometrical parameters (bond lengths in Å and bond angles in degree) of the *m*-benzyne (C_6H_4) obtained at the CCSD, CCSD(T), CCSDT, Mk-MRCCSD and Mk-MRCCSDT levels of theory using the cc-pVDZ basis set as well as RHF orbitals for single-reference and TCSCF orbitals for multireference computations.

	CCSD	CCSD(T)	CCSDT	Mk-MRCCSD	Mk-MRCCSDT
$R(C_1C_2)$	1.3638	1.3891	1.3870	1.3809	1.3880
$R(C_2C_3)$	1.3939	1.3927	1.3920	1.3869	1.3919
$R(C_3C_4)$	1.4208	1.4149	1.4148	1.4098	1.4148
$R(C_1H)$	1.0947	1.0915	1.0914	1.0897	1.0914
$R(C_3H)$	1.0912	1.0958	1.0956	1.0938	1.0957
$R(C_4H)$	1.0978	1.0998	1.0996	1.0976	1.0996
$R(C_2C_6)$	1.5902	2.1265	2.1084	2.0965	2.1224
$\measuredangle(C_2C_1C_6)$	71.33	99.89	98.94	98.77	99.73
$\measuredangle(C_1C_2C_3)$	160.23	135.28	136.06	136.26	135.44
$\measuredangle(C_2C_3C_4)$	108.18	117.52	117.32	117.19	117.45
$\measuredangle(C_3C_4C_5)$	111.85	114.51	114.30	114.34	114.50
$\measuredangle(C_2C_3H)$	125.95	120.40	120.47	120.56	120.46

particular for *m*-benzyne, where CCSD yields a very small C_2C_6 distance corresponding to a bicyclic structure.

The change in the C_2C_6 distance due to triple excitations is considerably more pronounced for the single-reference methods than for Mk-MRCC. While the change in this distance from CCSD to CCSDT is 0.1316, 0.0626 and 0.5182 Å, respectively, a difference of only 0.0038, 0.0119 and 0.0259 Å is observed when comparing Mk-MRCCSD and Mk-MRCCSDT results. Interestingly, the C_2C_6 distance in 2,6-pyridyne computed at the Mk-MRCCSD level lies between the CCSDT and Mk-MRCCSDT results. For the other two compounds Mk-MRCCSD yields a distance that is slightly shorter than the corresponding CCSDT result. The CCSD(T) method yields in all three cases a longer C_2C_6 distance (by 0.0081, 0.0141 and 0.0181 Å, respectively) than CCSDT.

5 Parallelization of CCSDT and Mk-MRCCSDT

When aiming for quantitative accuracy it is essential to consider in the CC treatment triple-excitation effects. While in most calculations triple excitations are often treated using approximate schemes such as the CC singles and doubles (CCSD) approach with a perturbative treatment of triples [CCSD(T)],[6] the full inclusion of triple excitations within the CC singles, doubles and triples (CCSDT)[7,8] model has turned out to be of importance in areas where quantitative accuracy is needed.[10,147–152] The same holds when applying multireference methods. Beyond the recently proposed Mk-MRCCSD(T) approaches,[137,153] explicit expressions for the implementation of full triples have been presented within the Mk-MRCC framework in order to tackle multireference cases with high accuracy.[68] However, the application of CC methods including a full treatment of triple excitations to larger chemical problems is hampered by the considerable increase of computational effort with increasing number of electrons and basis functions. If N represents a measure of the system size, the operation count and therefore the execution time scales as N^8 for CCSDT and $d \cdot N^8$ for Mk-MRCCSDT with d denoting the number of chosen reference determinants. In comparison the storage requirements for intermediates and CC amplitudes only scales as N^6 and $d \cdot N^6$, respectively. Therefore, the limiting factor of CCSDT calculations is the execution time and not the storage requirement.

To circumvent limitations due to the execution time and motivated by the cheap computing power available through computer clusters, several parallel implementations of single-reference CC methods have been recently presented.[11–20] For most of these parallelization schemes additional tools have been developed. The parallelization in Ref. 12, for example, is based on the use of Global Arrays (GA)[154] as a parallelization tool. GA simulates shared memory programming on distributed memory computer clusters by striping large arrays across nodes. In view of the large memory and disk space available nowadays, the striping of individual arrays may no longer be necessary. Therefore, an alternative approach, namely Array Files (AF),[155] has been developed where the whole array is stored on a given node. The concept of AF has been used for a parallel im-

plementation of CCSD energy calculations by Janowski et al.[14] A highly sophisticated parallel algorithm for the computation of CCSD(T) energies has been furthermore reported by Olson et al. thereby combining distributed and shared memory techniques by using the Distributed Data Interface (DDI/3).[13,156] This implementation is tailored to multiprocessor and multicore nodes connected via a dedicated communication network. An ansatz which works without an additional layer of complexity provided by libraries such as GA, AF or DDI/3 has been reported recently for the parallel calculation of CCSD and CCSD(T) energies as well as analytic first and second derivatives.[15] This scheme is based on the message passing interface (MPI)[157] and the adaptation of an efficient serial algorithm to parallel environments where all nonparallel steps run redundantly on all available processors at the same time.

In the field of MRCC theory, parallel algorithms are hardly found as MRCC calculations are so far not considered a routine application. Only Piecuch and Landman reported a parallelization scheme for state-universal CCSD calculations.[158] In this scheme the underlying serial algorithm has been modified by parallelizing the most time-determining steps using OpenMP.[159]

To the best of my knowledge, most of the parallel CC algorithms are so far only capable to compute perturbative treatments of triple excitations such as in CCSD(T). Parallel implementations for CCSDT or a corresponding multireference ansatz have been reported for CCSDT within the general CC program of Kállay[20] and the NWChem program package[18] which has been developed for computations using parallel supercomputers. In contrast to these approaches, a more practical approach is described in this work based on the adaptation of an efficient serial algorithm that can be run on workstation clusters. Furthermore, a detailed analysis of the time-determining steps for a full treatment of triple excitations as well as the resulting parallel algorithm in the quantum-chemical program package CFOUR[49] is presented. The applicability of the parallelization strategy is demonstrated by computations on N_2O, ozone (O_3), benzene (C_6H_6) and 2,6-pyridyne (C_5NH_3). The hardware specifications of the computers used for the calculations carried out in this chapter can be found in the appendix.

5.1 Parallelization of CCSDT and Mk-MRCCSDT Energy Computations

In the efforts to parallelize CCSDT and Mk-MRCCSDT energy calculations, the strategy already described in Ref. 15 has been followed for the parallel computation of CCSD and CCSD(T) energies as well as analytic first and second derivatives. To avoid the communication of intermediate quantities, most of the quantities needed within the CC iterations are stored completely on every node. Thus, the algorithm presented here is tailored to cluster architectures with moderate hardware specifications as well as inexpensive and rather slow standard interconnect structures such as Gigabit Ethernet. Furthermore, is is assumed that enough fast memory and disk space are available locally on every node to store the full set of t-amplitudes. In this way communication is minimized as only the CC amplitudes need to be communicated.

In the actual algorithm, parts of the intermediates are contracted with the proper t_3-amplitudes to yield parts of the resulting quantities which, at the end of the parallel operation, are broadcasted to all other nodes. The costs associated with the communication of the triples amplitudes thus scales as $n_{\mathrm{occ}}^3 n_{\mathrm{vrt}}^3$ for CCSDT and $d \cdot n_{\mathrm{occ}}^3 n_{\mathrm{vrt}}^3$ for Mk-MRCCSDT, where n_{occ} (n_{vrt}) denotes the number of occupied (virtual) orbitals. This is two orders of magnitudes smaller than the required time for the computation of the amplitudes which has a scaling of $n_{\mathrm{occ}}^3 n_{\mathrm{vrt}}^5$ and $d \cdot n_{\mathrm{occ}}^3 n_{\mathrm{vrt}}^5$, respectively. Disregarding communication latencies, the dominating steps have been implemented in such a way that the total amount of communication between the parallel processes does not depend on the number of involved processors due to the MPI routine used. Thus, the distribution of the time-determining steps to different nodes reduces the overall walltime significantly, particularly when larger examples are considered.

As for the parallelization of CCSD and CCSD(T) calculations,[15] it is important to identify the time-determining steps. CCSDT energy calculations are dominated by the computation of the t_3-amplitudes yielding a scaling of $n_{\mathrm{occ}}^3 n_{\mathrm{vrt}}^5$. Furthermore, contributions of the t_3-amplitudes to the t_2-amplitude equations having a formal scaling of N^7 need to be considered. Thus, the time spent for the calculation of the triples amplitudes and the resulting contributions to the t_2-amplitude equations increases more rapidly with the number of basis functions than in the pure CCSD part (the scaling of CCSD is $n_{\mathrm{occ}}^2 n_{\mathrm{vrt}}^4$) which renders the triples part by far the time-determining step in CCSDT calculations. This becomes obvious when considering the timings for a CCSDT energy

Table 5.1: Timings (walltime in s) for the N_2O molecule for one CC iteration and the triples part within this iteration. The code has been parallelized outside or inside the loop over occupied orbitals. The computation has been carried out at the CCSDT/cc-pCVTZ level (129 basis functions). For the communication outside the loop the ratio of the triples part to the whole CC iteration is given in parenthesis. On each node 1 cpu has been used.

# nodes	CC iter., outside	CC iter., inside	triples, outside	triples, inside
1	1065	1062	1046 (98%)	1043
2	547	545	528 (97%)	526
4	288	289	269 (93%)	269
8	158	157	139 (88%)	138
16	93	94	74 (80%)	75

calculation, e.g., for the N_2O molecule employing the cc-pCVTZ basis set[128] (Table 5.1). For this example the time spent in the triples part for a serial calculation is about 98 % of a CC iteration.

The approach to parallelize the computation of the triple amplitudes starts with the t_3-amplitude equations given as

$$t_{ijk}^{abc} D_{ijk}^{abc} = \left\langle \Phi_{ijk}^{abc} \middle| e^{-\hat{T}} \left[\hat{H}_N - \hat{H}_0 \right] e^{\hat{T}} \middle| 0 \right\rangle \ , \tag{5.1}$$

with

$$\hat{H}_0 = \sum_p f_{pp} \{ \hat{a}_p^\dagger \hat{a}_p \} \ . \tag{5.2}$$

The denominator array D_{ijk}^{abc} is defined as

$$D_{ijk}^{abc} = f_{ii} + f_{jj} + f_{kk} - f_{aa} - f_{bb} - f_{cc} \tag{5.3}$$

where $i, j, k, \ldots$ denotes occupied and $a, b, c, \ldots$ virtual spin orbitals. The normal-ordered Hamiltonian $\hat{H}_N$ is given as

$$\hat{H}_N = \sum_{pq} f_{pq} \left\{ \hat{a}_p^\dagger \hat{a}_q \right\} + \frac{1}{4} \sum_{pqrs} \langle pq||rs \rangle \left\{ \hat{a}_p^\dagger \hat{a}_q^\dagger \hat{a}_s \hat{a}_r \right\} \ , \tag{5.4}$$

with the Fock-matrix elements computed as

$$f_{pq} = h_{pq} + \sum_{k}^{n_{occ}} \langle pk||qk\rangle \ , \tag{5.5}$$

from the one-electron integrals h_{pq} and the antisymmetrized two-electron integrals $\langle pq||rs\rangle$. The strings $\{\hat{a}_p^\dagger \hat{a}_p\}$, $\{\hat{a}_p^\dagger \hat{a}_q\}$ and $\{\hat{a}_p^\dagger \hat{a}_q^\dagger \hat{a}_s \hat{a}_r\}$ denote normal-ordered sequences of creation ($\hat{a}_p^\dagger$) and annihilation ($\hat{a}_q$) operators.

As described in Chapter 3, the basic feature in the serial CFOUR algorithm for the formation of the t_3-amplitudes in a CCSDT energy calculation is an outer loop over an index triple i, j, k of the t_{ijk}^{abc}-amplitudes (for a detailed description of the implementation see Refs. 87 and 97). Blocks of a, b, c index triples are computed within the loop one at a time and stored on disk for the next iteration. In addition, these blocks are used immediately to calculate the contributions to the singles and doubles amplitude equations. A schematic representation of this algorithm is depicted in the upper box of Fig. 5.1.

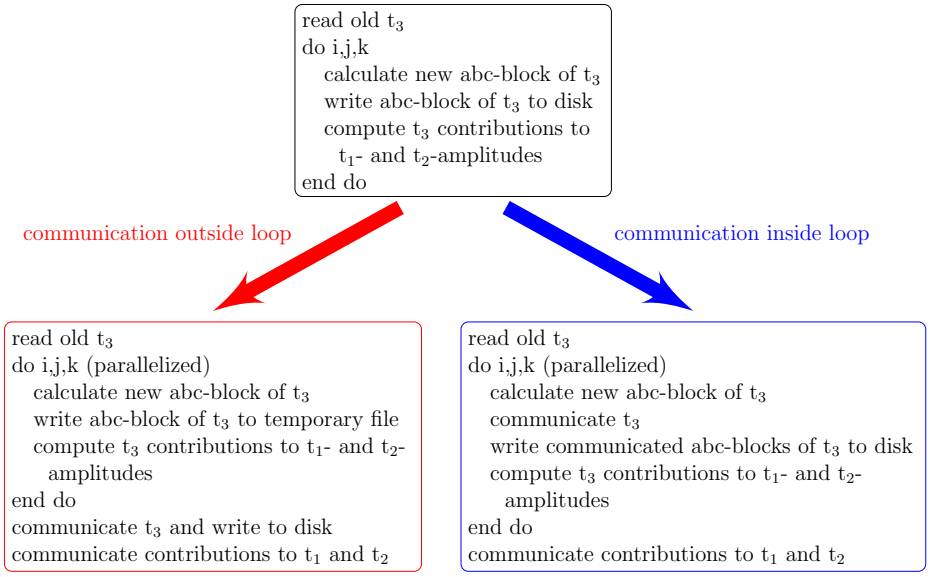

Figure 5.1: Schematic representation of the two different parallelization strategies. The serial algorithm (top) has been parallelized by communicating the triples amplitudes outside (left) or inside (right) the loop over occupied orbitals i,j,k.

The Mk-MRCCSDT ansatz is implemented using the same loop structure over indices

i, j, k. The triples amplitude equations of the Mk-MRCC ansatz are given as

$$\left\langle \Phi_{ijk}^{abc}(\mu) \middle| e^{-\hat{T}_\mu} \hat{H} e^{\hat{T}_\mu} \middle| \Phi_\mu \right\rangle c_\mu^\alpha + \sum_{\nu(\neq\mu)} \left\langle \Phi_{ijk}^{abc}(\mu) \middle| e^{-\hat{T}_\mu} e^{\hat{T}_\nu} \middle| \Phi_\mu \right\rangle H_{\mu\nu}^{\text{eff}} c_\nu^\alpha = 0 \ , \tag{5.6}$$

The computational cost for Eq. (5.6) is given for d reference determinants as $d \cdot n_{\text{occ}}^3 n_{\text{vrt}}^5$. Within the Mk-MRCC approach the amplitude equations [Eq. (5.6)] can be separated into a single-reference and a coupling part.[42] The first part is very similar to Eq. (5.1) with the only difference that all quantities are now specific for one reference determinant μ. Consequently, the Mk-MRCC ansatz can be implemented within a single-reference CC (SRCC) code as, for example, provided by the CFOUR package by looping over the reference determinants and adding the coupling terms.[31] This does not affect the general structure of the algorithm for the calculation of the t_3-amplitudes as mentioned before. The only difference is an extra loop over reference determinants around the loop over the index triples i, j, k and the additional coupling terms which are added inside the i, j, k loop.

For a parallelization of the loop over the index triples i, j, k the t_3-amplitudes and the triples contributions to the t_1- and t_2-amplitudes computed on separate nodes need to be communicated. For the communication of the triples amplitudes two different strategies are possible as shown in Fig. 5.1. The t_3-amplitudes are either written to a temporary file and communicated outside the loop or communicated directly after their computation inside the loop. The contributions to the t_1- and t_2-amplitudes are in both cases computed within the same i, j, k loop and communicated outside the loop. Using the strategy described above all triple terms and contributions are parallelized simultaneously. Each parallel process has to calculate a similar amount of i, j, k index triples which is then broadcasted to all other processors.

The performance of the two possible schemes is demonstrated via computations for the N_2O molecule at the CCSDT level of theory using the cc-pCVTZ basis (129 basis functions).[i] The timings for one CC iteration and the respective triples part are given in Table 5.1. It can be seen that the walltime for one CC iteration is reduced considerably with increasing number of processors. Thus, the implementation will make calculations at the CCSDT level that would take months feasible within days or weeks, provided that an appropriate number of nodes is used. In addition, with a larger number of nodes the triples part becomes less dominant in a CCSDT calculation. While for two

[i] The absolute energy obtained is -184.572494 Hartree when using the geometry parameters: R(NN)=1.1290 Å, R(NO)=1.1849 Å, ∠(NNO)=180.0 °.

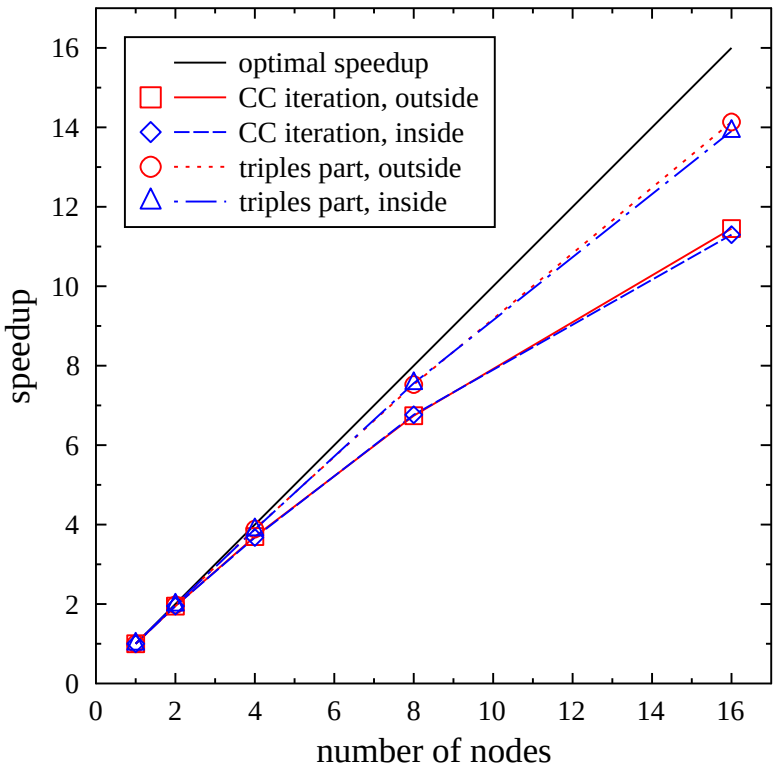

Figure 5.2: Parallel scaling of energy calculation at the CCSDT/cc-pCVTZ level of theory for N_2O. Depicted is the speedup for one CCSDT iteration and for the triples part within this iteration. The t_3-amplitudes are communicated either outside or inside the loop over i, j, k indices. On each node 1 cpu has been used.

nodes 97 % of the time are spent computing triples contributions, it is reduced to 80 % on 16 nodes. The corresponding speedup[ii] of the parallel algorithm is depicted in Fig. 5.2. The speedup observed with increasing number of nodes is quite close to the optimal one. With 16 nodes the speedup of one CCSDT iteration reaches values between 11 and 12, while the triples part alone yields a speedup of 14. It is interesting to note that the two outlined communication strategies for the t_3-amplitudes (outside and inside the i, j, k loop) show very similar performance. However, a careful investigation of Fig. 5.2 indicates some preferences to the "outside communication". Therefore, this communication strategy is used in the following.

As the full inclusion of triple excitations in CC calculation is computational demanding

[ii]The speedup is defined as the ratio of the serial execution time and the execution time on n nodes.

Table 5.2: Timings (walltime in s) for one CC iteration of the computation for the N_2O molecule using approximate schemes of CCSDT. The computations have been carried out using the cc-pV5Z basis set (273 basis functions). The speedups for the corresponding computations are given in parentheses. On each node 1 cpu has been used.

# nodes	CCSDT-1a	CCSDT-1b	CCSDT-2	CCSDT-3	CC3
1	596	605	650	660	667
2	311 (1.9)	318 (1.9)	356 (1.8)	373 (1.8)	373 (1.8)
4	170 (3.5)	175 (3.5)	214 (3.0)	231 (2.9)	229 (2.9)
8	99 (6.0)	102 (5.9)	142 (4.6)	158 (4.2)	157 (4.2)
16	64 (9.3)	67 (9.0)	106 (6.1)	123 (5.4)	123 (5.4)

due to its scaling behavior (N^8), several approximate iterative schemes of CCSDT have been developed, namely CCSDT-n (n=1a, 1b, 2, 3)[160,161] and CC3.[162] In these schemes certain terms of the CCSDT amplitude equations are skipped so that the computational scaling is reduced to N^7. As these methods are implemented within the same i, j, k loop in CFOUR their parallelization is straightforward, but should be mentioned at this point. The timings for these methods obtained for the computation on N_2O using the cc-pV5Z basis[143] (273 basis functions)[iii] are reported in Table 5.2. As for CCSDT the walltime is reduced considerably when increasing the number of nodes used, e.g., the calculation time for one iteration of the CCSDT-1a method is about 10 minutes on 1 node in comparison to about 1 minute on 16 nodes yielding a speedup of 9.3. The speedup for 16 nodes observed here is smaller than for CCSDT which is explained by the fact that these computations are less dominated by the triples part. While the time spent calculating the triples contributions for the CCSDT-1a method is 95 % of the whole CC iteration on 1 node (compared to 98 % for CCSDT using a smaller basis) it is reduced to 58 % on 16 nodes (80 % for CCSDT).

The performance of the parallel computation of Mk-MRCCSDT energies is shown for the ozone molecule. The computation[iv] has been performed using the cc-pCVTZ basis set and two-configurational SCF orbitals (with the active-space orbitals having b_1 and a_2 symmetry) using the experimental geometry (R=1.2717 Å, $\measuredangle$=116.8 °).[142] The timings for one CC iteration and the corresponding triples part are given in Table 5.3.

[iii] The absolute energies obtained are (in Hartree): CC3: -184.595095, CCSDT-1a: -184.594467, CCSDT-1b: -184.594525, CCSDT-2: -184.588903, CCSDT-3: -184.589449.

[iv] The absolute energy obtained is -225.306818 Hartree.

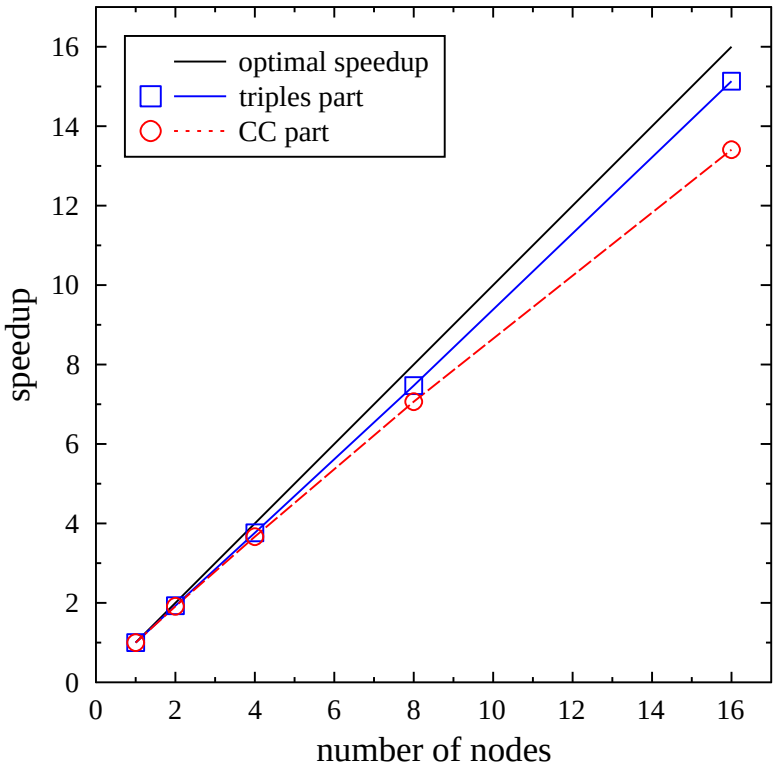

Figure 5.3: Parallel scaling of energy calculation at the Mk-MRCCSDT/cc-pCVTZ level of theory for O_3. Depicted is the speedup for one Mk-MRCCSDT iteration and for the triples part within this iteration. The t_3-amplitudes are communicated outside the loop over i, j, k indices. On each node 1 cpu has been used.

Table 5.3: Timings (walltime in s) for the O_3 molecule for one CC iteration and the triples part within this iteration. The communication has been performed outside the loop. The computation has been carried out at the Mk-MRCCSDT/cc-pCVTZ level (129 basis functions). The ratio of the triples part to the whole CC iteration is given in parenthesis. On each node 1 cpu has been used.

# nodes	CC iter.	triples part
1	5864	5811 (99%)
2	3065	3013 (98%)
4	1597	1544 (97%)
8	830	778 (94%)
16	436	384 (88%)

The time for one CC iteration is considerably reduced with an increasing number of processors yielding a computation time of about 7 minutes on 16 nodes in comparison to 98 minutes on 1 node. The triples part of this calculation is even more dominant than for a single-reference CCSDT case. For Mk-MRCCSDT the time spent in the triples part is 99% on 1 node and 88% on 16 nodes (compared to 98% and 80% for CCSDT). The speedup obtained for the Mk-MRCCSDT computations is displayed in Fig. 5.3. With 16 nodes the speedup observed lies between 13 and 14, while the triples part alone yields a speedup of over 15. These speedups are even closer to the optimal speedup as the ones obtained for the CCSDT calculation of N_2O, thus, demonstrating the efficiency of the parallelization scheme presented here for Mk-MRCCSDT computations.

5.2 Results and Discussion

In this section the overall performance and applicability of the parallelization scheme is demonstrated. Results of two applications are presented that involve typical problems in quantum chemistry for which the inclusion of triple excitation is desirable but so far extremely time consuming.

5.2.1 The CCSDT Energy of Benzene

For the investigation of the energetics of molecules, such as the atomization energy, several schemes have been reported in the literature to achieve high-accuracy results.[147,150,151] From these studies it is obvious that triple excitations are of importance and that contributions beyond CCSD(T) due to a full treatment of triple excitations at the CCSDT level of theory are non-negligible: the contribution from non-perturbative triple excitations, approximated by the difference of CCSDT and CCSD(T) extrapolated from triple- and quadruple-zeta quality basis sets is found for example to be crucial for obtaining chemical accuracy (about 1 kcal/mol) for the molecules N_2, C_2H_2, CO_2, HCN, O_2 (see Ref. 151), as well as for vinyl chloride,[163] cyclopropenylidene, propadienylidene[164] and many others. However, these computations are often very time consuming and the applicability of these schemes thus is limited to rather small molecules. Using the parallelization scheme presented here, high-level computations on larger molecules as benzene or substituted benzenes become feasible.

To demonstrate the applicability of the parallelization scheme for medium-sized molecules, benzene (with geometrical parameters R(CC)=1.3911 Å, R(CH)=1.0800 Å)[165] has

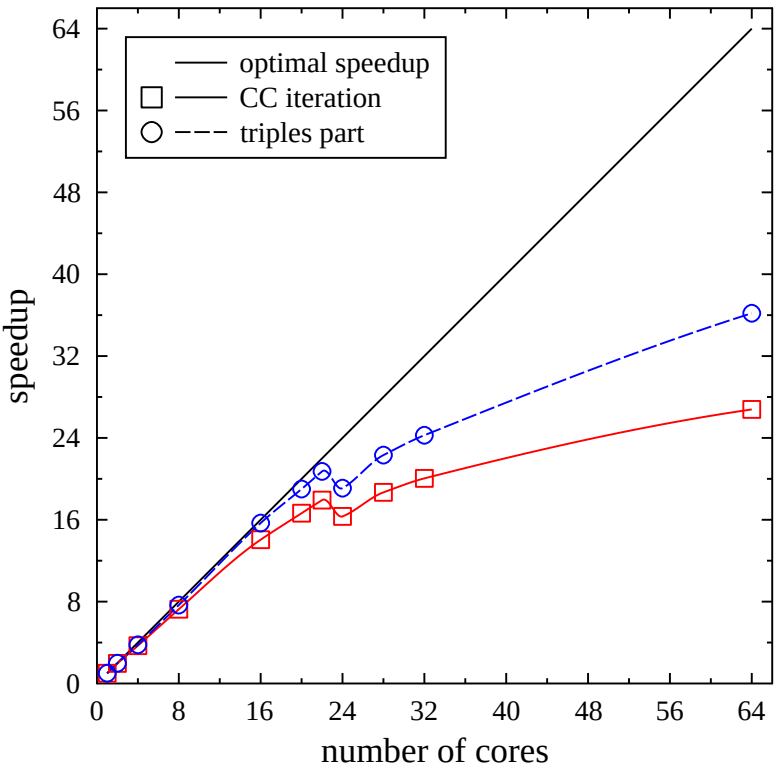

Figure 5.4: Parallel scaling of frozen-core energy calculation at the CCSDT/cc-pVTZ level for benzene. Depicted is the speedup for one CCSDT iteration and for the triples part within this iteration. The jobs have been distributed in a round-robin fashion.

been chosen as a typical representative example. The timings for the frozen-core (fc) energy calculation at the CCSDT level of theory using the cc-pVTZ basis set[143] are given in Table 5.4. As for N_2O, the walltime is reduced considerably with increasing number of nodes. The walltime for one CC iteration on one node is about six hours whereas the same computation on 16 nodes only requires about 25 minutes. Thus, the whole calculation is carried out within hours instead of days. In Fig. 5.4 the corresponding speedup is visualized. In comparison to the results obtained for N_2O (Fig. 5.2) the speedup for benzene is closer to the optimal speedup. Using 16 nodes the speedup observed is 14 for one CC iteration and larger than 15 for the triples part (compare to 11-12 and 14 in the case of N_2O). Thus, the scaling of the total time with the number of processors is improving for increasing system size (129 basis functions and 16 correlated electrons for N_2O, 264 basis functions and 30 correlated electrons for benzene) as the importance of

Table 5.4: Timings (walltime in s) for one CC iteration for the benzene molecule and the triples part within this iteration. The computation has been carried out at the fc-CCSDT/cc-pVTZ level (264 basis functions). The jobs have been distributed in a round-robin fashion.

# nodes	CC iteration	triples part
1	21669	21494
2	11036	10861
4	5866	5685
8	2986	2805
16	1542	1371
20	1302	1131
22	1209	1037
24	1327	1126
28	1160	963
32	1081	886
64	809	594

the parallelized, time-determining steps is even larger. It is worthwhile to note the drop in the speedup when using 24 instead of 22 nodes. All the computations presented in this section have been carried out on 22 nodes with four cores each. The jobs are distributed in a round-robin fashion, i.e., every node first obtains only one job. After that all remaining jobs are distributed in the same way. This means that for computations with up to 22 nodes only one core per node has been used. After that point at least some of the nodes need to handle more than one job at a time, i.e., these nodes enter the region of so-called symmetric multiprocessing. The influence of this on the computation time is shown in Table 5.5 for a computation using 16 cores. The same calculation has been carried out using a different number of cores per node. While using one core per node the walltime observed is 25 minutes, the computation of one iteration takes about five minutes longer when the number of cores is increased from one to two yielding a speedup of 12 instead of 14. Increasing the number of cores per node again by one, the computational effort grows by additional 9 minutes, lowering the speedup to nine. Thus, when increasing the number of cores per node used in a calculation a loss of hardware efficiency is observed which worsens with higher number of cores per node.

Table 5.5: Timings (walltime in s) and corresponding speedup for one iteration in the calculation of benzene at the fc-CCSDT/cc-pVTZ level (264 basis functions) when the number of CPUs per node is increased. The computation has been performed using 16 cores.

# CPUs per node	timing	speedup
1	1542	14
2	1812	12
3	2360	9

5.2.2 The 2,6-Pyridyne (C_5NH_3) Molecule

The applicability of the parallelization scheme is further demonstrated by investigating the 2,6-isomer of the didehydropyridine (pyridyne) studied in Section 4.5.2. This study of the geometry of 2,6-pyridyne at the CCSD, CCSD(T) and Mk-MRCCSD level did not provide a final answer for this class of molecules.[31] While CCSD and Mk-MRCCSD predicts both forms to be a minimum (with the monocyclic form to be more stable at the Mk-MRCCSD level and the bicyclic form to be more stable for CCSD) CCSD(T) only yields a minimum for the monocyclic structure. In order to narrow down the problem high-level multireference ab-initio calculations are necessary. The recent development of the Mk-MRCCSDT approach[68] allows the inclusion of full triple excitations. However, calculations at this level of theory are demanding and time consuming when proper basis sets are to be used.

To extend the previous study of 2,6-pyridyne single-point energy calculations at the Mk-MRCCSDT/cc-pVTZ level have been carried out. The geometries of the bicyclic and the monocyclic form as well as the transition state are obtained at the Mk-MRCCSD/cc-pCVTZ level (see Sec. 4.5.2.2). Two closed-shell determinants are used as reference as explained in Sec. 4.5.2.

The resulting energies are depicted in Fig. 5.5. For comparison, the single-point energies computed at the fc-CCSD and fc-Mk-MRCCSD levels have been added to the figure. The CCSD energy for the bicyclic form is lower (2.9 kcal mol^{-1}) than that for the monocyclic form. The energy of the transition state lies in between. Mk-MRCCSD yields a lower energy for the monocyclic isomer (3.9 kcal mol^{-1}) and a barrier of 0.2 kcal mol^{-1} from the bicyclic form. When the effect of triple excitations is included at the CCSDT and Mk-MRCCSDT levels of theory the monocyclic form is found to be

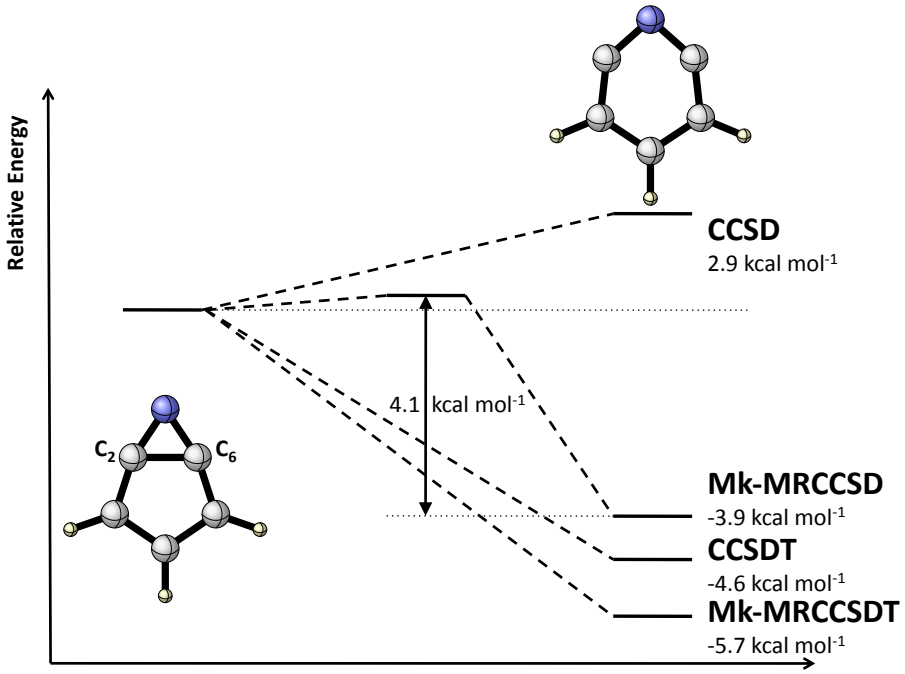

Figure 5.5: Schematic representation of the energetic ordering of the monocyclic and bicyclic forms of 2,6-pyridyne as obtained in frozen-core computations at the CCSD, Mk-MRCCSD, CCSDT and Mk-MRCCSDT levels of theory using the cc-pVTZ basis set and the RHF-Mk-MRCCSD/cc-pCVTZ geometries from Ref. 31. The energies are given relative to the bicyclic form.

lower in energy than the bicyclic one. The energy computed at the Mk-MRCCSD/cc-pCVTZ transition-state geometry lies in between. The inclusion of triple excitations at the CCSDT level leads to an considerable stabilization of the monocyclic isomer (7.5 kcal mol^{-1}). The additional stabilization at the Mk-MRCCSDT level is significantly smaller (1.8 kcal mol^{-1}).

These results indicate that the energy minimum of the bicyclic isomer of 2,6-pyridyne may be an artifact of theory due to the lack of triple excitations. Interestingly, computations at the Mk-MRCCSD(T) level, where triple excitations are treated in an approximate manner, yield comparable findings supporting this conclusion.[153]

As the calculations at the Mk-MRCCSDT level are computationally demanding they have only been carried out using 8 and 16 nodes. The walltimes observed for the calculations are given in Table 5.6. The computation time for the monocyclic isomer is about 178 minutes on 8 nodes and about 102 minutes on 16 nodes yielding a speedup of 1.8.

For the corresponding computation at the CCSDT level a speedup of 1.6 is observed.

Table 5.6: Timings (walltime in s) for one CC iteration for the energy computations of 2,6-pyridyne at geometries for the bicyclic and monocyclic form as well as the transition state. The frozen-core calculations have been carried out on 8 nodes (using 1 cpu each) employing the cc-pVTZ basis set (222 basis functions) and the Mk-MRCCSD/cc-pCVTZ geometry.

	bicyclic	transition state	monocyclic
Mk-MRCCSDT	10707	10718	10699
CCSDT	2529	2548	2526

6 Summary

Coupled-cluster theory in its single-reference formulation represents one of the most successful approaches in quantum chemistry for the description of atoms and molecules. To extend the applicability of single-reference coupled-cluster theory to systems with degenerate or near-degenerate electronic configurations, multireference coupled-cluster methods have been suggested in the literature. However, many of the methods are not formulated in a general way, i.e., they have been formulated to describe only specific multireference problems (exceptions are for example the state-specific MRCC methods such as the Mk-MRCC approach suggested by Mukherjee and coworkers,[41,42] as well as the BW-MRCC ansatz[40] or the renormalized coupled-cluster approach[166]) and do not represent black-box approaches. For only few of these MRCC theories there is an efficient algorithm available, e.g., for Mk-MRCC (e.g., developed in this work or within the PSI program package[167]) or BW-MRCC.[40] Additionally, the lack of analytic derivatives limits the application of such methods to small model systems when aiming for properties such as the equilibrium geometry.

This work deals with developments to overcome these limitations and to extend the range of applicability of one of the most promising multireference coupled-cluster theories, namely the Mk-MRCC approach to larger molecular systems of chemical interest. The strategies followed here cover areas such as the development of efficient algorithms, analytic gradient techniques, and parallelization of calculations which now allow computations on systems previously inaccessible by theory. The approaches developed here have been tested and applied to chemically relevant systems. The following paragraphs provide a detailed summary of the results presented in this thesis.

Development of an Efficient Multireference Algorithm

An efficient multireference algorithm has been implemented to perform Mk-MRCC energy calculations within the singles and doubles (Mk-MRCCSD) and singles, doubles, and triples (Mk-MRCCSDT) approximations. This algorithm exploits the special structure of the Mk-MRCC working equations that allows to adapt existing efficient

single-reference coupled-cluster codes and, thus, to reduce the work required for the implementation. The algorithm has the correct computational scaling of $d \cdot N^6$ for Mk-MRCCSD and $d \cdot N^8$ for Mk-MRCCSDT, where N denotes the system size and d the number of reference determinants. The algorithm allows the use of a model space containing determinants derived from distributing two electrons in two active orbitals. Both methods can be used in conjunction RHF and TCSCF reference wave functions. Additionally, UHF and ROHF open-shell singlet reference wave functions can be used with Mk-MRCCSD.

Analytic First Derivatives for the Mk-MRCC Ansatz

The theory of analytic first derivatives for the Mk-MRCC method has been formulated using a Lagrange formalism. The resulting equations have been separated in a single-reference part and additional coupling terms. As in the case of energy computations, this represents an enormous advantage because it reduces the effort required to implement the theory. The Mk-MRCC gradients within the singles and doubles (Mk-MRCCSD) and singles, doubles and triples (Mk-MRCCSDT) approximation have been implemented in the CFOUR package. The algorithm is capable of using RHF and TCSCF reference wave functions, and as for the energy calculation, the correct scaling of $d \cdot N^6$ for Mk-MRCCSD and $d \cdot N^8$ for Mk-MRCCSDT has been achieved.

The applicability of analytic Mk-MRCC gradients has been demonstrated for various compounds. While for 2,6-pyridyne, single-reference CCSD calculations predict the bicyclic form to be the most stable one, the Mk-MRCCSD results favor the correct monocyclic form, although a minimum for the bicyclic structure can still be found. This finding indicates that for a correct description of the whole potential energy surface, triple excitations should be included. The application of Mk-MRCC gradients for the determination of geometry parameters of the ozone molecule indicate that a balanced description of dynamical and non-dynamical correlation effects together with proper basis-sets is necessary in order to correctly predict the equilibrium geometry. The deviations to experiment obtained for geometry optimizations using Mk-MRCC are always smaller than the deviations from the corresponding single-reference coupled-cluster calculations. For example, the computation at the Mk-MRCCSDT/cc-pVTZ level for the bond length (1.2732 Å) yield a deviation from experiment (1.2717 Å) of only 0.0015 Å.

The development of analytic gradients for Mk-MRCC offers the possibility of rou-

tinely locating minima and transition states on the potential energy surface. It can be considered as a key step towards routine investigation of multireference systems and calculation of their properties.

Parallelization of Mk-MRCCSDT and CCSDT

As the full treatment of triple excitations in coupled-cluster calculations is rather time-consuming a parallelization scheme for Mk-MRCCSDT and CCSDT energy calculations has been outlined and implemented. A detailed analysis of CCSDT and Mk-MRCCSDT energy computations indicates that these calculations are completely dominated by the determination of the triples amplitudes and their contributions to the singles and doubles amplitude equations. Starting from the highly efficient serial CFOUR computer code, a program which can be used on workstation clusters by parallelizing the most time-consuming steps of the algorithm, i.e., steps related to the triple amplitudes, has been developed. The central aspect of the parallel implementation is the distributed computation of the triple amplitudes as well as their contributions to the single and double amplitudes. In this way an algorithm is obtained for which sufficient local memory and disk space are needed but which does not depend on high-speed network connections.

Benchmark calculations demonstrate the excellent scaling of computation time with an increasing number of processors. For calculations on benzene at the CCSDT/cc-pVTZ level (264 basis functions) and on ozone molecule at the Mk-MRCCSDT/cc-pCVTZ level (129 basis functions) a speedup of about 14 is obtained when 16 nodes are used. In this way Mk-MRCC computations for the 2,6-pyridyne with 222 basis functions have become feasible and can be carried out in a reasonable amount of time, i.e., within days or weeks instead of months or years. Thus, this kind of implementation opens the field of application for Mk-MRCCSDT and CCSDT where high accuracy is decisive.

In summary, it can be stated that the work presented here represents an important step in turning multireference coupled-cluster methods from a highly experimental field into approaches which can be routinely applied to chemically relevant systems. This offers the possibility to obtain the high accuracy provided by coupled-cluster approaches when intermediates or transition states in chemical reactions are to be correctly described. In this way, pathways on the potential energy surface that have not been accessible so far by coupled-cluster methods can be investigated with the hope that this will yield a

deeper insight into chemical reactions.

Although the Mk-MRCC approach has its deficiencies, such as the lack of energy invariance with respect to orbital rotations within the active space, Mk-MRCC theory has opened the field of routine application of MRCC methods to chemical problems and the number of publications concerning pure application of the method has been increased in the last years.[168–170] Furthermore, an efficient program capable to perform calculations at the Mk-MRCC level of theory allows for new developments for the treatment of multireference problems, as for example the inclusion of relativistic effects, the investigation of excited-state properties via response theory or the implementation of second derivatives.

To overcome the problems of Mk-MRCC theory, it needs to be investigated in the future whether it is necessary to modify the Mk-MRCC approach or to replace it by a new theory. One possible strategy might be to retain the Jeziorski-Monkhorst ansatz and use alternative sufficiency conditions that fulfill the desirable requirements without loss of size-extensivity. Beside that, it would also be possible to follow a completely different approach as, for example, the development of a theory based on an internally contracted ansatz where only one universal exponential operator acts on a linear combination of reference determinants. However, even if new methods will be developed to solve the problems of the Mk-MRCC approach it is likely that the structure of the new approach or the underlying equations might be similar to Mk-MRCC theory. Therefore, the knowledge obtained from this work can directly be used to understand new approaches in more detail which will considerably simplify the extension of the applicability of these new methods.

Bibliography

[1] J. Gauss, in *The Encyclopedia of Computational Chemistry*, edited by P. v. R. Schleyer, N. L. Allinger, T. Clark, J. Gasteiger, P. A. Kollman, H. F. Schaefer, and P. R. Schreiner, p. 615, Wiley, Chichester, 1998.

[2] T. D. Crawford and H. F. Schaefer, *Rev. Comp. Chem.* **14**, 33 (2000).

[3] R. J. Bartlett and M. Musiał, *Rev. Mod. Phys.* **79**, 291 (2007).

[4] I. Shavitt and R. J. Bartlett, *Many-Body Methods in Chemistry and Physics: MBPT and Coupled-Cluster Theory*, Cambridge University Press, Cambridge, 2009.

[5] G. D. Purvis and R. J. Bartlett, *J. Chem. Phys.* **76**, 1910 (1982).

[6] K. Raghavachari, G. W. Trucks, J. A. Pople, and M. Head-Gordon, *Chem. Phys. Lett.* **157**, 479 (1989).

[7] J. Noga and R. J. Bartlett, *J. Chem. Phys.* **86**, 7041 (1987).

[8] G. E. Scuseria and H. F. Schaefer, *Chem. Phys. Lett.* **152**, 382 (1988).

[9] J. D. Watts and R. J. Bartlett, *J. Chem. Phys.* **93**, 6104 (1990).

[10] T. Helgaker, P. Jørgensen, and J. Olsen, *Molecular Electronic-Structure Theory*, Wiley, Chichester, 2000.

[11] A. P. Rendell, T. J. Lee, and R. Lindh, *Chem. Phys. Lett.* **194**, 84 (1992).

[12] S. Hirata, *J. Phys. Chem. A* **107**, 9887 (2003).

[13] R. M. Olson, J. L. Bentz, R. A. Kendall, M. W. Schmidt, and M. S. Gordon, *J. Chem. Theory. Comput.* **3**, 1312 (2007).

[14] T. Janowski, A. R. Ford, and P. Pulay, *J. Chem. Theory. Comput.* **3**, 1368 (2007).

[15] M. E. Harding, T. Metzroth, J. Gauss, and A. A. Auer, *J. Chem. Theory. Comput.* **4**, 64 (2008).

[16] V. Lotrich, N. Flocke, M. Ponton, A. D. Yau, A. Perera, E. Deumens, and R. J. Bartlett, *J. Chem. Phys.* **128**, 194104 (2008).

[17] J. R. Hammond, W. A. de Jong, and K. Kowalski, *J. Chem. Phys.* **128**, 224102 (2008).

[18] E. J. Bylaska, W. A. de Jong, N. Govind, K. Kowalski, T. P. Straatsma, M. Valiev, D. Wang, E. Aprà, T. L. Windus, J. Hammond, P. Nichols, S. Hirata, M. T. Hackler, Y. Zhao, P.-D. Fan, R. J. Harrison, M. Dupuis, D. M. A. Smith, J. Nieplocha, V. Tipparaju, M. Krishnan, Q. Wu, T. V. Voorhis, A. A. Auer, M. Nooijen, E. Brown, G. Cisneros, G. I. Fann, H. Früchtl, J. Garza, K. Hirao, R. Kendall, J. A. Nichols, K. Tsemekhman, K. Wolinski, J. Anchell, D. Bernholdt, P. Borowski, T. Clark, D. Clerc, H. Dachsel, M. Deegan, K. Dyall, D. Elwood, E. Glendening, M. Gutowski, A. Hess, J. Jaffe, B. Johnson, J. Ju, R. Kobayashi, R. Kutteh, Z. Lin, R. Littlefield, X. Long, B. Meng, T. Nakajima, S. Niu, L. Pollack, M. Rosing, G. Sandrone, M. Stave, H. Taylor, G. Thomas, J. van Lenthe, A. Wong, and Z. Zhang, *NWChem, A Computational Chemistry Package for Parallel Computers, Version 5.1* (2007), Pacific Northwest National Laboratory, Richland, Washington 99352-0999, USA.

[19] H.-J. Werner, P. J. Knowles, R. Lindh, F. R. Manby, M. Schütz, P. Celani, T. Korona, A. Mitrushenkov, G. Rauhut, T. B. Adler, R. D. Amos, A. Bernhardsson, A. Berning, D. L. Cooper, M. J. O. Deegan, A. J. Dobbyn, F. Eckert, E. Goll, C. Hampel, G. Hetzer, T. Hrenar, G. Knizia, C. Köppl, Y. Liu, A. W. Lloyd, R. A. Mata, A. J. May, S. J. McNicholas, W. Meyer, M. E. Mura, A. Nicklass, P. Palmieri, K. Pflüger, R. Pitzer, M. Reiher, U. Schumann, H. Stoll, A. J. Stone, R. Tarroni, T. Thorsteinsson, M. Wang, and A. Wolf, MOLPRO, version 2009.1, a package of ab initio programs, 2009, see http://www.molpro.net.

[20] M. Kállay and M. E. Harding, parallel version of the string-based general coupled-cluster program MRCC, 2006, see http://www.mrcc.hu.

[21] J. Hoffner, M. J. Schottelius, D. Feichtinger, and P. Chen, *J. Am. Chem. Soc.* **120**, 376 (1998).

[22] F. A. Evangelista, W. D. Allen, and H. F. Schaefer, *J. Chem. Phys.* **127**, 024102 (2007).

[23] J. Shen, T. Fang, S. Li, and Y. Jiang, *J. Phys. Chem. A* **112**, 12518 (2008).

[24] M. Barbatti, J. Paier, and H. Lischka, *J. Chem. Phys.* **121**, 11614 (2004).

[25] X. Li and J. Paldus, *J. Chem. Phys.* **126**, 234303 (2007).

[26] J. W. Grissom, G. U. Gunawardena, D. Klingberg, and D. H. Huang, *Tetrahedron* **52**, 6453 (1996).

[27] M. Winkler, B. Cakir, and W. Sander, *J. Am. Chem. Soc.* **126**, 6135 (2004).

[28] M. Winkler and W. Sander, *Aust. J. Chem.* **63**, 1013 (2010).

[29] R. G. Parr and W. Yang, *Density-Functional Theory of Atoms ans Molecules*, Science Publications, Oxford, 1994.

[30] S. L. Debbert and C. J. Cramer, *Int. J. Mass. Spectrom.* **201**, 1 (2000).

[31] E. Prochnow, F. A. Evangelista, H. F. Schaefer, W. D. Allen, and J. Gauss, *J. Chem. Phys.* **131**, 064109 (2009).

[32] N. Oliphant and L. Adamowicz, *J. Chem. Phys.* **94**, 1229 (1991).

[33] S. A. Kucharski and R. J. Bartlett, *J. Chem. Phys.* **95**, 8227 (1991).

[34] X. Z. Li and J. Paldus, *J. Chem. Phys.* **107**, 6257 (1997).

[35] K. Kowalski and P. Piecuch, *J. Chem. Phys.* **113**, 18 (2000).

[36] D. Mukherjee, R. K. Moitra, and A. Mukhopadhyay, *Mol. Phys.* **33**, 955 (1977).

[37] I. Lindgren, *Int. J. Quantum Chem. Symp.* **12**, 33 (1978).

[38] B. Jeziorski and H. J. Monkhorst, *Phys. Rev. A* **24**, 1668 (1981).

[39] J. Mášik and I. Hubač, in *Quantum Systems in Chemistry and Physics: Trends in Methods and Applications*, edited by R. McWeeny, J. Maruani, Y. G. Smeyers, and S. Wilson, pp. 283–308, Kluwer Academic, Dordrecht, 1997.

[40] J. Pittner, P. Nachtigall, P. Čársky, J. Mášik, and I. Hubač, *J. Chem. Phys.* **110**, 10275 (1999).

[41] U. S. Mahapatra, B. Datta, and D. Mukherjee, *Mol. Phys.* **94**, 157 (1998).

[42] U. S. Mahapatra, B. Datta, and D. Mukherjee, *J. Chem. Phys.* **110**, 6171 (1999).

[43] M. Hanrath, *J. Chem. Phys.* **123**, 084102 (2005).

[44] F. A. Evangelista, W. D. Allen, and H. F. Schaefer, *J. Chem. Phys.* **125**, 154113 (2006).

[45] L. Kong, *Int. J. Quantum. Chem.* **109**, 441 (2009).

[46] A. Szabo and N. S. Ostlund, *Modern Quantum Chemistry: Introduction to Advanced Electronic Structure Theory.*, Dover Publications, Mineola, New York, 1996.

[47] I. Hubač, J. Pittner, and P. Čársky, *J. Chem. Phys.* **112**, 8779 (2000).

[48] M. Hanrath, *J. Chem. Phys.* **128**, 154118 (2008).

[49] CFOUR, a quantum chemical program package written by J.F. Stanton, J. Gauss, M.E. Harding, and P.G. Szalay; with contributions from A.A. Auer, R.J. Bartlett, U. Benedikt, C. Berger, D.E. Bernholdt, Y. J. Bomble, O. Christiansen, M. Heckert, O. Heun, C. Huber, D. Jonsson, J. Jusélius, K. Klein, W.J. Lauderdale, D. A. Matthews, T. Metzroth, D.P. O'Neill, D.R. Price, E. Prochnow, K. Ruud, F. Schiffmann, S. Stopkowicz, M.E. Varner, J. Vázquez, F. Wang, J.D. Watts and the integral packages MOLECULE (J. Almlöf and P.R. Taylor), PROPS (P.R. Taylor), ABACUS (T. Helgaker, H.J. Aa. Jensen, P. Jørgensen, and J. Olsen), and ECP routines by A. V. Mitin and C. van Wüllen. For the current version, see http://www.cfour.de.

[50] M. Born and J. R. Oppenheimer, *Ann. Physik* **389**, 457 (1927).

[51] C. C. J. Roothaan, *Rev. Mod. Phys.* **23**, 69 (1951).

[52] G. G. Hall, *Proc. Roy. Soc.* **A205**, 541 (1951).

[53] H. J. Werner, *Adv. Chem. Phys.* **69**, 1 (1987).

[54] R. Shepard, *Adv. Chem. Phys.* **69**, 63 (1987).

[55] G. Das and A. C. Wahl, *J. Chem. Phys.* **44**, 87 (1966).

[56] J. Čížek, *J. Chem. Phys.* **45**, 4256 (1966).

[57] J. Čížek, *Adv. Chem. Phys.* **14**, 35 (1969).

[58] J. Čížek and J. Paldus, *Int. J. Quantum. Chem.* **5**, 359 (1971).

[59] C. D. Sherrill and H. F. Schaefer, in *Advances in Quantum Chemistry: The Configuration Interaction Method*, edited by P.-O. Löwdin, E. Brändas, J. R. Sabin, and M. C. Zerner, p. 143, Academic Press, New York, 1999.

[60] S. Hassani, *Mathematical Physics*, Springer, New York, 1999.

[61] J. F. Stanton, J. Gauss, J. D. Watts, and R. J. Bartlett, *J. Chem. Phys.* **94**, 4334 (1991).

[62] G. E. Scuseria, C. L. Janssen, and H. F. Schaefer, *J. Chem. Phys.* **89**, 7382 (1988).

[63] N. Oliphant and L. Adamowicz, *J. Chem. Phys.* **95**, 6645 (1991).

[64] S. A. Kucharski and R. J. Bartlett, *J. Chem. Phys.* **97**, 4282 (1992).

[65] I. Lindgren, *J. Phys. B: Atom. Molec. Phys.* **7**, 2441 (1974), Bloch equation, perturbation theory.

[66] D. Pahari, S. Chattopadhyay, S. Das, and D. Mukherjee, *Chem. Phys. Lett.* **381**, 223 (2003).

[67] J. Mášik, I. Hubač, and P. Mach, *J. Chem. Phys.* **108**, 6571 (1998).

[68] F. A. Evangelista, A. C. Simmonett, W. D. Allen, H. F. Schaefer, and J. Gauss, *J. Chem. Phys.* **128**, 124104 (2008).

[69] S. Das, D. Mukherjee, and M. Kállay, *J. Chem. Phys.* **132**, 074103 (2010).

[70] F. A. Evangelista and J. Gauss, *J. Chem. Phys.* **133**, 044101 (2010).

[71] X. Li and J. Paldus, *J. Chem. Phys.* **132**, 114103 (2010).

[72] J. Gauss, in *Modern Methods and Algorithms of Quantum Chemistry*, edited by J. Grotendorst, Neumann Institute for Computing, Jülich, 2002.

[73] J. Gauss and J. F. Stanton, *J. Chem. Phys.* **102**, 251 (1995).

[74] M. Kállay and J. Gauss, *J. Chem. Phys.* **120**, 6841 (2004).

[75] J. Pittner and J. Šmydke, *J. Chem. Phys.* **127**, 114103 (2007).

[76] E. Kordel, C. Villani, and W. Klopper, *Mol. Phys.* **105**, 2565 (2007).

[77] P. G. Szalay, *Int. J. Quantum Chem.* **55**, 151 (1995).

[78] P. Jørgensen and T. Helgaker, *J. Chem. Phys.* **89**, 1560 (1988).

[79] H. Koch, H. J. Aa. Jensen, P. Jørgensen, T. Helgaker, G. E. Scuseria, and H. F. Schaefer, *J. Chem. Phys.* **92**, 4924 (1990).

[80] J. Gerratt and I. M. Mills, *J. Chem. Phys.* **49**, 1719 (1968).

[81] J. Gauss, J. F. Stanton, and R. J. Bartlett, *J. Chem. Phys.* **95**, 2623 (1991).

[82] N. C. Handy and H. F. Schaefer, *J. Chem. Phys.* **81**, 5031 (1984).

[83] J. Rice and R. Amos, *Chem. Phys. Lett.* **122**, 585 (1985).

[84] J. D. Watts, J. Gauss, and R. J. Bartlett, *J. Chem. Phys.* **98**, 8718 (1993).

[85] T. J. Lee, W. D. Allen, and H. F. Schaefer, *J. Chem. Phys.* **87**, 7062 (1987).

[86] R. Shepard, H. Lischka, P. G. Szalay, T. Kovar, and M. Ernzerhof, *J. Chem. Phys.* **96**, 2085 (1992).

[87] J. Gauss and J. F. Stanton, *Phys. Chem. Chem. Phys.* **2**, 2047 (2000).

[88] A. C. Scheiner, G. E. Scuseria, J. E. Rice, T. J. Lee, and H. F. Schaefer, *J. Chem. Phys.* **87**, 5361 (1987).

[89] E. A. Salter, G. W. Trucks, and R. J. Bartlett, *J. Chem. Phys.* **90**, 1752 (1989).

[90] J. Gauss, J. F. Stanton, and R. J. Bartlett, *J. Chem. Phys.* **95**, 2639 (1991).

[91] J. Gauss, W. J. Lauderdale, J. F. Stanton, J. D. Watts, and R. J. Bartlett, *Chem. Phys. Lett.* **182**, 207 (1991).

[92] G. E. Scuseria, *J. Chem. Phys.* **94**, 442 (1991).

[93] T. J. Lee and A. P. Rendell, *J. Chem. Phys.* **94**, 6229 (1991).

[94] J. D. Watts, J. Gauss, and R. J. Bartlett, *Chem. Phys. Lett.* **200**, 1 (1992).

[95] J. Gauss and J. F. Stanton, *Chem. Phys. Lett.* **276**, 70 (1997).

[96] P. G. Szalay, J. Gauss, and J. F. Stanton, *Theor. Chem. Acc.* **100**, 5 (1998).

[97] J. Gauss and J. F. Stanton, *J. Chem. Phys.* **116**, 1773 (2002).

[98] J. Gauss, *J. Chem. Phys.* **116**, 4773 (2002).

[99] M. Kállay, J. Gauss, and P. G. Szalay, *J. Chem. Phys.* **119**, 2991 (2003).

[100] M. Kállay and J. Gauss, *J. Chem. Phys.* **120**, 6841 (2004).

[101] P. G. Szalay and R. J. Bartlett, *J. Chem. Phys.* **101**, 4936 (1994).

[102] J. F. Stanton and J. Gauss, *J. Chem. Phys* **101**, 8938 (1994).

[103] S. V. Levchenko, T. Wang, and A. I. Krylov, *J. Chem. Phys.* **122**, 224106 (2005).

[104] O. Demel and J. Pittner, *J. Chem. Phys.* **124**, 144112 (2006).

[105] J. Pittner, X. Z. Li, and J. Paldus, *Mol. Phys.* **103**, 2239 (2005).

[106] T. Helgaker and P. Jørgensen, *Adv. Quantum Chem.* **19**, 183 (1988).

[107] D. J. Thouless, *The Quantum Mechanics of Many-Body Systems*, Academic Press, New York, 1961.

[108] A. G. Myers, S. B. Cohen, and B. M. Kwon, *J. Am. Chem. Soc.* **116**, 1670 (1994).

[109] M. J. Schottelius and P. Chen, *J. Am. Chem. Soc.* **118**, 4896 (1996).

[110] R. Lindh, T. J. Lee, A. Bernhardsson, B. J. Persson, and G. Karlström, *J. Am. Chem. Soc.* **117**, 7186 (1995).

[111] R. Lindh and M. Schütz, *Chem. Phys. Lett.* **258**, 409 (1996).

[112] N. Koga and K. Morokuma, *J. Am. Chem. Soc.* **113**, 1907 (1991).

[113] R. Lindh and B. J. Persson, *J. Am. Chem. Soc.* **116**, 4963 (1994).

[114] C. J. Cramer, J. J. Nash, and R. R. Squires, *Chem. Phys. Lett.* **277**, 311 (1997).

[115] C. J. Cramer, *J. Am. Chem. Soc.* **120**, 6261 (1998).

[116] E. B. Wang, C. A. Parish, and H. Lischka, *J. Chem. Phys.* **129**, 044306 (2008).

[117] X. Li and J. Paldus, *J. Chem. Phys.* **129**, 174101 (2008).

[118] E. Kraka and D. Cremer, *Chem. Phys. Lett.* **216**, 333 (1993).

[119] E. Kraka and D. Cremer, *J. Am. Chem. Soc.* **116**, 4929 (1994).

[120] T. D. Crawford, E. Kraka, J. F. Stanton, and D. Cremer, *J. Chem. Phys.* **114**, 10638 (2001).

[121] P. U. Manohar and A. I. Krylov, *J. Chem. Phys.* **129**, 194105 (2008).

[122] P. R. Schreiner, *Chem. Commun.* 483 (1998).

[123] P. R. Schreiner and M. Prall, *J. Am. Chem. Soc.* **121**, 8615 (1999).

[124] M. Winkler and W. Sander, *J. Phys. Chem. A* **105**, 10422 (2001).

[125] E. Kraka, J. Anglada, A. Hjerpe, M. Filatov, and D. Cremer, *Chem. Phys. Lett.* **348**, 115 (2001).

[126] P. R. Schreiner, M. Prall, and V. Lutz, *Angew. Chem. Int. Edit.* **42**, 5757 (2003).

[127] C. E. Smith, T. D. Crawford, and D. Cremer, *J. Chem. Phys.* **122**, 174309 (2005).

[128] D. E. Woon and T. H. Dunning, Jr., *J. Chem. Phys.* **103**, 4572 (1995).

[129] C. J. Cerjan and W. H. Miller, *J. Chem. Phys.* **75**, 2800 (1981).

[130] J. Nichols, H. Taylor, P. Schmidt, and J. Simons, *J. Chem. Phys.* **92**, 340 (1990).

[131] T.-C. Jagau, *Analytische Ableitungstechniken für Mehrdeterminantenansätze*, Diplomarbeit, Johannes Gutenberg-Universität Mainz, Germany, 2009.

[132] T.-C. Jagau, E. Prochnow, F. A. Evangelista, and J. Gauss, *J. Chem. Phys.* **132**, 144110 (2010).

[133] Y. Yamaguchi, Y. Osamura, and H. F. Schaefer, *J. Am. Chem. Soc.* **105**, 7506 (1983).

[134] Y. Yamaguchi, J. D. Goddard, Y. Osamura, and H. F. Schaefer, *A New Dimension to Quantum Chemistry: Analytic Derivative Methods in Ab Initio Molecular Electronic Structure Theory*, Oxford University Press, New York, 1994.

[135] E. Prochnow, M. E. Harding, and J. Gauss, *J. Chem. Theory. Comput.* **6**, 2339 (2010).

[136] O. Hino, T. Kinoshita, G. K. L. Chan, and R. J. Bartlett, *J. Chem. Phys.* **124**, 114311 (2006).

[137] K. Bhaskaran-Nair, O. Demel, and J. Pittner, *J. Chem. Phys.* **129**, 184105 (2008).

[138] O. Demel, K. R. Shamasundar, L. Kong, and M. Nooijen, *J. Phys. Chem. A* **112**, 11895 (2008).

[139] X. Li and J. Paldus, *J. Chem. Phys.* **131**, 114103 (2009).

[140] U. S. Mahapatra, S. Chattopadhyay, and R. K. Chaudhuri, *J. Phys. Chem. A* **114**, 3668 (2010).

[141] D. W. Whitman and B. K. Carpenter, *J. Am. Chem. Soc.* **104**, 6473 (1982).

[142] T. Tanaka and Y. Morino, *J. Mol. Spectrosc.* **33**, 538 (1970).

[143] T. H. Dunning, Jr., *J. Chem. Phys.* **90**, 1007 (1989).

[144] Y. J. Bomble, J. Stanton, M. Kállay, and J. Gauss, *J. Chem. Phys.* **123**, 054101 (2005).

[145] S. A. Kucharski and R. J. Bartlett, *J. Chem. Phys.* **110**, 8233 (1999).

[146] W. T. Borden, E. R. Davidson, and D. Feller, *J. Am. Chem. Soc.* **103**, 5725 (1981).

[147] A. G. Császár, W. D. Allen, and H. F. Schaefer, *J. Chem. Phys.* **108**, 9751 (1998).

[148] A. Halkier, H. Larsen, J. Olsen, P. Jørgensen, and J. Gauss, *J. Chem. Phys.* **110**, 734 (1999).

[149] J. A. Sordo, *J. Chem. Phys.* **114**, 1974 (2001).

[150] A. Karton, E. Rabinovich, J. M. L. Martin, and B. Ruscic, *J. Chem. Phys.* **125**, 144108 (2006).

[151] M. E. Harding, J. Vázquez, B. Ruscic, A. K. Wilson, J. Gauss, and J. F. Stanton, *J. Chem. Phys.* **128**, 114111 (2008).

[152] D. Feller and K. A. Peterson, *J. Chem. Phys.* **131**, 154306 (2009).

[153] F. A. Evangelista, E. Prochnow, J. Gauss, and H. F. Schaefer, *J. Chem. Phys.* **132**, 074107 (2010).

[154] J. Nieplocha, R. J. Harrison, and R. Littlefield, In Proceedings of Supercomputing, IEEE Computer Society Press: Washington, DC, 1994.

[155] A. R. Ford, T. Janowski, and P. Pulay, *J. Comput. Chem.* **28**, 1215 (2007).

[156] R. M. Olson, M. W. Schmidt, M. S. Gordon, and A. P. Rendell, *Enabling the Efficient Use of SMP Clusters: The GAMESS/DDI Approach*, In Supercomputing, ACM/IEEE Conference: Phoenix, AZ, 2003.

[157] The MPIForum, *MPI: a message passing interface*, In Proceedings of the 1993 ACM/IEEE conference on Supercomputing, ACM Press: Portland, OR, USA, 1993.

[158] P. Piecuch and J. I. Landman, *Parallel Comput.* **26**, 913 (2000).

[159] OpenMP Fortran Application Programming Interface, http://www.openmp.org.

[160] M. Urban, J. Noga, S. J. Cole, and R. J. Bartlett, *J. Chem. Phys.* **83**, 4041 (1985).

[161] J. Noga, R. J. Bartlett, and M. Urban, *Chem. Phys. Lett.* **134**, 126 (1987).

[162] H. Koch, O. Christiansen, P. Jørgensen, A. S. de Merás, and T. Helgaker, *J. Chem. Phys.* **106**, 1808 (1997).

[163] M. E. Harding, J. Gauss, K. Pflüger, and H.-J. Werner, *J. Phys. Chem. A* **111**, 13623 (2007).

[164] J. Vázquez, M. E. Harding, J. Gauss, and J. F. Stanton, *J. Phys. Chem. A* **113**, 12447 (2009).

[165] J. Gauss and J. F. Stanton, *J. Phys. Chem. A* **104**, 2865 (2000).

[166] P. Piecuch, K. Kowalski, I. S. O. Pimienta, and M. J. McGuire, *Int. Rev. Phys. Chem.* **21**, 527 (2002).

[167] T. D. Crawford, C. D. Sherrill, E. F. Valeev, J. T. Fermann, R. A. King, M. L. Leininger, S. T. Brown, C. L. Janssen, E. T. Seidl, J. P. Kenny, and W. D. Allen, *Journal of Computational Chemistry* **28**, 1610 (2007).

[168] S. Chattopadhyay, P. Ghosh, and U. S. Mahapatra, *J. Phys. B: At. Mol. Opt. Phys.* **37**, 495 (2004).

[169] T. Lu, A. C. Simmonett, F. A. Evangelista, Y. Yamaguchi, and H. F. Schaefer, *J. Phys. Chem. A* **113**, 13227 (2009).

[170] T. Saito, S. Nishihara, Y. Kataoka, Y. Nakanishi, Y. Kitagawa, T. Kawakami, S. Yamanaka, M. Okumura, and K. Yamaguchi, *J. Phys. Chem. A* **114**, 7967 (2010).

[171] G. Burns, R. Daoud, and J. Vaigl, LAM: An Open Cluster Environment for MPI, in *Proceedings of Supercomputing Symposium*, p. 379, 1994.

[172] J. M. Squyres and A. Lumsdaine, A Component Architecture for LAM/MPI, in *Proceedings, 10th European PVM/MPI Users' Group Meeting*, number 2840 in Lecture Notes in Computer Science, p. 379, Venice, Italy, 2003, Springer-Verlag.

A Technical Details

All calculations were carried out on a 22 node cluster. The cluster nodes were equipped with two dual core Intel Xeon 5160 processors running at 3 GHz, 32 GB FB-DIMM RAM, and 8 striped SATA disks. For the network communication the onboard Gigabit Ethernet controller was used.

For the parallel implementation the message passing interface (MPI)[157] is used. The results presented here are obtained by using LAM/MPI.[171,172] The communication of the t_3-amplitudes is done by the MPI_BCAST subroutine. The triples contributions to the t_1- and t_2-amplitudes are communicated using the MPI_ALLREDUCE routine.

B SRCC Gradients

B.1 Explicit Expression for the Orbital Response Part in SRCC Theory

The one-particle intermediate I'_{pq} is defined by

$$I'_{pq} = -\frac{1}{2}\Big\{ f_{pp}\Big[D_{pq} + D_{qp}\Big] + \sum_{rst}\Big[\langle pr||st\rangle \, \Gamma_{qrst} + \langle rp||st\rangle \, \Gamma_{rqst} + \langle rs||pt\rangle \, \Gamma_{rsqt} + \langle rs||tp\rangle \, \Gamma_{rstq}\Big]\Big\} - \sum_{rs} \langle pr||qs\rangle \, D_{rs}\delta_{qi} \ . \tag{B.1}$$

The last term is only apparent when the index q refers to an occupied orbital as indicated by δ_{qi}:

$$\delta_{qi} = \begin{cases} 1 & \text{if } q \in \text{occ} \\ 0 & \text{otherwise} \end{cases} \ . \tag{B.2}$$

The one-particle intermediate $I_{\mu\nu}$ in its MO representation is given as

$$I_{ij} = I''_{ij} - \sum_{e}\sum_{m} D_{em}\left(\langle ei||mj\rangle + \langle im||je\rangle\right) \tag{B.3}$$

$$I_{ai} = I''_{ai} - f_{ii}D_{ai} \tag{B.4}$$

$$I_{ia} = I''_{ia} - f_{ii}D_{ai} \tag{B.5}$$

$$I_{ab} = I''_{ab} \ , \tag{B.6}$$

with the intermediate I''_{pq}:

$$I''_{pq} = \begin{cases} I'_{qp}(\mu) & \text{if } (p,q) = (a,i) \\ I'_{pq} & \text{otherwise} \end{cases} \ . \tag{B.7}$$

C Mk-MRCC Gradients

C.1 Explicit Expression for the Orbital Response Part in Mk-MRCC Theory

For the case of HF orbitals, the generalized energy-weighted density matrix in the MO representation, $I_{pq}(\mu)$, is defined by

$$I_{ij}(\mu) = I''_{ij}(\mu) - 2\sum_{e}\sum_{m} D_{em}^{(\mathrm{orb-resp})}(\mu)\,\langle ei||mj\rangle \tag{C.1}$$

$$I_{ai}(\mu) = I_{ia}(\mu) = I''_{ia}(\mu) - \sum_{m} f_{im}(\mu) D_{ma}^{(\mathrm{orb-resp})}(\mu) \tag{C.2}$$

$$I_{ab}(\mu) = I''_{ab}(\mu)\ , \tag{C.3}$$

where the intermediate $I''_{pq}(\mu)$ is given as

$$I''_{pq}(\mu) = \begin{cases} I'_{pq}(\mu) & \text{if } p < q \\ I'_{qp}(\mu) & \text{if } p > q \end{cases}\ . \tag{C.4}$$

$D_{em}^{(\mathrm{orb-resp})}(\mu)$ is obtained by solving the corresponding Z-vector equations.

D List of Publications

D.1 Publications Relevant for this Work

- E. Prochnow, M. E. Harding, J. Gauss, *Parallel calculation of CCSDT and Mk-MRCCSDT energies*, J. Chem. Theory Comput. **6**, 2339 (2010).
- T.-C. Jagau, E. Prochnow, F. A. Evangelista, J. Gauss, *Analytic gradients for Mukherjee's multireference coupled cluster method using two-configurational self-consistent-field orbitals*, J. Chem. Phys. **132**, 144110 (2010).
- E. Prochnow, F. A. Evangelista, W. D. Allen, H. F. Schaefer III, J. Gauss, *Analytic gradients for the state-specific multireference coupled cluster singles and doubles model*, J. Chem. Phys. **131**, 064109 (2009).

D.2 Further Publications

- F. A. Evangelista, E. Prochnow, J. Gauss, H. F. Schaefer III, *Perturbative triples corrections in state-specific multireference coupled cluster theory*, J. Chem. Phys. **132**, 074107 (2010).
- E. Prochnow, A. A. Auer, *Quantitative prediction of gas-phase* ^{15}N *and* ^{31}P *nuclear magnetic shielding constants*, J. Chem. Phys. **132**, 064109 (2010).
- M. Lehmann, J. Seltmann, A. A. Auer, E. Prochnow, U. Benedikt, *Synthesis and mesomorphic properties of new V-shaped shape-persistent nematogens containing a thiazole or a thiadiazole bending unit*, J. Mater. Chem. **19**, 1978-1988 (2009).
- E. Prochnow, A. A. Auer, K. Banert, *Ab initio study of molecular properties and decomposition products of 1-azidoalkynes – A challenge for experimentalists*, J. Phys. Chem. A **111**, 9945 (2007).